ABSTRACT

GROUNDWATER FLOW IN THE UPPER CASTLE HAYNE AQUIFER: NUMERICAL SIMULATIONS AND STRONTIUM ISOTOPIC INVESTIGATIONS

by

Samantha Eileen Kofroth

December 2019

Director of Thesis: Dr. Terri L. Woods

Major Department: Geological Sciences

The Castle Hayne Aquifer System (CHAS) is the most extensively used aquifer system in the North Carolina Coastal Plain. Heavy groundwater withdrawals from the Upper Castle Hayne Aquifer (UCH) have occurred since the 1960's and have caused changes in groundwater flow regimes. These changes require full understanding because they can lead to degradation of one of North Carolina's most valuable freshwater resources.

A Principal Component Analysis explained 86.82% of the variance in groundwater chemistry in the UCH. The Component Loadings indicated strong correlations between the changing concentrations of many chemical variables and suggested that influx of saline water into the UCH and limestone dissolution have major impacts on water chemistry.

The main goal of this project was to investigate groundwater movement within the UCH aquifer of North Carolina by comparing the results of a strontium-isotope-based, two-component, mixing model to the results of a computer-simulated flow model. The Sr-study suggests sources of water entering the UCH based on $^{87}Sr/^{86}Sr$ ratios and [Sr] concentrations. The Sr data utilized in this study were obtained from previous studies.

A groundwater flow model was developed using Visual MODFLOW. The model was calibrated to current conditions, which include heavy pumping of the UCH. The simulated UCH equipotential map showed that groundwater in the UCH is moving toward the Nutrien phosphate mine from all directions. The map also showed a cone of depression that is similar the observed equipotential map generated from the 2017 water level data.

Particle tracking simulations performed with MODPATH under current pumping conditions, and using effective porosities of 15%, 26% and 37 % for the UCH, yielded minimum total travel times from Earth's surface to well screens of 730 years, 825 years, and 920 years, respectively, and groundwater velocities of 0.002-22, 0.0014-13, and 0.001-9.15 (feet/day), respectively.

MODPATH simulation results performed under pumping conditions sometimes conflicted with the conclusions drawn from the Sr-study, except where the Sr-analysis indicate downward flow from the Surficial Aquifer through the overlying units. Therefore, alternative non-pumping simulations were performed. During non-pumping simulations, groundwater-flow vectors showed upward groundwater movement from the Lower Castle Hayne Aquifer (LCH) and the Beaufort Aquifer (BF) going into the UCH, for samples that plotted below or to the left of the calculated, two-component, Sr-mixing line. This means that vertical movement of water from units below the UCH could have occurred prior to pumping.

Overall, the results of this study indicate that heavy groundwater withdrawals have extensively altered groundwater flow patterns across the North Carolina Coastal Plain. Further research, including the development of a model calibrated to pre-pumping conditions is required to fully understand the groundwater processes that have caused the current Sr-signatures.

GROUNDWATER FLOW IN THE UPPER CASTLE HAYNE AQUIFER: NUMERICAL SIMULATIONS AND STRONTIUM ISOTOPIC INVESTIGATIONS

A Thesis

Presented to

The Faculty of the Department of Geological Sciences

East Carolina University

To be submitted in partial fulfillment of the requirements for the degree of

Master of Science in Geology

Samantha Eileen Kofroth

December, 2019

GROUNDWATER FLOW IN THE UPPER CASTLE HAYNE AQUIFER: NUMERICAL SIMULATIONS AND STRONTIUM ISOTOPIC INVESTIGATIONS

By

Samantha Eileen Kofroth

APPROVED BY:

DIRECTOR OF THESIS: _____
Dr. Terri L. Woods

COMMITTEE MEMBER: _____
Dr. Alex K. Manda

COMMITTEE MEMBER: _____
Dr. Richard L. Mauger

COMMITTEE MEMBER: _____
Mr. James K. Holley

CHAIR OF GEOLOGICAL SCIENCES:

_____
Dr. Stephen J. Culver

DEAN OF THE GRADUATE SCHOOL:

_____
Dr. Paul J. Gemperline

Acknowledgments

I would like to thank my parents, Scott and Detrina Kofroth, and my entire family for their love and support. I would like to give a special thank you to Drs. Terri L. Woods, Alex K. Manda, Richard L. Mauger, and Mr. James K. Holly for their support and guidance. I would also like to thank Amy W. Cressman for her steadfast support and friendship.

TABLE OF CONTENTS

LIST OF TABLES

LIST OF FIGURES

LIST OF ABBREVIATIONS

NACP ..... North Atlantic Coastal Plain

NCCP ..... North Carolina Coastal Plain

S ..... Surficial Aquifer

YCL ..... Yorktown Confining Layer

Y ..... Yorktown Aquifer

PR ..... Pungo River

UCHCL ..... Upper Castle Hayne Confining Layer

CH ..... Castle Hayne

CHAS ..... Castle Hayne Aquifer System

CAS ..... Cretaceous Aquifer System

UCH ..... Upper Castle Hayne Aquifer

LCHCL ..... Lower Castle Hayne Confining Layer

LCH ..... Lower Castle Hayne Aquifer

BFCL ..... Beaufort Confining Layer

BF ..... Beaufort Aquifer

PDCL ..... Peedee Confining Layer

K_h ..... Horizontal hydraulic conductivity

K_v ..... Vertical Hydraulic conductivity

T ..... Transmissivity

S_s ..... Specific Storage

Sr ..... Strontium

Rb ..... Rubidium

USGS ..... United States Geological Survey

PCA ..... Principal Component Analysis

RMS .....Root Mean Square error

NRMS .....Normalized Root Mean Square error

Mgd ..... Million Gallons per Day

Ft^3/d ..... Cubic Feet per Day

1.0 INTRODUCTION

1.1 Study Area

The Northern Atlantic Coastal Plain (NACP) aquifer system is a 50,000-square-mile area, composed of low rolling hills and flat ground, which extends from the coast of Long Island, New York to the North Carolina – South Carolina border. The portion of the NACP that lies within North Carolina is referred to as the North Carolina Coastal Plain (NCCP). The NCCP covers 25,000-square miles (Figure 1). Sea-level transgression and regression of the Cenozoic, Cretaceous and later periods, have resulted in little topographic relief. The area also has extensive swamps, many of which have been drained for agriculture.

The Castle Hayne Aquifer System (CHAS) underlies twenty-three counties in the NCCP and covers an area of approximately 11,500 square miles (Winner and Coble, 1996). This study focuses on Beaufort County and portions of adjoining counties, including: Pitt, Craven and Hyde (Figure 1). The groundwater hydrology of Beaufort County has been extensively investigated because of the large-scale phosphate mining operation near the town of Aurora, North Carolina. The mine is adjacent to the Pamlico Estuary at Lee Creek. Texas Gulf Sulfur Company (TGS) began full-scale mining in 1965. The Potash Corporation of Saskatchewan, also known as PCS Phosphate Company Inc., or PotashCorp Aurora, bought the mine from TGS in 1995. PotashCorp and Agrium Inc., merged in 2018 and the operation continues as Nutrien Phosphate Aurora. To ensure safe, dry mining conditions, the piezometric head of the UCH has been lowered from 7 feet above mean sea level (AMSL) to about 140 feet below mean sea level (BMSL). The mine's average daily pumping rate was 43 million gallons per day (mgd) during the 2017 calendar year (https://www.ncwater.org/Permits_and_Registration/Capacity_Use/Central_Coastal_Plain/ccpcu

adetail.php?permit=CU1003). Depressurizing the UCH for mining activities has affected the hydrogeological processes of this region. For example, a wide-spread cone of depression has developed in the potentiometric surface of the UCH, and drawdown has been observed in wells over 30 miles from the mine (Sherwani, 1980). Groundwater-flow regimes have also been altered since extensive pumping began, especially in areas near the mine (DeWiest, 1969).

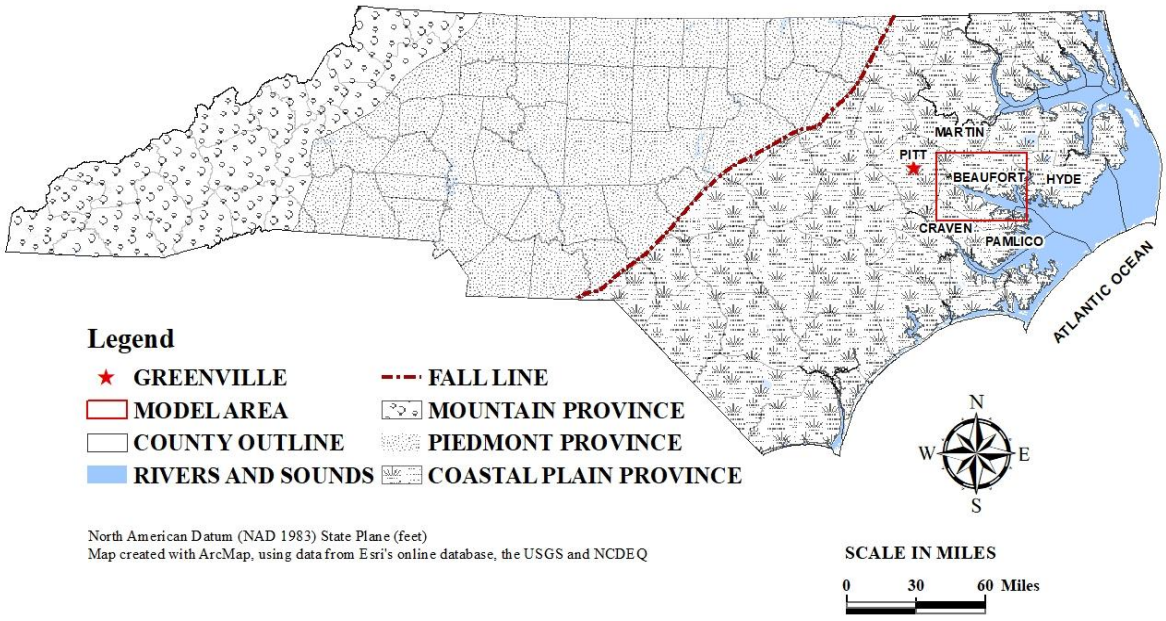

Figure 1. *Physiographic provinces and map of study area in North Carolina.*

1.2 Purpose

Vertical groundwater movement can significantly affect groundwater quality. The purpose of this research was to investigate the vertical movement of groundwater into and out of the UCH. This study compared a strontium-based geochemical model and a simulated

groundwater-flow model to evaluate the impacts that vertical flow has on UCH groundwater by attempting to identify where vertical movements occur. Chemical and isotopic data from previous studies were compiled for statistical analysis and chemical classification to help determine hydrogeologic processes that impact UCH groundwater.

1.2.1 Principal Component Analysis

In recent years, isotopic signatures and chemistry of the CHAS and its related aquifers such as the Cretaceous Peedee, has enhanced our understanding of the water-quality changes and movement of groundwater in these coastal limestones. Using SigmaPlot (version 13), Principal Component Analysis (PCA, a multivariate statistical technique) was applied to the compiled data to determine patterns and underlying processes that may not be directly evident. PCA creates principal components (PCs) to explain relationships between complexly related variables such as the concentrations of major constituents or stable isotopic ratios in the groundwater considered for this study. The PCs are independent of one another and help to characterize the correlations of the variables. In the case of natural waters, PCs can provide indications of specific hydrologic or geologic processes, such as saltwater intrusion or limestone dissolution.

1.2.2 Groundwater Flow Simulation

There are three general purposes for numerical groundwater models, the first of which is to forecast expected artificial or natural changes in the system. Secondly, groundwater models are used to generate a description of the system which is then used to analyze assumptions about its nature and dynamics. These models are used to further understanding of the system and for future planning. Thirdly, groundwater models are used to generate hypothetical systems which

are used to study the principles of groundwater flow that are associated with general and specific problems (Kresic, 2007). The purpose of creating the model in this study aligns most directly with the second purpose. Woods et al. (2000[a]) used a strontium-based geochemical model to determine hydrogeologic processes that affect UCH groundwater. The model presented in this study was developed to assess the results of the geochemical study by analyzing groundwater flow in the CHAS system with a computer-simulated flow model (Visual MODFLOW Classic).

2.0 PREVIOUS STUDIES

Several modeling studies have been done in the NCCP, because the UCH is the most productive and the most extensively used aquifer in North Carolina. Studies include works by Winner and Coble, 1996; Giese et al., 1997; Leahy and Martin, 1993; Leahy and Martin, 1980; and Reynolds, 1992. Most of these studies concern the Central Coastal Plain Capacity Use Area (CCPCUA) and the effects that extensive groundwater withdrawals have on the aquifer system. By 1980, estimated groundwater withdrawals in North Carolina exceeded 130 mgd (Leahy and Martin, 1993; Giese et al., 1997). Pumping centers withdrawing at least 100,000 gal/d were primarily south and west of the Pamlico Sound, although large withdrawals were also made farther north near the Albemarle Sound. The largest single withdrawal was associated with the phosphate-mining operation in Beaufort County. By 1980, withdrawals from the UCH associated with the mine were approximately 64 mgd (Giese et al., 1997). Consequently, this area experienced the greatest water-level decline. Water levels declined more than 20 ft from pre-pumping levels over a large part of the county; near the center of the cone of depression, decline was as great as 80 ft. (Giese et al., 1997). Extensive pumping of the UCH has locally altered groundwater movement, however, previous studies have determined that overall changes in recharge and discharge have been slight. Principal changes primarily involve the vertical movement of water from one hydrogeologic unit to another, and the reversal of vertical flow direction near the major pumping areas.

Giese et al., 1997, developed and compared a model simulating pre-pumping conditions (1900), and a model simulating pumping conditions (1980). Comparison of these two models determined that changes in the overall water budget for the NCCP aquifers was minor. However, pumping has caused large local decreases in the potentiometric surfaces of several

aquifers, including the UCH. The simulated pre-pumping potentiometric surfaces of the Surficial Aquifer and for the up-dip (western) parts of the other aquifers were high in the interstream divide areas and low in the valleys of perennial streams. This distribution indicates that most groundwater movement is within the local flow systems and discharge is to nearby streams. In the down-dip areas of the confined aquifers, the potentiometric surfaces have a gentle coastward gradient to the east-southeast (Giese et al., 1997). The simulated potentiometric surfaces indicate lowered levels in parts of most aquifers due to pumping, and drawdowns of 30 and 60 feet BSL has occurred in parts of the Beaufort and Castle Hayne Aquifers in the Beaufort County area. Large withdrawals from the UCH have caused groundwater to move upward into the UCH, through the underlying Beaufort Aquifer and Confining Layer, creating a large area of depressed potentiometric levels in the Beaufort Aquifer (Giese at al., 1997).

Previous studies of strontium isotopes to trace groundwater mixing and diagenesis in carbonate aquifers include: Banner, 1995; Banner et al., 1989; Cander, 1994; Collerson et al., 1988; Jacobson and Wasserburg, 2005; Katz and Bullen, 1996; McNutt et al., 1990; and Stueber et al., 1993. Jacobson and Wasserburg (2005) explain that $^{87}Sr/^{86}Sr$ ratios in groundwater systems are a powerful tool for examining geochemical interactions between aquifer rocks and migrating fluids. Radiogenic strontium (^{87}Sr) is produced by the β-decay of ^{87}Rb ($\tau_{1/2}$= 48.8Ga). Therefore, the $^{87}Sr/^{86}Sr$ ratio of strontium released into groundwater during water-rock interaction varies according to the Rb and Sr concentrations, age, and dissolution rate of aquifer materials. If there is a large contrast between the Sr-isotopic composition of groundwater aquifer rocks, it is possible to assess the extent of water-rock interactions during flow through the aquifer (Jacobson and Wasserburg, 2005).

Previous geochemical studies of the CHAS include works by: Woods et al., 2000[a]; Sutton and Woods, 1995; Harned et al., 1989; and Sherwani, 1980. Woods et al. (2000[b]) explain that chemical and isotopic analyses can provide information on the movement and mixing of groundwater along flowpaths. The aforementioned studies have provided evidence indicating that geographic variations of $^{87}Sr/^{86}Sr$ isotope ratios and Sr concentrations of UCH groundwater cannot solely be explained by the continuous reaction of water with aquifer materials. Other hydrogeologic processes must be occurring. $^{87}Sr/^{86}Sr$ ratios have provided information about groundwater movement that could not have been determined by studying only the physical and chemical characteristics of the water. The $^{87}Sr/^{86}Sr$ in groundwater in the NCCP reveal a complex mixing pattern and indicate that hydrogeochemical processes, such as limestone dissolution, weathering, other water-rock interactions, saline-mixing, and salt-water intrusion control groundwater quality (Bakari et al., 2013). Results of these studies illustrate the strength of combining isotopic measurements with more conventional chemistry data to obtain a better understanding of groundwater flow systems and the geochemical processes governing their chemistry (Bakari, 2013).

2.1 Regional Geology

The NCCP lies within the Coastal Plain province of North Carolina. This province is characterized by flat to gently undulating topography and covers approximately one-third of the state. The Coastal Plain province has been subjected to sea level transgressions and regressions. Topographic relief and elevations increase westward. The NCCP is underlain by a wedge-shaped mass of sedimentary strata that dip and thicken eastward. The wedge thins toward its western limit, which coincides with the position of the Fall Line (NCGS, 1985), an erosional

feature that separates the Piedmont and the Coastal Plain physiographic regions. The sedimentary wedge reaches a maximum thickness of approximately 10,000 feet at Cape Hatteras, NC. Mesozoic to Precambrian crystalline basement rocks underlie the NCCP sediments and sedimentary formations (Winner and Coble, 1996).

NCCP sediments are of marine, estuarine and terrestrial origin and range in age from Early Cretaceous to Holocene. A wide range of lithologies and degrees of induration occur, including: clay and silt, glauconitic and phosphatic sands, highly fossiliferous sand and clay, non-fossiliferous sand and clay, multiple varieties of limestone, sandstone, and peat (NCGS, 1985). Several Plio-Pleistocene formations have been identified in the NCCP, and include: the James City, the Flanner's Beach, the Waccamaw, and the Croatan Formations (NCGS, 1985). Cenozoic formations that comprise the NCCP, in descending order, are as follows: the undifferentiated Quaternary Unit (surficial sediments), the Yorktown, the Pungo River, the Castle Hayne, the Belgrade, the River Bend, and the Beaufort Formations. Mesozoic formations underlie the Cenozoic age formations, and are as follows: the Peedee Formation, Black Creek Group, which includes the Tar-Heel, the Bladen, and Donoho Creek Formations, and Cape Fear Formation. These formations overlie Mesozoic to Precambrian crystalline basement rock.

2.2 Hydrogeologic Framework

The subdivision of sedimentary formations generally coincides with the subdivision of hydrogeological units (Table 1). For the purposes of this study, "unit" refers to a specific aquifer and its associated overlying confining layer (when present). The system of regional hydrogeological units is defined by lateral distribution, thickness, hydraulic properties and composition. Figure 2 shows the location of cross-section trace (A-A') of the hydrogeologic

system and the cross-section is illustrated in Figure 3. In the main part of the study area, Beaufort County, the thickness of sedimentary strata ranges from 1,200 feet BSL in the west to about 4,500 feet eastern portion. Most of the deeper sedimentary strata contain residual sea water (N.C. Department of Water and Air Resources, 1971). The areal extents of each hydrogeologic unit are presented in Figures 4-10. These maps were constructed in ArcGIS, using geospatial data retrieved from the United States Geological Survey (USGS) website (https://water.usgs.gov/ogw/gwrp/activities/gspdata/Studies/NSCCoastal.html), except for the Pungo River Unit, which was inferred from (Winner and Coble, 1996). This study is primarily concerned with the sediments that lie above the Peedee Unit, and include: the Surficial, the Yorktown, the Pungo River, the Castle Hayne, and the Beaufort Aquifers and their associated confining layers.

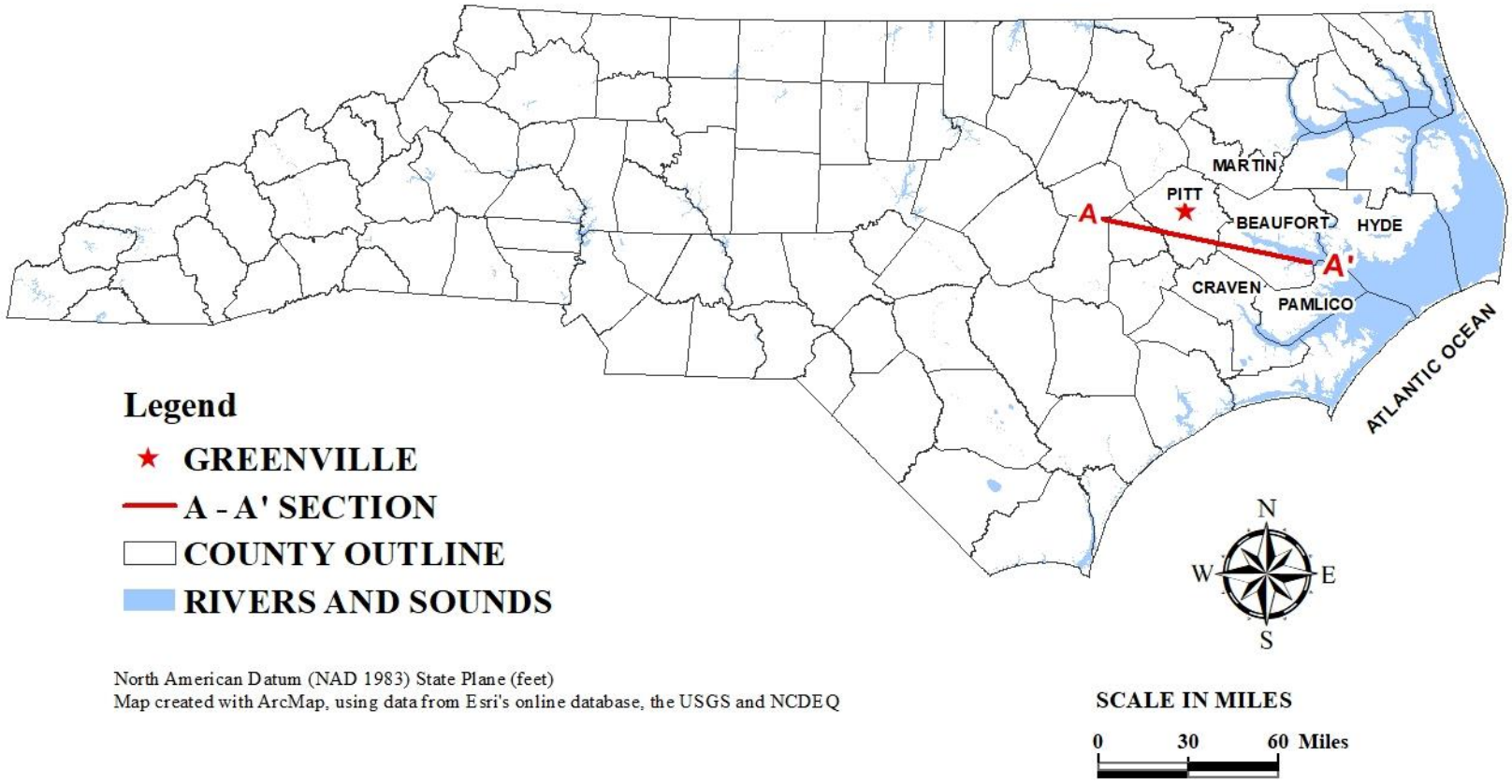

Figure 2. *Beaufort County, North Carolina with location of cross section A-A'.*

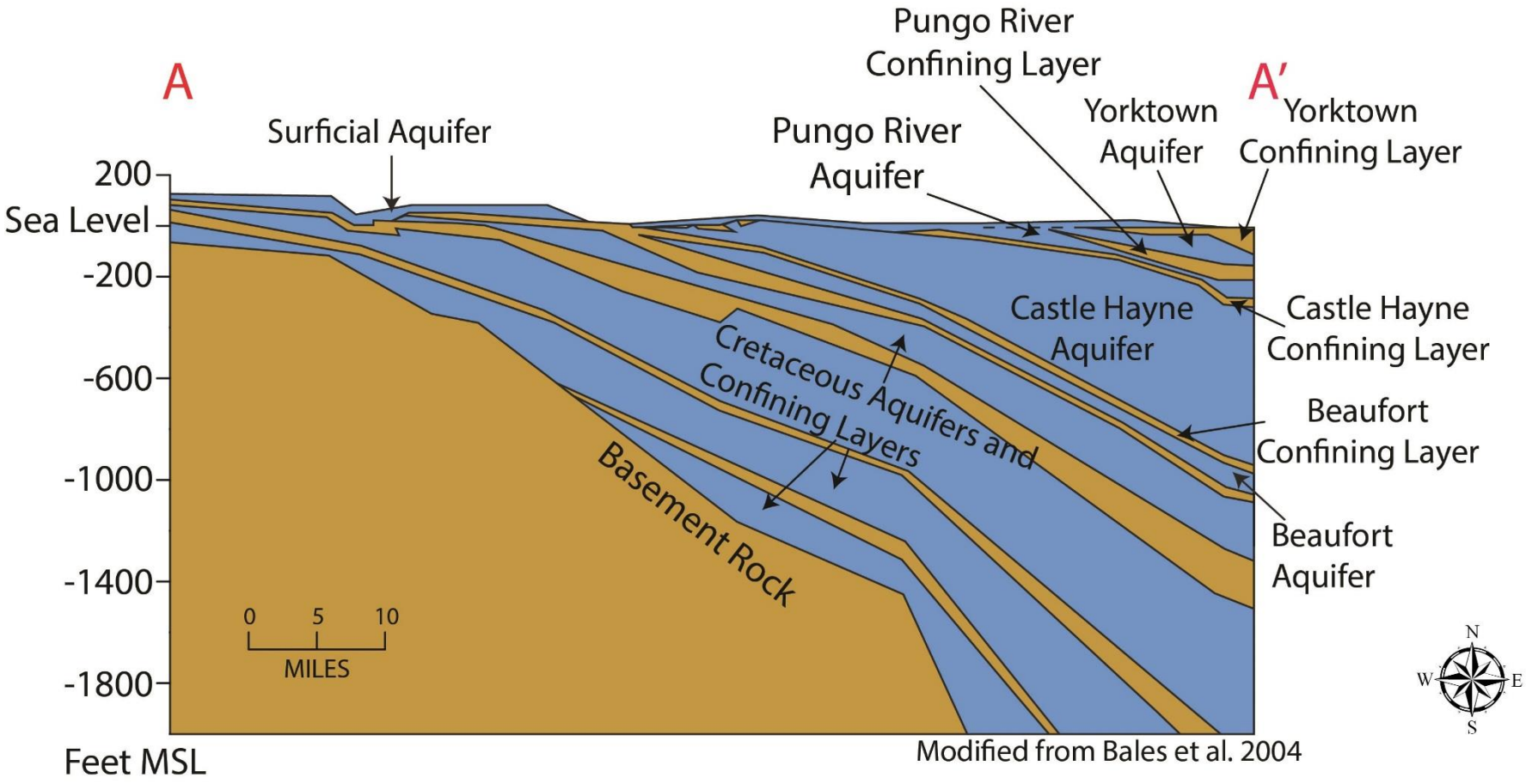

***Figure* 3.** *Generalized hydrologic cross-section of A- A' in the Pamlico River area. Vertical scale is in feet with respect to mean sea level; horizontal scale is in miles. Modified from Bales et al. 2004.*

Table 1. Generalized Stratigraphy and Hydrogeology of Coastal Plain Formations (Modified from Winner and Coble, 1996)				
Geologic Age	**Formation**		**Aquifer or Confining Unit Name**	**Description**
Quaternary (Recent and Pleistocene)	Surficial Sediments		Surficial Aquifer (unconfined)	Sand, silt, shells, clay and peat
Plio-Pliestocene	Yorktown, James City, Flanner's Beach, Waccamaw, and Croatan		Yorktown Confining Layer and Aquifer	Interbedded silt, sand and clay with some shell beds
Miocene	Pungo River		Pungo River Confining Layer and Aquifer	Phosphate and quartz sand, silt, clay and limestone
Oligocene Eocene	River Bend Castle Hayne	C H A S	Upper Castle Hayne Confining Layer and Aquifer	Well indurated, moldic limestone containing calcite, quartz, glauconite and dolomite with interlayered calcareous sands
			Lower Castle Hayne Confining Layer and Aquifer	Shell limestone interbedded with calcareous sands
Paleocene	Beaufort		Beaufort Confining Layer and Aquifer	Fine glauconite sand, silty and clayey in part
Upper Cretaceous	Peedee		Peedee Confining Layer and Aquifer	Interbedded clay, fine sand and silt becoming calcareous in the Peedee
	Black Creek Group		Black Creek Confining Layer and Aquifer	
	Cape Fear		Cape Fear Confining Layer and Aquifers	
Lower Cretaceous	Unnamed		Lower Cretaceous Aquifers	
Mesozoic- Precambrian Basement Complex				

2.2.1 Surficial Aquifer

The Surficial Aquifer (S) is at the surface in most of the NCCP (Lautier, 2001). The aquifer is Pleistocene to Holocene in age (Table 1) and consists of fine sand, silt, clay, shell, soil residuum, and peat beds (Giese et al., 1997). In relict beach ridges and alluvium, there are scattered deposits of coarser-grained sediment. Throughout the western and central parts of the NCCP, the thickness of the aquifer ranges from 0-30 feet; however, it thickens eastward and is locally greater than 200 feet thick in the Outer Banks (Giese et al., 1997). The aquifer overlies most of the confined aquifers at some point and it exchanges water with them either directly or through a confining layer. This aquifer is the source of water for the underlying confined aquifers and much of the base flow to steams (Lautier, 2001). Horizontal hydraulic conductivity ranges from 10 to 50 ft/day, and averages 29 ft/day (Winner and Coble, 1996). The transmissivity of the aquifer is probably a few thousand gallons per day per foot (N.C. Department of Water and Air Resources, 1971).

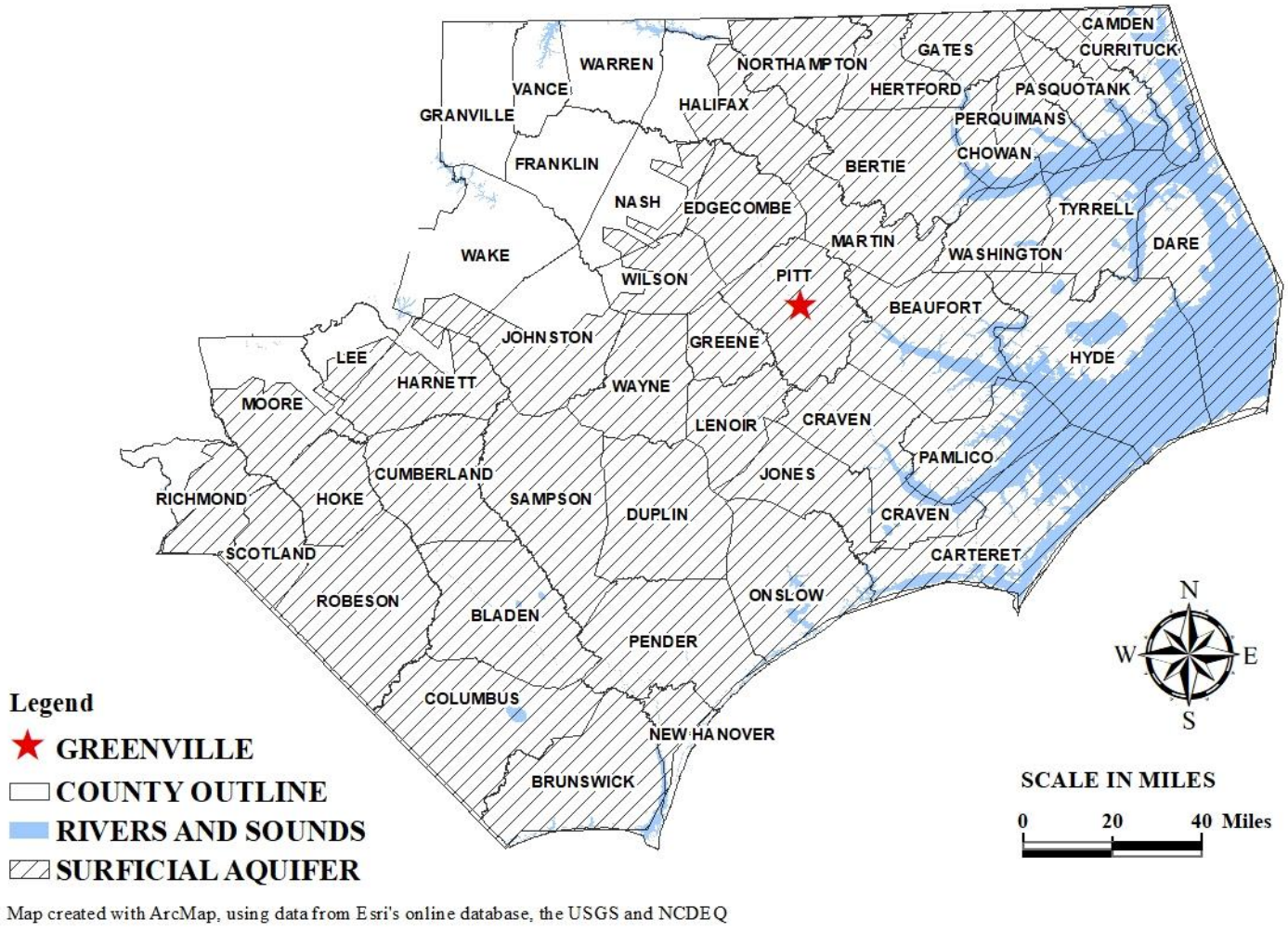

Figure 4. *Areal extent of the Surficial Aquifer.*

2.2.2 Yorktown Unit

The Yorktown Confining Layer (YCL) and the Yorktown Aquifer (Y) are generally composed of the Yorktown Formation (Table 1). Sometimes they contain younger, Quaternary sediments, where the confining bed is higher in the stratigraphic section (Lautier, 2001). The YCL is Pliocene to Pleistocene in age (Table 1). The top of the YCL represents the first extensive clay layer encountered below the land surface. Analysis of available data indicates a significant change in lithologic character and permeability of the YCL clays from west to east. In the west, the fine-grained units are largely silt; they grade eastward into finer grained, denser silty clays. Therefore, the permeability decreases from west to east (N.C. Department of Water and Air Resources, 1971). Thickness ranges from 10 -70 feet, and averages about 25 feet. The YCL also contains sandy clay and local beds of fine sand and shells. The YCL extends as far as the Yorktown Aquifer (Figure 5) although, stratigraphically equivalent beds are found beyond the aquifer's limits (Giese et al., 1997).

The Yorktown Aquifer (Y) (Figure 6) underlies the YCL and is composed of fine sand, silty sand, clayey sand, sand with shells, shell beds, some limestone and coarse sand beds (Table 1). The Yorktown Aquifer is less than 20 feet thick in many areas and has also been eroded away or incised by streams in some locations. The aquifer is thickest in Dare County where it reaches 300 feet (Winner and Coble, 1996). The horizontal hydraulic conductivity of the aquifer ranges from 19 feet to 33 feet/day and averages 22 feet/day (Giese at al., 1997). According to Lautier (2001), water from the aquifer is hard and contains iron above the drinking water-limit, so it is not as extensively used as the deeper aquifers in the area.

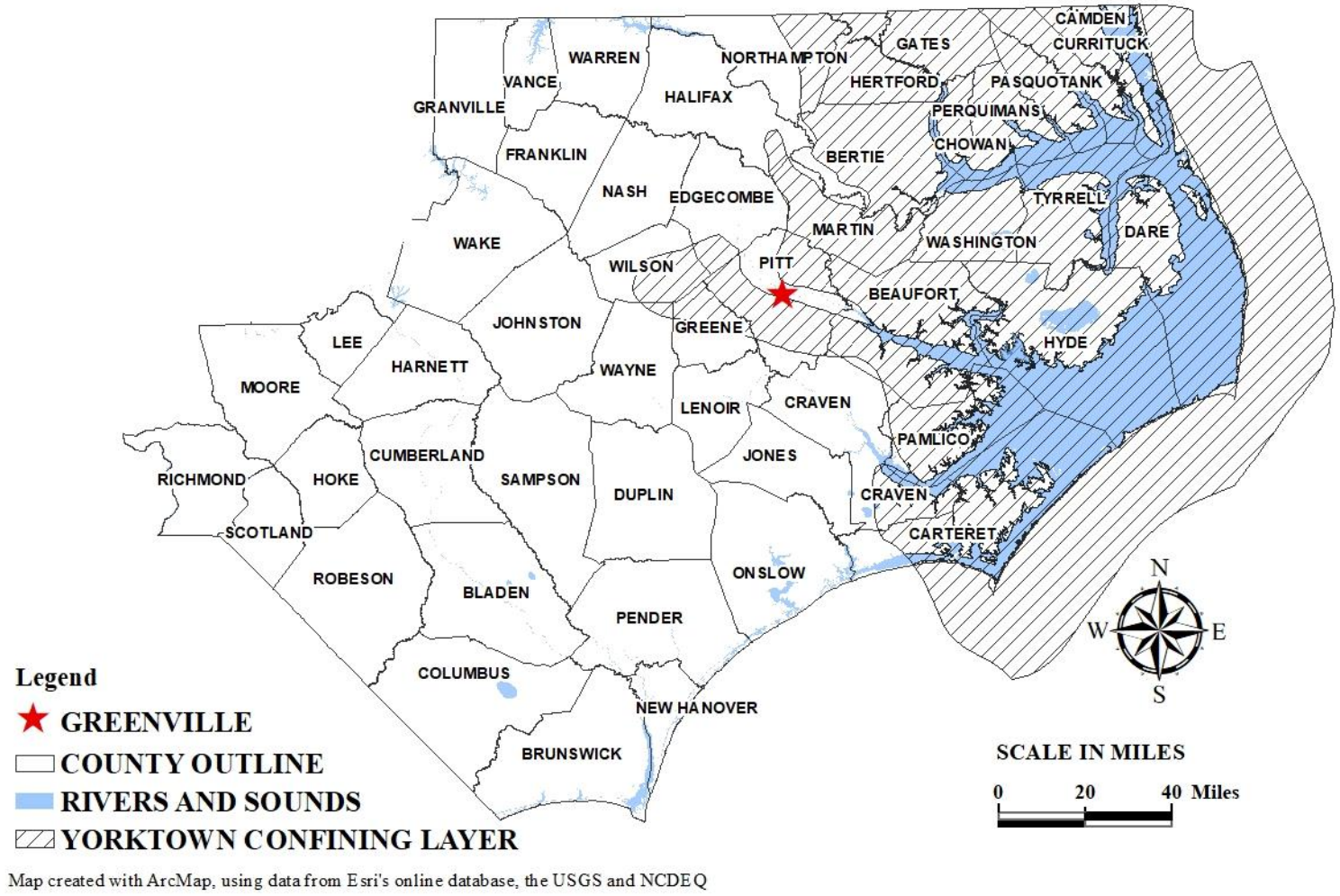

Figure 5. *Areal extent of the Yorktown Confining Layer.*

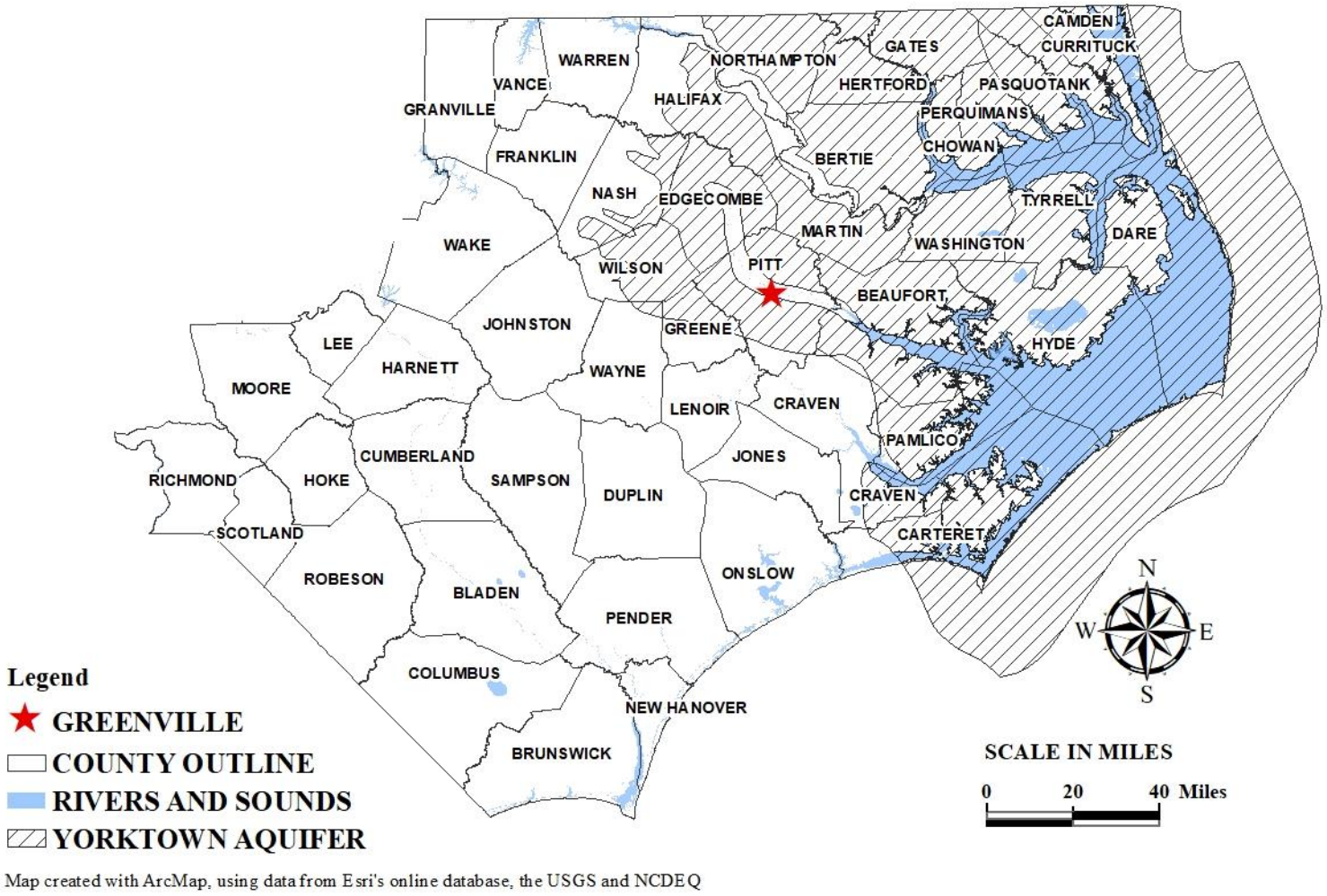

Figure 6. *Areal extent of the Yorktown Aquifer.*

2.2.3 Pungo River Unit

The Pungo River Formation is of Miocene age. It is fine-grained and composed of interbedded phosphatic clays, diatomaceous clays, phosphatic limestones, coquinas, calcareous clays, and phosphatic sands (Groundwater Management Associates, 2013). The Pungo River Aquifer (PR) includes the permeable portions of the Pungo River Formation and is predominantly composed of phosphatic sand (Groundwater Management Associates, 2013). The confining layer and aquifer are limited to the eastern part of the NCCP. The western limit (Figure 7) is a line that extends north from western Carteret County, through the center of Beaufort County to Gates County. The northern limit is a line that extends east from Gates County to Currituck County (Winner and Coble, 1996). The aquifer averages 15 feet in thickness near its western and northern limits; however, it thickens to more than 200 feet at the coast. Winner and Coble (1996) state that under natural conditions, the aquifer is entirely covered by the younger sediments of the Yorktown Unit and Surficial sediments, except in an area near New Bern where the Neuse River is close to incising the aquifer's western margin. The PR is artificially exposed in the mine near Aurora in Beaufort County.

The Pungo River Confining Layer (PRCL) overlies the aquifer and consists of the upper clay beds of the Pungo River Formation as well as the contiguous clays of the lowermost Yorktown Formation. The thickness of the PRCL averages 10 feet near the western margin of the aquifer, and thickens eastward (Winner and Coble, 1996). There is little water level data available for the aquifer, because it is not heavily utilized as a source of water. Therefore, it is difficult to determine the recharge-discharge relationship between the Pungo River Unit and the Yorktown Unit. Winner and Coble (1996) state that the Pungo River Aquifer is recharged through the Yorktown Aquifer in areas beneath the surface-water divides common to both

aquifers and that upward discharge from the aquifer occurs along stream valleys. The aquifer is underlain entirely by the Castle Hayne Unit. The Castle Hayne Confining Layer that separates the Pungo River and Castle Hayne Aquifers averages 10 feet in thickness and is absent in many places (Winner and Coble, 1996).

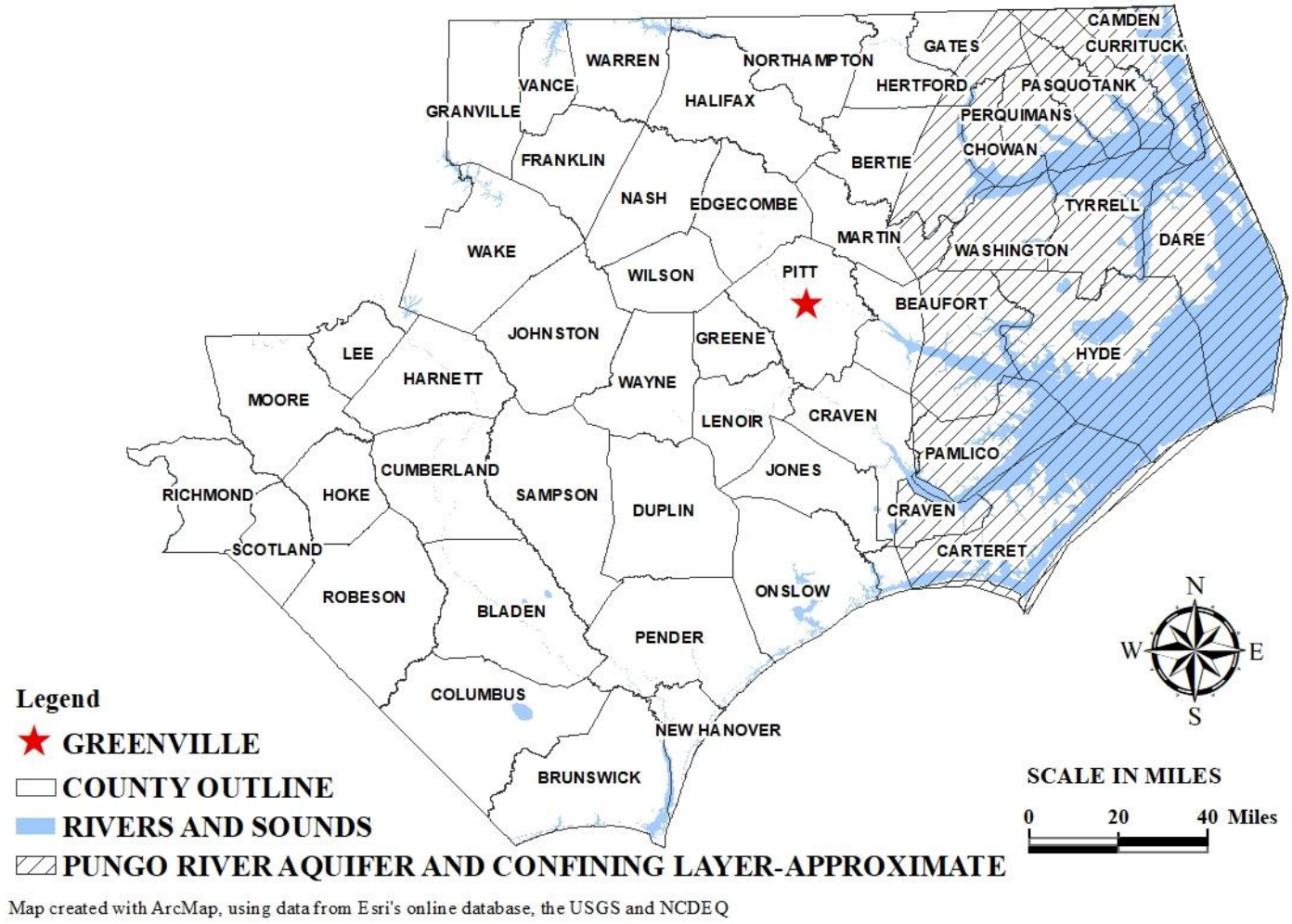

Figure 7. *Areal extents of the Pungo River Aquifer and Confining Layer.*

2.2.4 Castle Hayne Unit

The Castle Hayne Aquifer System (CHAS) includes the Oligocene Belgrade and River Bend, and the Castle Hayne Formations. The Castle Hayne Formation is commonly divided into the Spring Garden, the Comfort, and the New Hanover members. The Spring Garden member includes the Upper Castle Hayne Limestone. The Lower Castle Hayne is composed of the lower units of the Spring Garden, as well as the Comfort member. The New Hanover member is local to New Hanover County, and likely does not occur in the study area. Throughout the southern area of the NCCP, the CHAS is overlain by the Pungo River Unit, the Yorktown Unit, and surficial sediments. It is underlain everywhere by the Beaufort Unit (Giese at al., 1997). The Surficial Aquifer and the UCH have similar responses to seasonal recharge variations, which indicates that the UCH is not well confined (Lautier, 2001).

The Upper Castle Hayne Unit consists of a confining layer and an underlying aquifer. The Upper Castle Hayne Confining Layer (UCHCL) occurs above the Upper Castle Hayne Aquifer (UCH). It averages 10 feet in thickness and exceeds 25 feet in some areas. Figure 8 illustrates the areal extent of the UCHCL. The layer is highly irregular, and the top of the layer represents an unconformity. It is composed of beds of clay, sandy clay, and clay with sandy streaks. It is thinner than most of the other confining units in the NCCP and contains more sand, which makes it relatively more permeable and allows significant vertical leakage between the UCH and its overlying aquifers. The horizontal hydraulic conductivity of the confining layer is estimated to be 9.2×10^{-5} ft/day with a vertical hydraulic conductivity of 3.0×10^{-5} ft/day (Winner and Coble, 1989). The UCH is characterized as marine, calcareous sediments of Eocene age that correspond with the Upper Castle Hayne Limestone. The UCH Limestone contains sand and minor amounts of clay (Giese et al., 1997). The limestone may occur as shelly

limestone, dolomitic limestone and sandy limestone to calcareous sandstone, ranging from loosely consolidated to hard and recrystallized (Table 1). Along the western margin of the NCCP, the UCH occurs near the land surface. Figure 9 illustrates the areal extent of the UCH. Eastward, it thickens to 950 feet in Carteret County and to nearly 1,200 feet beneath Cape Hatteras. In Beaufort County, the UCH ranges in thickness from 90 to 250 feet. Near Albemarle Sound, limestone beds are thin and there are more clays in the sediments. The UCH is the most productive aquifer in North Carolina due to its thickness and high permeability (Table 1). Where it is composed of fine sand the horizontal hydraulic conductivity ranges from 15 ft/day to about 200 ft/day. Where the majority of the aquifer is composed of porous limestone, the horizontal hydraulic conductivity averages 65 ft/day, with some areas of 200 ft/day (Winner and Coble, 1996; and Groundwater Management Associates, 2013). In the study area, the top of the CHAS varies from approximately 40 to 80 feet BSL, with depths and thicknesses increasing to the east.

The Lower Castle Hayne is considered as a separate unit (N.C. Department of Air and Water Resources, 1971 and Gamus, 1972). The LCH unit consists of a thin confining layer and an underlying aquifer, and is composed of alternating layers of quartz sand, moldic limestone with minor amounts of phosphate and trace glauconite grains, and with spar-cement (N.C. Department of Water and Air Resources, 1971). The Lower Castle Hayne Confining Layer (LCHCL) and the Lower Castle Hayne Aquifer (LCH) contain higher sand and clay contents than the UCHCL and the UCH. Therefore, they have lower hydraulic conductivities (Table 1). The areal extent of the LCH is assumed to extend as far as the UCH, however, extent of the LCHCL is less certain. In this study the LCHCL was assumed to cover the same area as the LCH aquifer. The LCH ranges in thickness from 50 to 70 feet thick in Beaufort County.

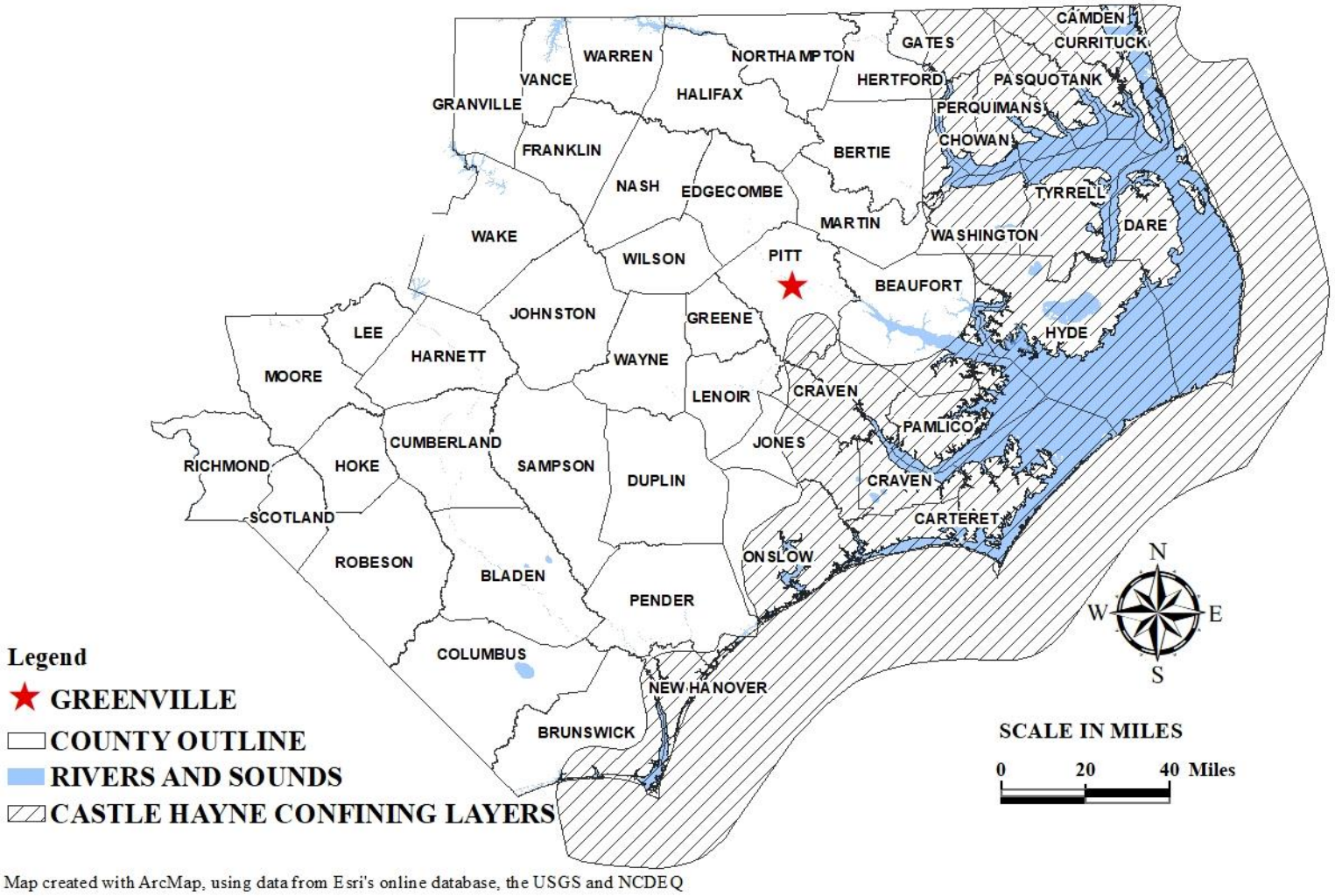

Figure 8. *Areal extents of the Upper and Lower Castle Hayne Confining Layers.*

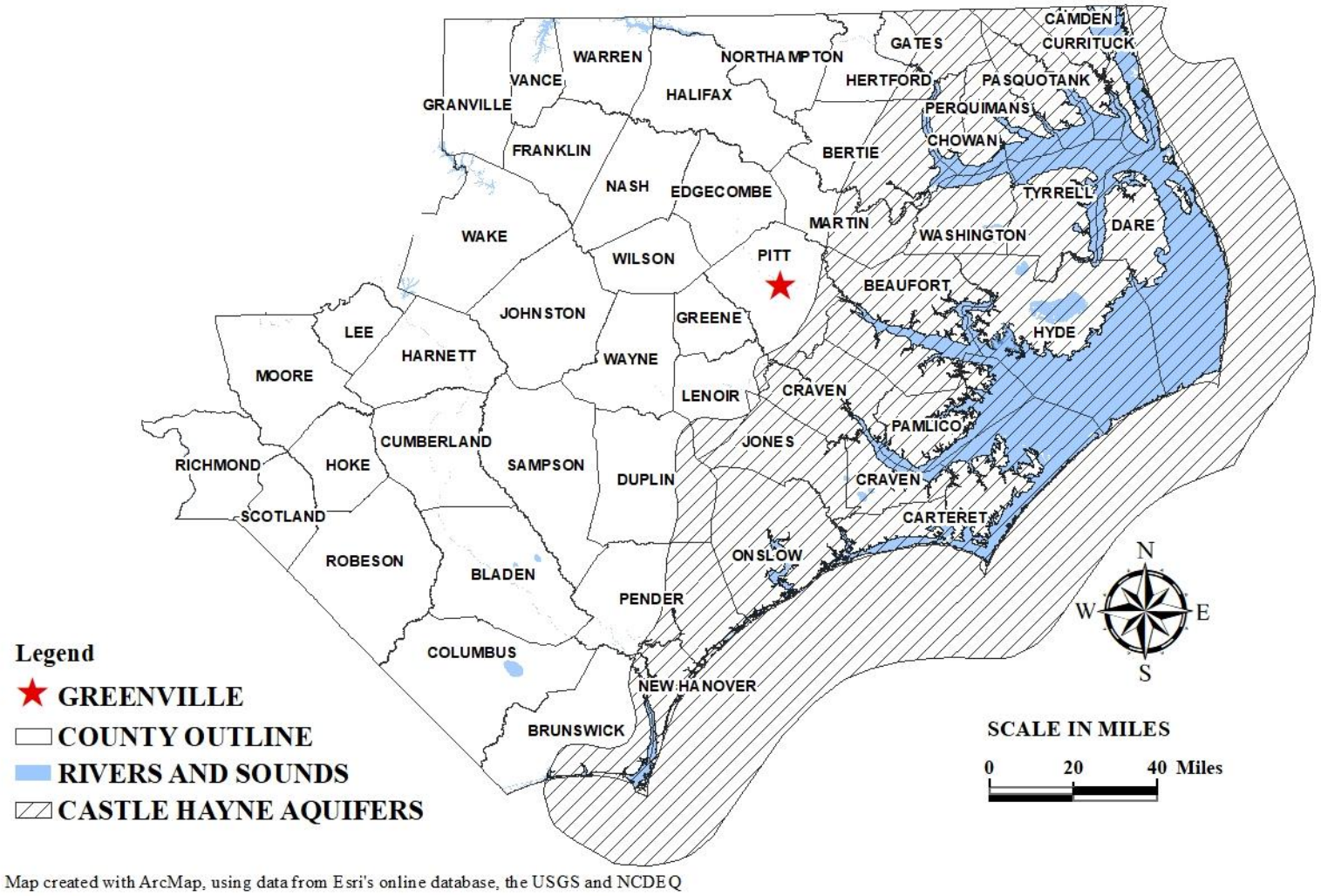

Figure 9. *Areal extent of the Upper and Lower Castle Hayne Aquifers.*

2.2.5 Beaufort Unit

In the study area, the Beaufort Unit (BF) does not include a recognizable confining layer; thus, for this study the Beaufort Confining Layer (BFCL) and the Beaufort Aquifer (BF) are undivided and grouped as one. The bulk of the BF is composed of the Paleocene Beaufort Formation (Table 1). As with the other hydrogeological units, the definition of this aquifer is not restricted to a single geologic formation and so, the BF may include strata that are older than the Beaufort Formation. The BF consists of fine to medium glauconitic sands, clayey sands and clay beds of marine origins. Shell and limestone beds are present but are less than 6 feet thick (N.C. Department of Water and Air Resources, 1971). The aquifer ranges in thickness from less than 10 feet along its western limit to more than 150 feet in the northern part of its eastern limit. In Camden and Currituck Counties it thins toward the east and northeast. The average horizontal hydraulic conductivity is estimated to be about 35 feet/day. However; lower-than-average values occur in the northern and easternmost parts of the aquifer where the sand is finer, and the aquifer contains more clay (Giese et al., 1997). The aquifer is covered entirely by younger rocks and about 90% of the aquifer and the upper confining layer are overlain by the CHAS, the Surficial and the Yorktown Unit overlie the remaining 10%, and the Peedee Unit underlies approximately 80% of the aquifer (Winner and Coble, 1996). The areal extent of the BF Unit is illustrated in Figure 10.

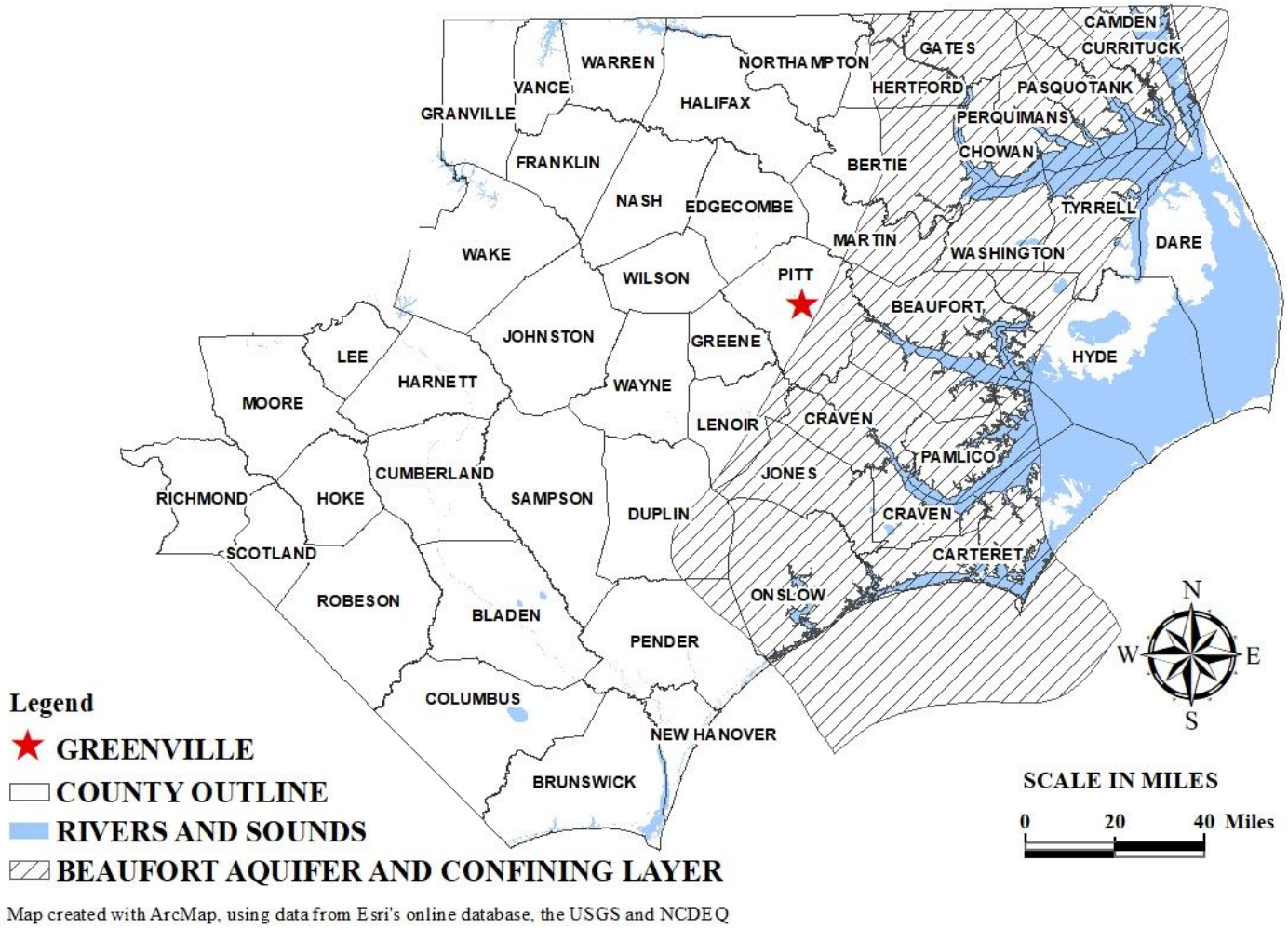

Figure 10. *Areal extents of the Beaufort Aquifer and Confining Layer.*

2.2.6 Cretaceous Aquifer System

Underlying the BF are the units of the Cretaceous Aquifer System (CAS) including the Late Cretaceous-age Peedee, the Black Creek, the Upper Cape Fear, and the Lower Cape Fear units. The Peedee includes a confining layer and an aquifer between the CHAS and the deeper aquifers, and the Peedee is composed of silts and clays interbedded with medium-grained sand (Reynolds and Spruill, 1995). The Black Creek is composed of tan to gray sands interbedded with thinly-laminated, gray to black clay. The Upper and Lower Cape Fear consist of alternating beds of sand and clay (Table 1). Underlying the Lower Cape Fear is the Lower Cretaceous unit, which is composed of limestone, shale, sand and gravel (Reynolds and Spruill, 1995). The CAS aquifers are extensively developed in the central part of the NCCP. However, in Beaufort County, the CAS aquifers are fully-confined and contain elevated salinity, and thus, were not addressed in the model evaluation of this study.

2.3 Hydrogeologic Conditions

2.3.1 Recharge and Leakage

The Surficial Aquifer receives direct recharge from precipitation and infiltration. It is the source of water for the deeper confined aquifers. The amount of recharge from precipitation averages about 12 inches/year and is dependent upon several factors, including: the annual amount of precipitation, slope of the land and the hydraulic conductivities of the soil. The estimated average, horizontal, hydraulic conductivity of the Surficial Aquifer is about 30 feet/day (Giese et al., 1997).

Most recharge to the confined aquifers occurs in the western portions of the NCCP where confining beds are relatively thin or do not exist. Most recharge occurs in freshwater wetlands.

However, some studies have shown that there is also vertical leakage from overlying aquifers entering into the CHAS. For, example; a study conducted by Consolvo (1998) concluded that the UCH is recharged through an overlying semi-pervious layer with a vertical hydraulic conductivity of 3.6 $x10^{-3}$ feet/day. Recharge that occurs due to leakage from overlying and underlying units ultimately depends on the vertical hydraulic conductivity of the confining layers and the head differences between aquifers (Giese et al., 1997). DeWiest (1969) estimated the area of direct recharge to the UCH is about 290 square miles with a rate of 20 mgd in areas north of the Pamlico River and about 45 mgd in areas south of the Pamlico River.

The UCH is hydraulically connected to the overlying and underlying units of the NCCP aquifer system. Water moves downward into the UCH in areas where the head of the overlying units is higher than the UCH. In areas where the UCH head is higher than the overlying units, water will move upward. In areas where the head of the UHC is lower than the underlying units, water will move upward into the UCH. The magnitudes of these vertical movements (leakage) are dependent upon the vertical hydraulic conductivity, the thickness of materials through which flow takes place, and the head differences between the units (Sherwani, 1980).

2.3.2 Discharge from Aquifers

According to DeWiest (1969), water from the CHAS discharges naturally into streams, estuaries and the sea. However, heavy groundwater withdrawals will alter the natural flow direction of groundwater, both horizontally and vertically. Changes in flow direction increase potential contamination by surface pollutants and from other aquifers of lower water quality.

2.3.3 Hydrologic Relationship of the CHAS and the Pamlico River and Estuary

A previous study by Johnson, 2007 showed that in western Beaufort County, near Tranter's Creek, river incision through the uppermost confining layers provides a direct connection to the deeper aquifers. Previous studies also indicate that large groundwater withdrawals have resulted in a reversal of hydraulic gradients in areas along the Pamlico River and Estuary (Lyke and Treece, 1988; DeWeist, 1969). Prior to anthropogenic withdrawals, groundwater from the UCH moved upward toward the Pamlico River and Estuary. Under current conditions of groundwater withdrawals, the Pamlico River and Estuary is a losing stream, and is a recharge source to the UCH. Lyke and Treece (1988) also reported that changes in flow direction have taken place along the Neuse River and at the U.S. Marine Corps Air Station at Cherry Point. Groundwater withdrawals have caused water from the river and estuary to move downward into the CHAS (DeWiest, 1969).

2.4 Chemical and Isotopic Composition of Castle Hayne Groundwater

Bicarbonate is the dominant anion in UCH water. HCO_3^- and Ca^{2+} ions in the western portions of the study area come from the dissolution of limestone which is enhanced by dissolved CO_2 in the recharge water. Carbonate buffering maintains the pH of UCH water between 6.9 and 8.1, where HCO_3^- is the dominant carbonate species. Alkalinity tends to increase in the UCH from west to east and is comparable to other waters with compositions dominated by calcium carbonate dissolution (Sprinkle, 1989). Chloride is the dominant anion of the LCH but also dominates the anion concentrations of the UCH in the easternmost portions of the region. In both the UCH and LCH, chloride concentrations increase from west to east,

(Sutton, 1994). In the UCH and LCH, total dissolved solids (TDS) generally increase from west to east but the highest concentrations are in the northeast. According to Sutton (1994), eastward increases of TDS are due to increased mixing with saline water.

The UCH contains fresh, high-quality water, but the LCH is relatively brackish (Sherwani, 1980). Sutton and Woods (1995) determined the following:

- Groundwater from the LCH is alkali-rich and Cl-rich.
- TDS, chloride, and sulfate concentrations increase from west to east in the LCH, and these concentrations are generally greater than those in the UCH.
- LCH wells tend to have higher sodium, potassium, calcium and magnesium concentrations than UCH wells at the same location.
- Potassium and sodium increase from west to east throughout the study area.
- Iron concentrations in the UCH and LCH have been observed to decrease from west to east in the study area.
- There is a discernable relationship of pH between the UCH and LCH aquifers at the same well site.
- UCH has higher Eh values, which means UCH water is more oxidizing than LCH water.

Chemical analyses from previous studies are provided in Appendix A.

2.5 Strontium Mixing-Line Equations

Woods et al. (2000[a]) concluded that strontium-isotopic composition is useful in tracing groundwater movements. There is no fractionation of strontium isotopes during the formation of strontium-bearing marine precipitates; therefore, paleo-seawaters and coeval rocks from marine

formations have the same $^{87}Sr/^{86}Sr$ ratios (Veizer, 1989). $^{87}Sr/^{86}Sr$ ratios of Eocene seas were constant and varied only by about 0.0001, which makes the UCH an excellent candidate for strontium-isotopic studies. Because strontium-isotopic ratios remained constant throughout UCH deposition, this aquifer can be treated as a large reservoir of strontium with an isotopic ratio of about 0.70775 (Woods et al., 2000[a]).

Woods et al. (2000[a]) developed a two-component, mixing line to predict the change in the strontium-isotopic signature of UCH groundwater as it acquires strontium from aquifer materials along a flowpath. The mixing model uses Sr-isotopic ratios ($^{87}Sr/^{86}Sr$) and [Sr^{2+}] concentrations of groundwater, modern sea water, and local river waters (Sutton and Woods, 1995; Beck, 1997; Sirtariotis, 1998; Brown, 1999; and Fullagar, 2003). Values for rocks and fossils in Coastal Plain formations are from Denison et al. (1993). The data used to create the mixing line included samples collected throughout the NCCP, however for this study, only the samples that lie within the study area were included (Table 2).

Table 2. *Strontium Composition of Local Waters* *Data sources:* Woods et al., 2000[b]; personal comm. - P.D. Fullagar 1993			
Sample ID	**[Sr] ppm**	$^{87}Sr/^{86}Sr$	**Date**
Modern Seawater	7.6	0.709180	
RIVERS			
Pamlico	0.051	0.7095	1993
SURFICIAL			
O28K6	0.189	0.711332	3/14/01
P22U9	0.048	0.709677	3/16/01
YORKTOWN			
L13I2	0.7080	0.709200	1/30/97
Hyde Plant	0.4270	0.709111	11/8/95
PUNGO RIVER			
Plant	0.320	0.709051	8/31/95
UPPER CASTLE HAYNE			
P21K6	0.301	0.708810	5/17/93
MAS30	0.178	0.707991	9/12/02
TGS15	0.632	0.709263	5/9/97
WWWF2	0.300	0.709096	5/26/93
O17i2	0.958	0.708699	5/17/93
O13F1	0.824	0.708308	5/10/93
TGS11	0.717	0.708555	6/21/93
Q15U3	1.118	0.708158	5/18/93
TGS757	0.679	0.708688	NA
TGS772	0.700	0.708722	NA
P16O4	0.900	0.708547	5/27/93
LOWER CASTLE HAYNE			
Q15U5	2.643	0.708036	5/27/93
BEAUFORT			
TGS11A	2.654	0.708217	6/21/93

NA= Not Available

The equations that follow describe the expected variation of $^{87}Sr/^{86}Sr$ ratios in a two-component mixture where the Surficial Aquifer represents end-member A, and UCH limestone is

end-member B; the mixing line (Figure 11) was calculated using binary mixing equations from (Faure, 1998). Figure 12 illustrates spatial variations in the (a) $^{87}Sr/^{86}Sr$ and the (b) strontium concentration (ppm) of groundwater from the Upper Castle Hayne Aquifer. The slope and the y-intercept are used to calculate the mixing line. The Sr-concentration and $^{87}Sr/^{86}Sr$ ratios of the mixtures (m) are a function of various combinations of Sr from UCH Limestone with Sr from the original recharge water. The strontium mixing line equation is from Faure (1998).

$$(^{87}Sr/^{86}Sr)_m = [A/[Sr]_m] + B$$

Where: the slope and Y-intercept are represented, respectively, by:

$$A = \frac{\{[Sr]_A[Sr]_B[(^{87}Sr/^{86}Sr)_B - (^{87}Sr/^{86}Sr)_A\}}{[Sr]_A - [Sr]_B}$$

$$B = \frac{\{[Sr]A(^{87}Sr/^{86}Sr)_A - [Sr]B(^{87}Sr/^{86}Sr)_B\}}{[Sr]_A - [Sr]_B}$$

and $[Sr]_A$ and $[Sr]_B$ represent the concentrations (ppm) of strontium in the end-members.

The Surficial Aquifer's end-member A is the sample with the highest $^{87}Sr/^{86}Sr$ ratio (sample 028K6)

$[Sr]$ = 0.189ppm

$^{87}Sr/^{86}Sr$ = 0.711332

Characteristics of end-member B were calculated by averaging values for the UCH limestone rocks from Denison et al., 1993:

$[Sr]$ = 470ppm

$^{87}Sr/^{86}Sr$ = 0.707747

Slope and Y-Intercept

Slope = 0.000677

Y-Intercept (B) = 0.7077456

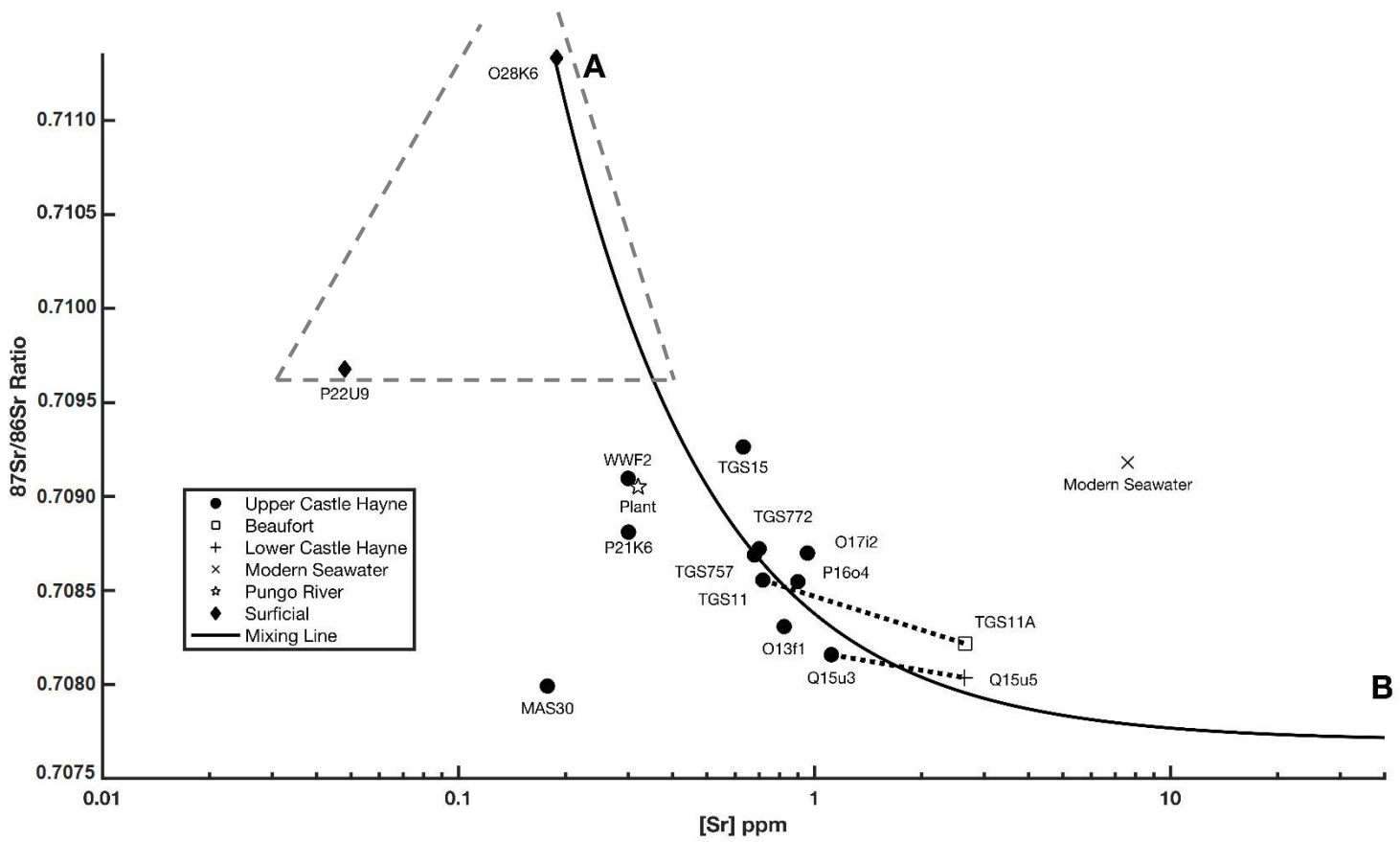

Figure 11. *Strontium mixing line and groundwater samples from wells within the study area. Dotted lines connect UCH wells to LCH or BF well at the same location, and the area inside the dashed field represents the field containing likely strontium compositions of recharge waters to the UCH. Modified from Woods et al. (2000[a]).*

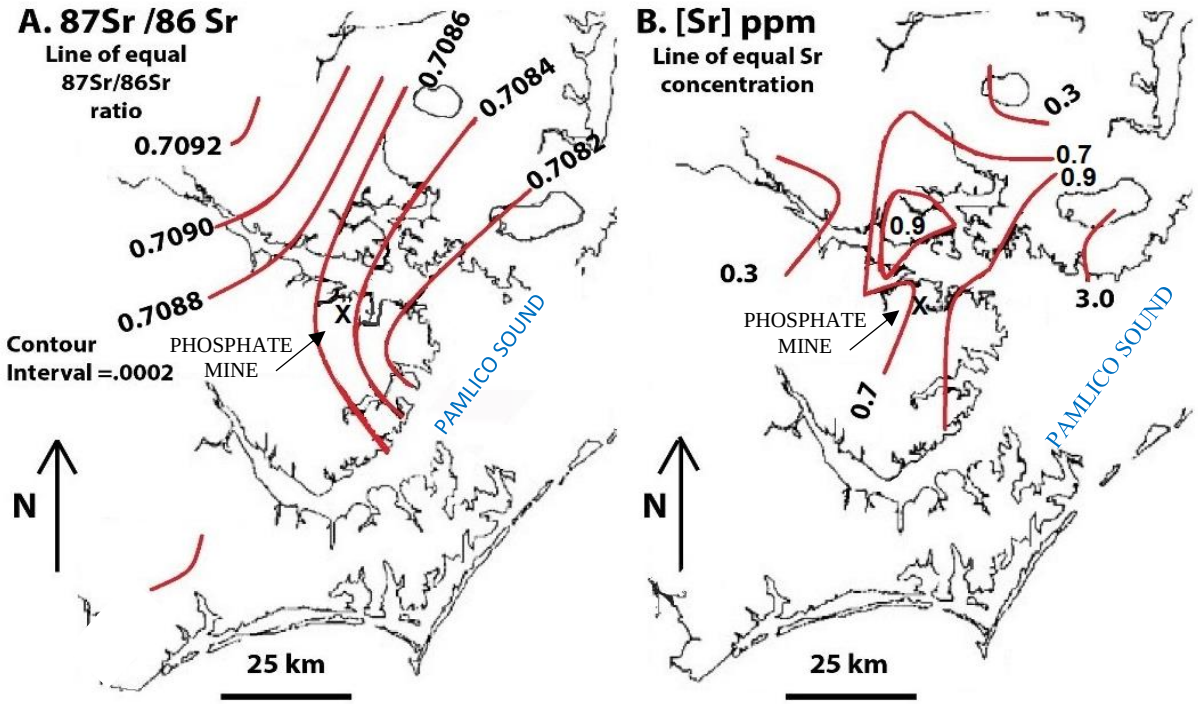

Figure 12. *Spatial variations in the $^{87}Sr/^{86}Sr$ ratios (A) and (B) strontium concentration (ppm) of Upper Castle Hayne groundwater, modified from Woods et al. (2000[a]).*

2.6 Potential Sources of Strontium to the Castle Hayne Aquifer

Woods et al. (2000[a]) used strontium-isotopic analysis to identify potential sources of water leaking into the UCH and described the following as possible sources:

- Downward movement of brackish water from the Pamlico River Estuary entering the UCH, which has the potential to increase the $^{87}Sr/^{86}Sr$ above the mixing line, and either raise or lower the Sr content, depending on the proportion of modern seawater included.
- Upconing of brackish water from the aquifers below the UCH. These waters are characterized by lower $^{87}Sr/^{86}Sr$ ratios and higher Sr than water from the UCH. Upward groundwater movement from these aquifers has the potential to lower the $^{87}Sr/^{86}Sr$ ratio and increase Sr content of UCH water.
- Westward migration of the freshwater-saltwater interface. Westward migrating saline water in the UCH will have variable $^{87}Sr/^{86}Sr$ ratio. The major element chemistry of saline water that mixes with freshwater in the aquifer should be similar to modern seawater because of the numerous, multiple, sea-level cycles that have occurred in the NC coastal plain during the Quaternary age. However, after modern or recent sea water (7.6 ppm Sr; 0.70918 $^{87}Sr/^{86}Sr$) has reacted with aquifer materials for thousands of years, it may incorporate more strontium by aquifer dissolution and have a lower $^{87}Sr/^{86}Sr$ ratio. To date, an insufficient number of UCH groundwater samples from the eastern part of the study area have been analyzed to characterize the Sr chemistry of sea water in the coastal portion of the aquifer.

3.0 METHODS

3.1 Data Compilation

Data compiled in this study were from published and unpublished sources, on-line databases provided by the North Carolina Department of Environmental Quality (NCDEQ) and the USGS. A reference list of sources is provided in section 7.0. **S**amples used in this study were analyzed for chemical constituents including major and minor elements, pH, alkalinity, stable isotopes, temperature, etc. (Appendix A). The data were used to construct a Visual MODFLOW model and, a Piper Diagram, and to perform statistical analysis using Principal Component Analysis (PCA).

The data review included:

A. Well construction records

B. Water-level measurement records

C. Chemical analyses

D. Chloride maps

E. Topographic maps

F. Geologic and hydrogeologic maps

G. Geologic and hydrogeologic cross-sections

H. Input parameters and results from previous models of the area

I. Data and interpretations presented in published and unpublished reports

3.2 Piper Diagram

Piper trilinear diagrams are commonly used to identify hydrochemical patterns and involve concentrations of Ca^{2+}, Mg^{2+}, and $Na^{+}+K^{+}$ plotted on the lower left-hand triangle and concentrations of Cl^{-}, HCO_3^{-}, and SO_4^{2-} plotted on the lower right-hand triangle as percentages of the total milliequivalents per liter of cations and anions (Piper, 1944). Compositions on the two triangles are projected along straight lines toward the central diamond-shaped field, and a single point is plotted at the intersection of these lines. The positions of these points in the diamond-shaped area are used to classify the hydrochemical facies of the water. Piper diagrams are useful for determining sources that contribute ions to the groundwater samples.

The USGS open-source "GW_Chart" version 1.29.0 (Winston, 2018), was used to construct the Piper Diagram and can be found at the following website (https://www.usgs.gov/software/gwchart-a-program-creating-specialized-graphs-used-nn-groundwater-studies).

3.3 Principal Component Analysis

Principal Component Analysis (PCA) of water chemistry, including isotopic data, provides a useful tool for classifying the sources of groundwater and identifying the significant factors governing groundwater quality (Bakari, 2011). PCA summarizes associations between chemical variables to suggest underlying hydrogeochemical processes. The first step is to create the correlation matrix from the input data set. Creating the correlation matrix is equivalent to standardizing the data, to yield a mean of zero and a standard deviation of one. This allows the input data to have units that differ, and values that may range over several orders of magnitude. Creating the correlation matrix from non-standardized data is a default option available in

SigmaPlot, so the input data are not required to have the same units and variables can cover a wide range of values without the solution being biased toward the sample with the largest variance (σ^2).

$$\sigma^2 = \overline{(\text{elemental concentration} - \text{average concentration})^2}$$

To calculate variance, the mean is subtracted from the observed value, the result is squared, and then the average of the squared differences is calculated. The PCA dataset included 18 variables, thereby providing a simultaneous analysis of the entire data set.

3.4 Groundwater Flow Simulation

Following the suggested protocol by Anderson and Woessner (2002), a conceptual model of the groundwater system in the study area was developed (Figure 13). Then groundwater flow modeling software, Visual MODFLOW (Version 4.0), was used to construct, and the model. Visual MODFLOW utilizes the three-dimensional, modular, finite-difference, groundwater flow code MODFLOW to simulate flow in steady-state or transient calibration (McDonald and Harbaugh, 1988). The model was calibrated manually and with Parameter Estimation (PEST), using average heads from 2017 to represent static water levels of the aquifers. Calibration of the model was completed using groundwater withdrawal data and observed potentiometric heads of the UCH by visual comparison. After calibration of the model, a post-processing, particle-tracking program (MODPATH) was applied to produce groundwater flow pathlines. The computer-simulated flowpaths were compared to the results produced by the strontium-geochemical mixing-model in Woods et al. (2000[a]). The steps of the modeling process were adopted from Anderson and Woessner (2002), and are as follows:

1. Identify vertical groundwater movement in and out of the UCH

2. Develop conceptual model to represent the groundwater flow system
3. Construct the model
4. Calibrate the model using static heads from the aquifers
5. Conduct sensitivity analysis
6. Model groundwater flowpaths using MODPATH to identify vertical groundwater flow in the system

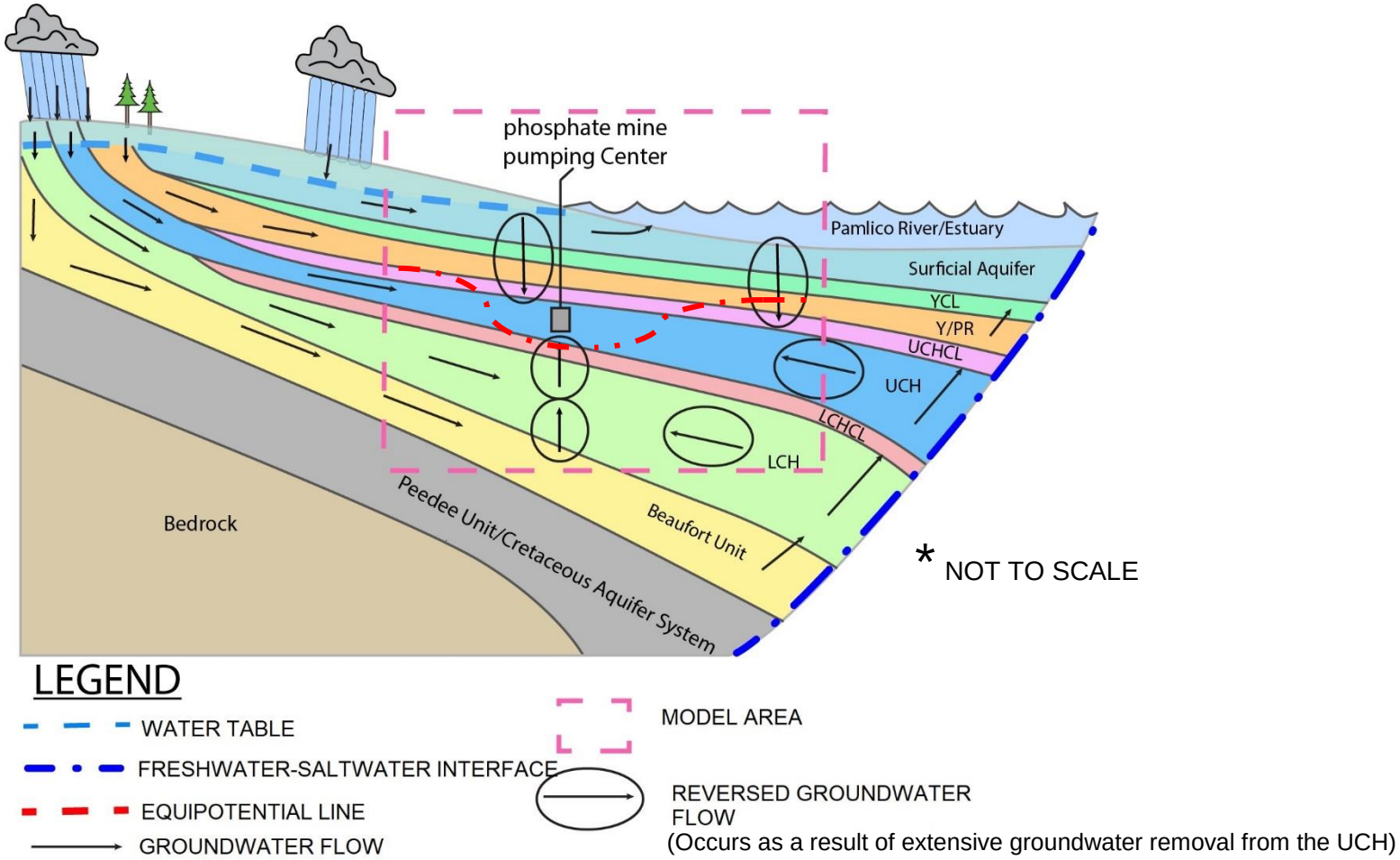

Figure 13. *Conceptual model of the groundwater flow system.*

3.4.1 Groundwater Modeling Objective

The Visual MODFLOW model was created to back-track particles from their sample location in the UCH to where they originated, to identify vertical groundwater movements between the UCH and its overlying and underlying units. The simulated groundwater flowpaths were compared to the flow patterns predicted by the strontium-isotopic geochemical model. A goal of this study was to elucidate the geological and hydrogeological processes that affect the groundwater chemistry of the UCH. The hypothesis of this study is that the MODPATH results should support the vertical groundwater movement in and out of the UCH as predicted by the changes in strontium isotopic signatures. The modeling portion of this study was conducted in three stages:

1. A conceptual model of the groundwater flow system was developed (Figure 13). The hydrogeologic framework, hydrostratigraphy, and aquifer properties were compiled from previous studies and available publications. Land elevation and water-level data were obtained through e-mail correspondence with Nutrien Phosphate Aurora and on-line databases (NCDEQ and USGS).
2. Visual MODFLOW was used to create a groundwater-flow model by integrating the compiled data into a three-dimensional model. Simulated water levels were compared with observed levels measured during a portion of 2017. Model parameters, such as hydraulic conductivity were varied in order to decrease errors between observed and simulated water levels. When the model produced simulated water levels that matched observed water levels within an acceptable range of error, the model was considered to be manually calibrated. A parameter estimation process

(PEST) was subsequently performed to increase agreement of the model with the observed water-levels and to decrease errors.

3. MODPATH was performed on the calibrated steady-state model which produced groundwater Pathlines, and these results were compared to the predictions of groundwater flow that were inferred by the strontium geochemical model.

3.5 Governing Equations

There are several integrated pre- and post-processing packages otherwise known as GUI's for MODFLOW that assist in data input and visualization of modeling results. Visual MODFLOW, created by Waterloo Hydrogeologic, is one of these packages and was used in this project. Visual MODFLOW uses a numeric solution for the equation governing groundwater flow through porous media. The numeric solution is as follows:

$$\frac{\partial}{\partial X}\left(K_{xx}\frac{\partial h}{\partial x}\right)+\frac{\partial}{\partial y}\left(K_{yy}\frac{\partial h}{\partial y}\right)+\frac{\partial}{\partial z}\left(K_{zz}\frac{\partial h}{\partial z}\right)\text{-W}=S_s\frac{\partial h}{\partial t}$$

where:

K_{xx}, K_{yy} and K_{zz}, are values of hydraulic conductivity along the x, y and z coordinate axes, respectively (assumed to be parallel to the major axes of hydraulic conductivity); (h) is hydraulic head; W is the volumetric flux per unit volume and represents sources or sinks of water; S_s is the specific storage of the porous material, and t is time. This equation describes groundwater flow in a heterogeneous and anisotropic medium, provided the principal axes of hydraulic conductivity are aligned with the coordinate directions (Kresic, 2007).

3.6 Model Domain

The MODFLOW program develops a numerical representation of a hydrogeological environment at a specific site. The model domain was divided into rows, columns and layers (dimension) to create the model cells (grid). The cells are assigned different property values and boundary values. Visual MODFLOW uses the assigned values to formulate finite-difference equations which produce the head values at the center of each cell (Bogdon, 2012). This model consists of nine layers that represent the Post-Cretaceous aquifers and their associated confining layers in the study area (Table 3). For modeling purposes, the Pungo River Unit is accounted for in the layer above the UCH (layer 3), and the Beaufort Unit was not divided into a confining layer, but instead, was considered a single unit (layer 8). The model represents an area that is 42 by 30 miles or approximately 1,260 mi^2. Beaufort County was chosen for the study area based on the available strontium data and for modeling purposes (Figure 14).

Table 3. Model Layers

Model Layer	Aquifer/ Confining Layer	Abbreviation
Layer 1	Surficial Aquifer	S
Layer 2	Yorktown Confining Layer	YCL
Layer 3	Yorktown Aquifer/Pungo River Aquifer and Confining Layer	Y/PR
Layer 4	Upper Castle Hayne Confining Layer	UCHCL
Layer 5	Upper Castle Hayne Aquifer	UCH
Layer 6	Lower Castle Hayne Confining Layer	LCHCL
Layer 7	Lower Castle Hayne Aquifer	LCH
Layer 8	Beaufort Confining Layer/Aquifer	BFCL/BF
Layer 9	Peedee Confining Layer	PDCL

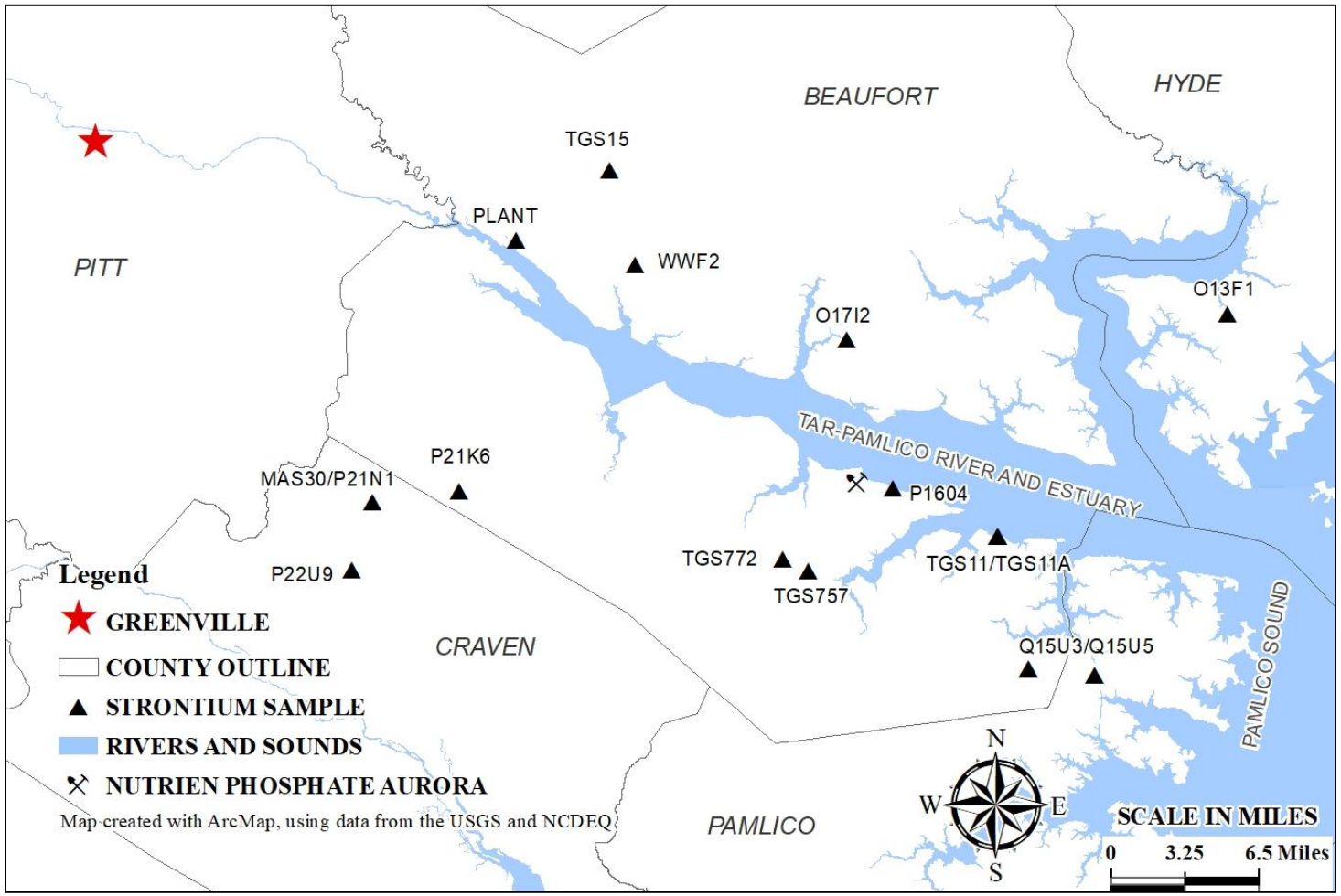

Figure 14. *Location of strontium samples.*

3.7 Finite-Difference Grid Selection

Defining the grid is the starting point in model design; the grid is formed by two sets of orthogonal parallel lines. The resulting blocks are the cells and in the center of each cell is a node; the node is the point at which hydraulic head is calculated. Cell properties are represented by the values of the node because it is assumed that the hydraulic and hydrogeologic properties are uniform across the entirety of the cell (Kresic, 2007).

The model area includes Beaufort County and parts of Pitt, Craven, and Hyde Counties (Figure 15). A grid of 100 x 100 cells was used for this study because the entire model area of interest is equally important and the available UCH aquifer data are evenly distributed across the model area. The model grid was rotated 23 degrees west for the model axes to align with the principal direction of groundwater flow to the east-southeast. Figure 16 depicts the nine layers of the model grid in cross-sectional view.

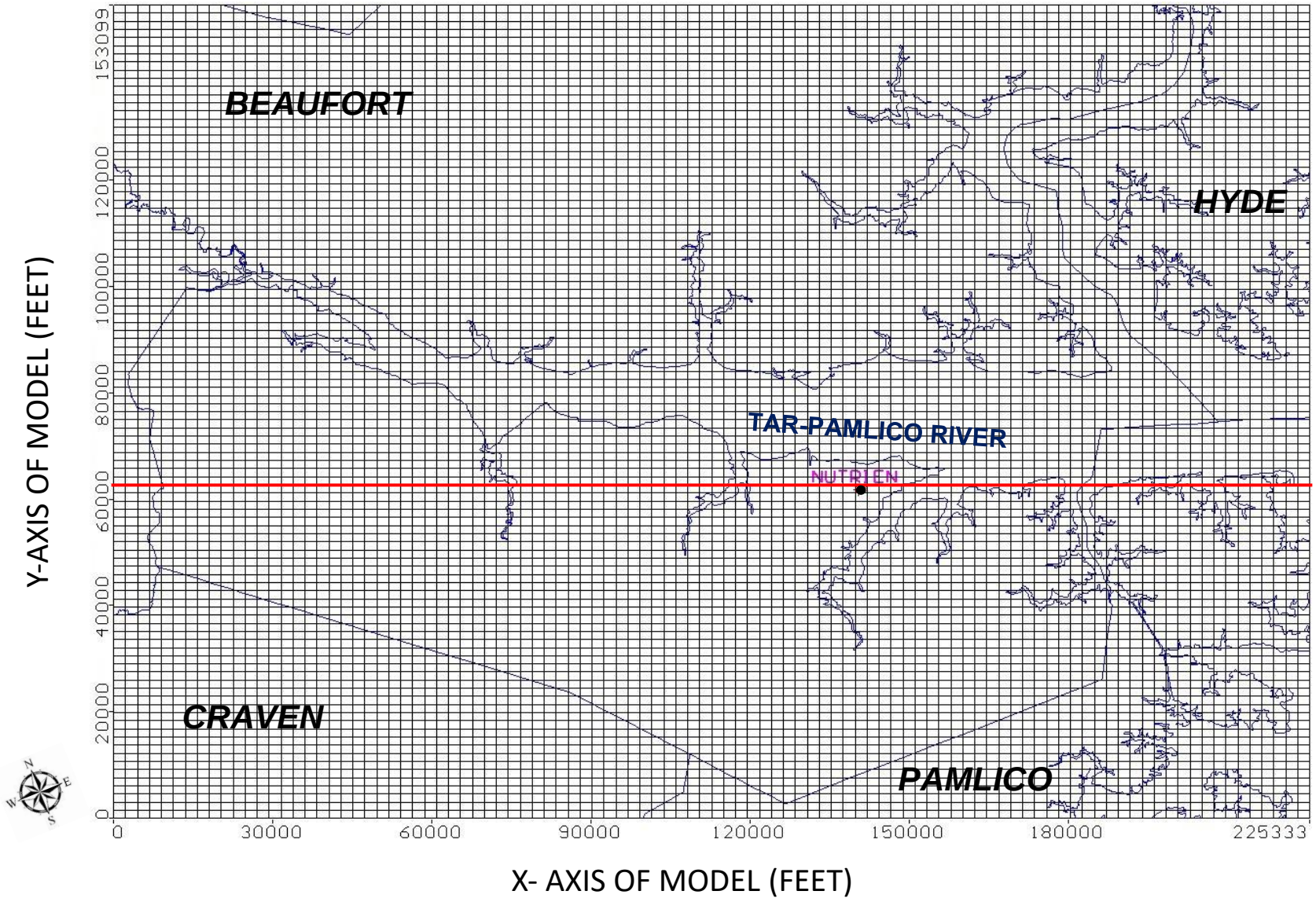

Figure 15. *Model grid. Row 60 highlighted in red.*

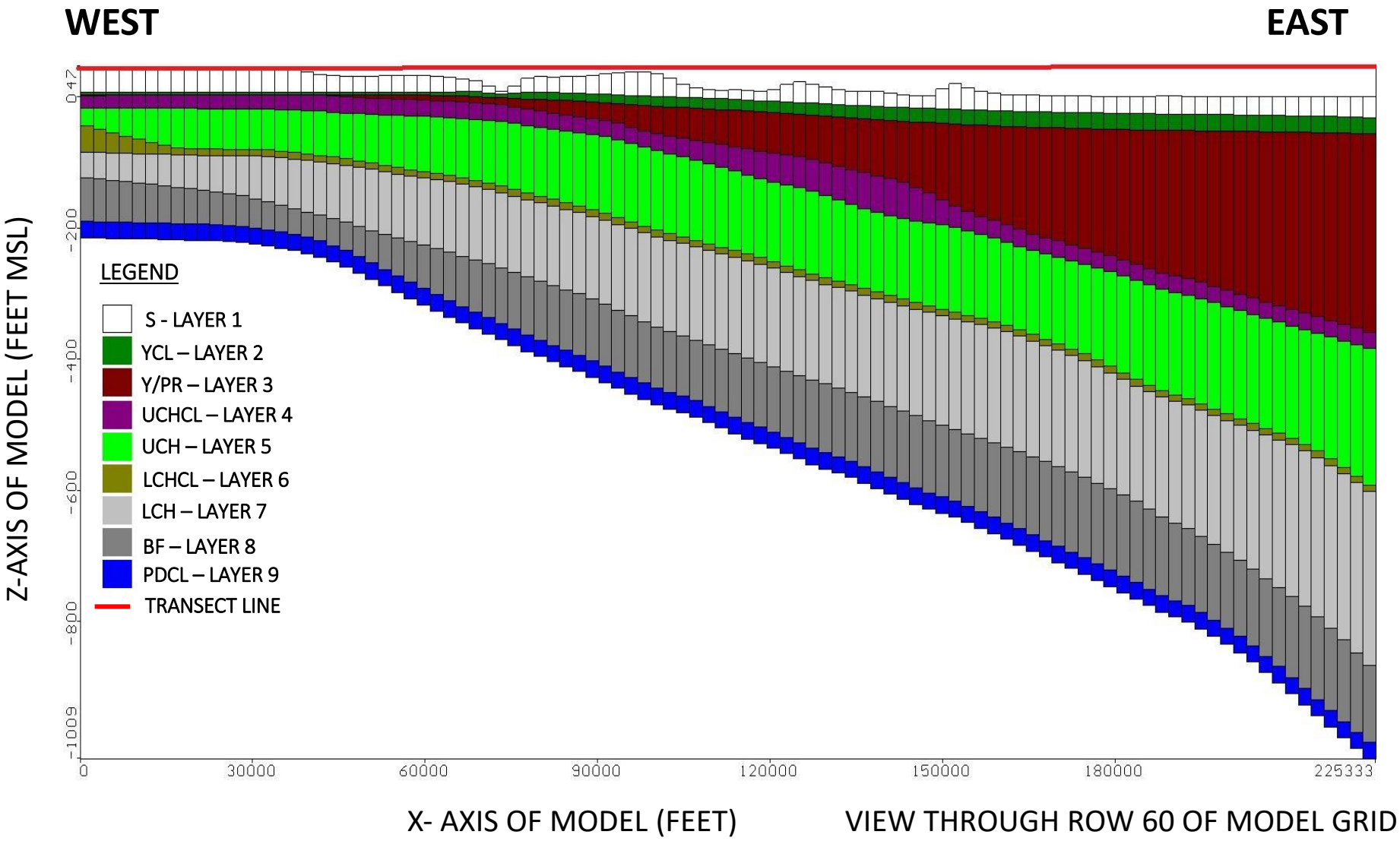

Figure 16. *Model layers in cross-section view.*

3.8 Model Parameters

3.8.1 Water Levels and Equipotential Maps

Water-level data were collected from NCDEQ's online database (https://www.ncwater.org/?page=343), which includes county well data and data from the monitoring well network of the Nutrien phosphate mine. Average water levels used as input data for the model were selected for a portion of 2017, when they did not fluctuate or fluctuated very little (Table 4 and Figure 17). These average heads were chosen to more accurately represent a steady-state system.

An equipotential map of the Castle Hayne Aquifer (Figure 18) was created with head data from 2017 (Table 4), and these data can be found at NCDEQ's online interactive map interface (https://www.ncwater.org/GWMS/openlayers/ol.php?menulist=bl). The equipotential map assisted in building and calibrating the model (Figure 18). NCDEQ's online mapping tool was also used to create equipotential maps for the Yorktown Unit and the Beaufort Unit with data observed from 2017. These maps, and previous studies, provided assistance in understanding regional groundwater flow characteristics prior to creating the model. Important observations include: 1) a cone of depression has developed in the UCH, as well as in the underlying LCH and Beaufort aquifers, 2) west of the mine (in the recharge areas) the potentiometric surface elevations of the LCH and BF aquifers are lower than those of the UCH, which indicates that recharge occurs through the overlying UCH, and 3) to the east of the mine, the potentiometric surfaces of the underlying LCH and BF aquifers are higher than that of the UCH, which indicates upward movement from the LCH and BF into the UCH.

WELL ID	HEAD (FT)
21A	22.1
HILLFLOUR1	-18.6
O13F1	-5.2
O15N3	0.2
O17I1	0.8
O22L2	37.1
O22V7	37.6
P17E3	0.7
P17I12	-49.0
P17I13	0.1
P17I7	0.0
P18V5	-21.0
P21K3	42.0
PCS829	-30.0
PCSCOUNTY5B	25.7
Q15U3	-16.1
Q15U5	-16.1
Q15U8	0.5
Q16G8	-42.8
SENT22A	-83.4
SENT26	-86.9
SENT31	24.6
SENT4	-33.4
SENT5	-30.0
SENT7	-31.6
SENT8	-21.3
SENT9	-28.4
SENTS28	30.0
21A	22.1
HILLFLOUR1	-18.6
O13F1	-5.2
O15N3	0.2
O17I1	0.8
O22L2	37.1

Table 4. *Average water-level data from 2017, relative to mean sea level.*

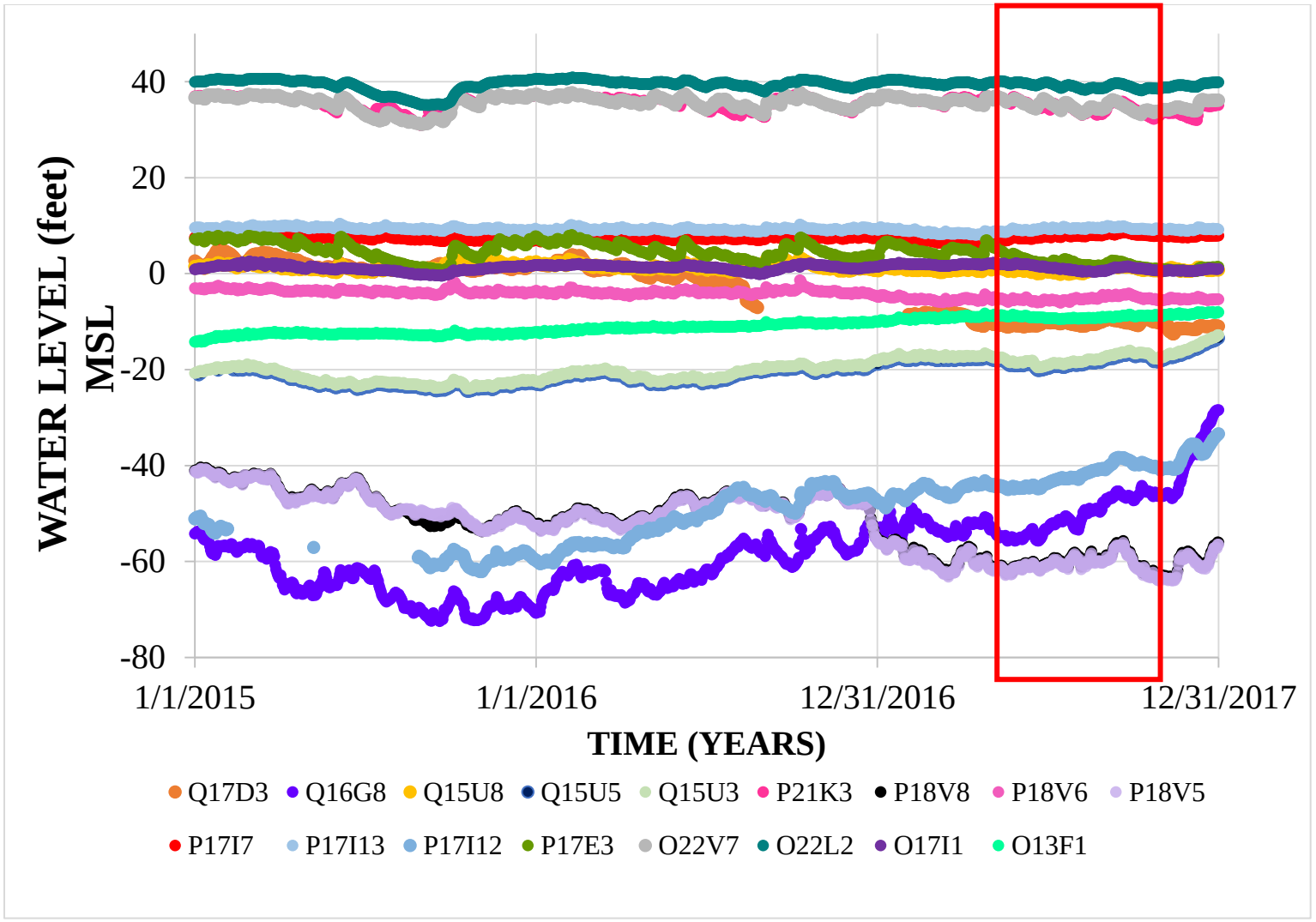

Figure 17. *Observed water-level graph depicting relatively stable water-levels of the aquifers. Red box indicates time frame selected for model construction.*

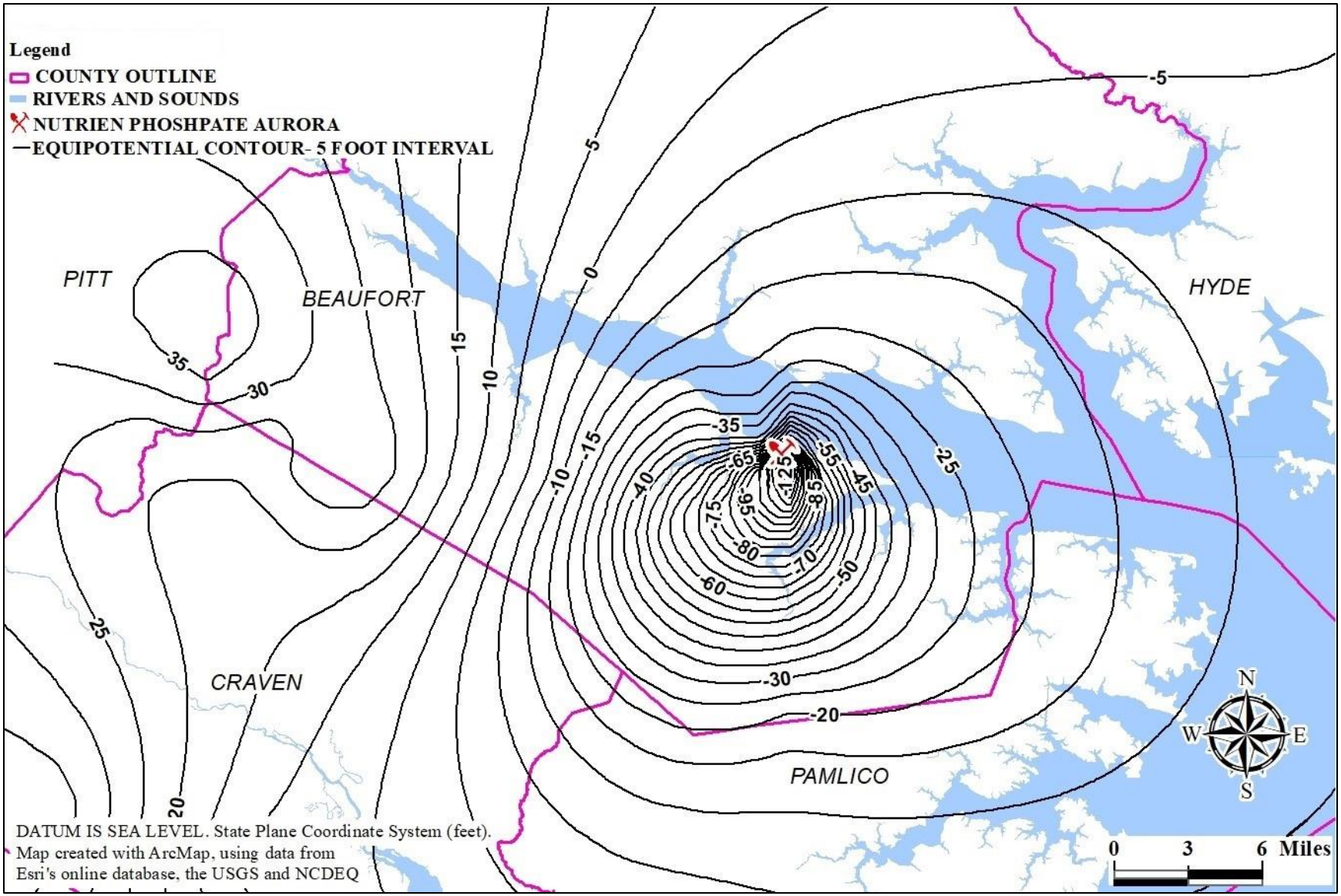

Figure 18. *Equipotential Map of the Upper Castle Hayne Aquifer, 2017.*

3.8.2 Top and Bottom Elevations

Geospatial data were obtained from the U.S.G.S website https://water.usgs.gov/ogw/gwrp/activities/gspdata/Studies/NSCCoastal.html, and were used to determine the land surface elevation and elevations of the top surface of each hydrogeologic unit in the model. An example of the UCH top surface is provided in Figure 19. These surfaces were used to characterize the dip of each hydrogeologic unit in the model; elevation contour maps for each surface are provided in Appendix B. The data are referenced to the North American Datum, 1983, North Carolina State Plane Coordinate System (feet) and are relative to mean sea level.

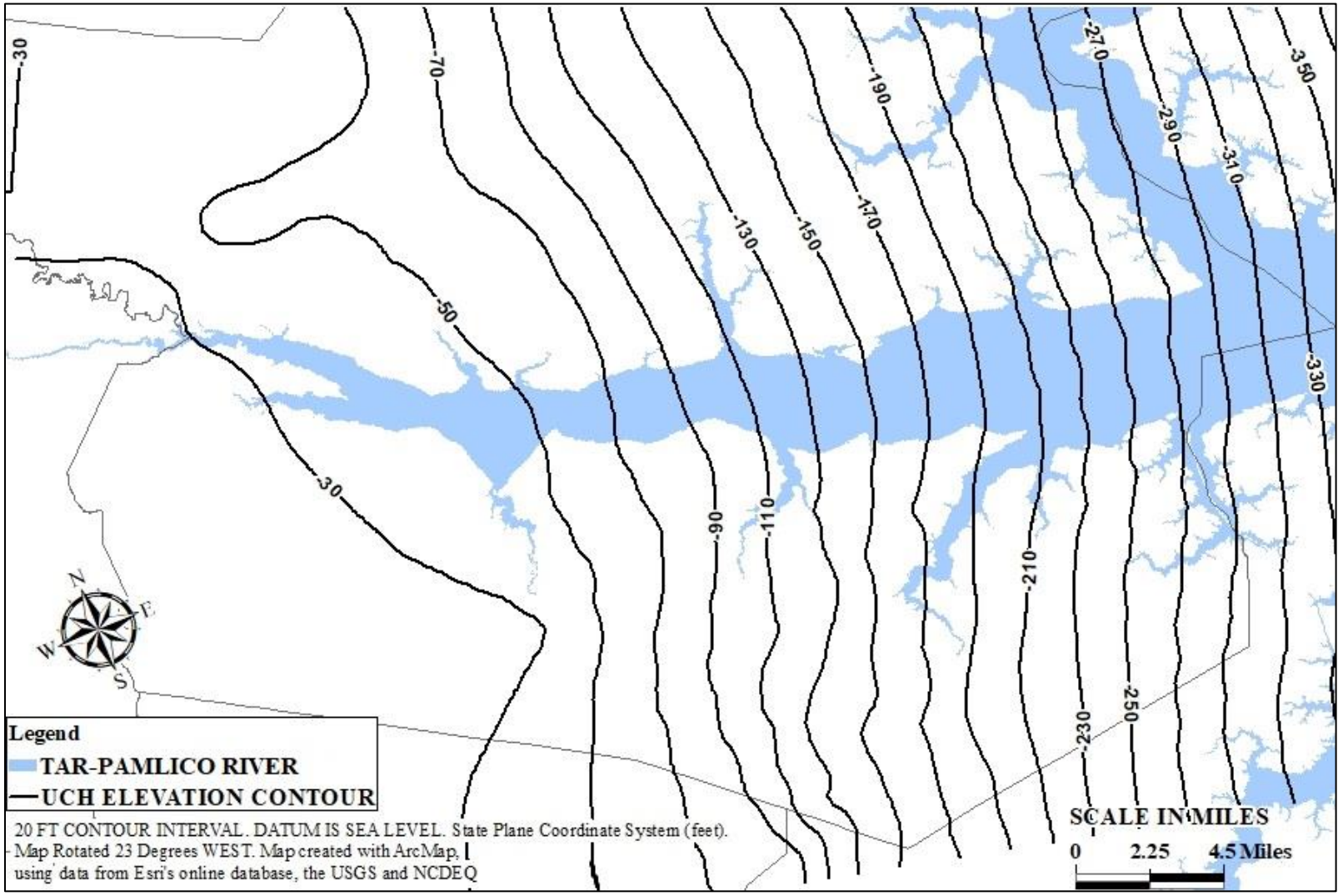

Figure 19. *Elevation of the Upper Castle Hayne Aquifer top surface.*

3.8.3 System Properties

The groundwater flow system was modeled by acquiring hydrogeologic properties from various sources and assigning the properties to the appropriate hydrogeologic units in the model. Best estimates of hydraulic properties were derived from available data and previous modeling studies (Heath, 1983, Reynolds, 1992, Winner and Coble, 1996; Giese et al., 1997; and Groundwater Management Associates, 2013). Property values and ranges for each of the model layers are summarized in Table 5. The initial input values of hydraulic conductivity for each model layer are listed in Table 6. During model calibration, hydraulic conductivities were adjusted between the minimum and maximum observed values to allow for optimization.

Storage properties, including specific storage, and specific yield, are not required for steady-state MODFLOW calculations. However, the porosity (effective porosity in MODFLOW) component of aquifer storage is required for MODPATH calculations, because MODPATH requires effective porosity values to calculate average linear velocities of groundwater and time markers along pathlines. Effective porosity, for the purposes of this study, refers to the percentage of interconnected pore space available for fluid movement (Lohman, 1972). For this study, all pores in the Coastal Plain sediments of the study area are assumed to be interconnected, and average effective porosity values were used as model input parameters for all aquifers and confining layers except for the CH limestone (Table 5). Average values of effective porosity were used for confining layers and other aquifers in the model due to a lack of available data (Heath, 1988). Sediments that contain clay and silt particles usually have greater porosity than sand and gravel-sized particles; however, the size of the pores in sediments containing clay and silt is small, the hydraulic conductivity is small, and fluid movement is much slower than through sand and gravel. The slower movement is attributed to increased molecular attraction

between the porous medium and the fluid as pores become small and as the surface area common to the particles and the fluid increases (Freethey, et al., 1994). Therefore, larger values of effective porosity, and the small hydraulic conductivity associated with the confining layers that are composed primarily of clay, would yield the slowest average linear velocity values during the MODPATH calculations.

A petrographic analysis performed by Neal et al., 2013, determined that the average porosity of the CH limestone ranges from 15% to 37%. All confining layers were assigned an effective porosity of 50%, the Surficial Aquifer was assigned an effective porosity of 40%; the Yorktown/Pungo River aquifer, the Lower Castle Hayne aquifer, and the Beaufort unit were assigned an effective porosity of 20%.

3.8.4 Vertical Hydraulic Conductivity and Leakage

For the purposes of this model, flow through the confining units is primarily vertical and flow through the aquifers is horizontal. A ratio of 1:10 for vertical to horizontal hydraulic conductivity was assumed for all hydrogeologic units during the manual calibration of the model.

Table 5. Hydraulic Properties of Regional Aquifers		
Model Layer	**Hydrogeologic Unit**	**Hydraulic Properties**
Layer 1	Surficial Aquifer	Winner and Coble, 1996 = horizontal hydraulic conductivity ranges from 1-120 ft/day Reynolds, 1992 = horizontal hydraulic conductivity ranges from 50-80 ft/day Waddell et al., 1987, = porosity of sand, silt and clay ranges from 38-42%.
Layer 2	Yorktown Confining Layer	Giese et al., 1997 = vertical hydraulic conductivity ranges from 0.002-0.00087 ft/day Reynolds, 1992 = vertical hydraulic conductivity ranges from 0.015-0.00015 ft/day (Reynolds combined the Yorktown, Pungo River and Upper Castle Hayne confining layers into one unit.) Heath, 1983 = porosity of clay = 50%
Layer 3	Yorktown Aquifer /Pungo River Unit	Giese et al., 1997 = horizontal hydraulic conductivity ranges from 19-33 ft/day and averages 22 ft/day. Groundwater Management Associates = porosity = 20%
Layer 4	Upper Castle Hayne Confining Layer	Giese et al., 1997 = vertical hydraulic conductivity ranges from 0.015-0.00015 ft/day. Heath, 1983 = porosity of clay = 50%
Layer 5	Upper Castle Hayne Aquifer	Giese et al., 1997 = horizontal hydraulic conductivity 200 ft/day Neal et al., 2013 = porosity of CH limestone ranges 15-37%
Layer 6	Lower Castle Hayne Confining Layer	Groundwater Management Associates, 2013 = vertical hydraulic conductivity of 0.001 ft/day. Heath, 1983 = porosity of clay = 50%
Layer 7	Lower Castle Hayne Aquifer	Reynolds and Spruill, 1995 = horizontal hydraulic conductivity ranges from 0.15-2 ft/day. Groundwater Management Associates, 2013 = 2 ft/day Less permeable than the Upper Castle Hayne aquifer due to increased sand content. Groundwater Management Associates = porosity = 20%
Layer 8	Beaufort Confining Layer/ Aquifer	Giese et al., 1997 = horizontal hydraulic conductivity ranges from 30-100 ft/day Groundwater Management Associates, 2013 = horizontal hydraulic conductivity is 3 ft/day Groundwater Management Associates = porosity = 20%
Layer 9	Peedee Confining Layer	Giese et al., 1997 = vertical hydraulic conductivity is 0.0075 ft/ day Heath, 1983 = porosity of clay = 50%

Table 6. Initial Hydraulic Conductivities of Model Layers		
Model Layer	**Hydrogeologic Unit**	**Hydraulic Conductivity**
Layer 1	Surficial Aquifer	29 ft/day
Layer 2	Yorktown Confining	9.1×10^{-5} ft/day
Layer 3	Yorktown Aquifer /Pungo River Unit	19 ft/day
Layer 4	Upper Castle Hayne	1.0×10^{-5} ft/ day
Layer 5	Upper Castle Hayne	200 ft/day
Layer 6	Lower Castle Hayne	0.001 ft/day
Layer 7	Lower Castle Hayne	2 ft/day
Layer 8	Beaufort Confining	3 ft/day
Layer 9	Peedee Confining	1.0×10^{-6} ft/day

3.8.5 Occurrence of Saltwater

Each aquifer in this study extends seaward where freshwater grades into saltwater outside of the study area (Figure 20). According to Meisler, 1989, water that contains chloride concentrations greater than 10,000 milligrams per liter (mg/L) is saltwater, so the saltwater-freshwater interface occurs where chloride concentrations are greater than or equal to 10,000 milligrams per liter (mg/L). At this interface the effect of saltwater density balances the freshwater head equipotential so that groundwater movement becomes insignificant. Therefore, the freshwater- saltwater interface acts as a no-flow boundary for modeling purposes, since water does not readily flow across this boundary.

Leahy and Martin (1993), developed a calibrated constant-density flow model and a variable-density flow model of the NACP to ascertain the sensitivity of the model to the location

of the saltwater-freshwater interface. The variable-density model simulated flow in parts of the aquifer system where groundwater contained chloride concentrations greater than 10,000 mg/L. The model calculated the head difference along the 10,000-chloride concentration line and it was discovered that head differences between the calibrated constant-density flow model and the variable-density flow model were generally less than 10 feet. Leahy and Martin (1993) concluded that only a small percentage of water in the system is derived from salty water, and so the exact location of the saltwater-freshwater interface was not accounted for in this study.

Chloride concentrations increase to the east.
Map created with ArcMap, using data from Esri's online database,
the USGS and NCDEQ. Chloride data from Meisler, 1989, Figure 6.

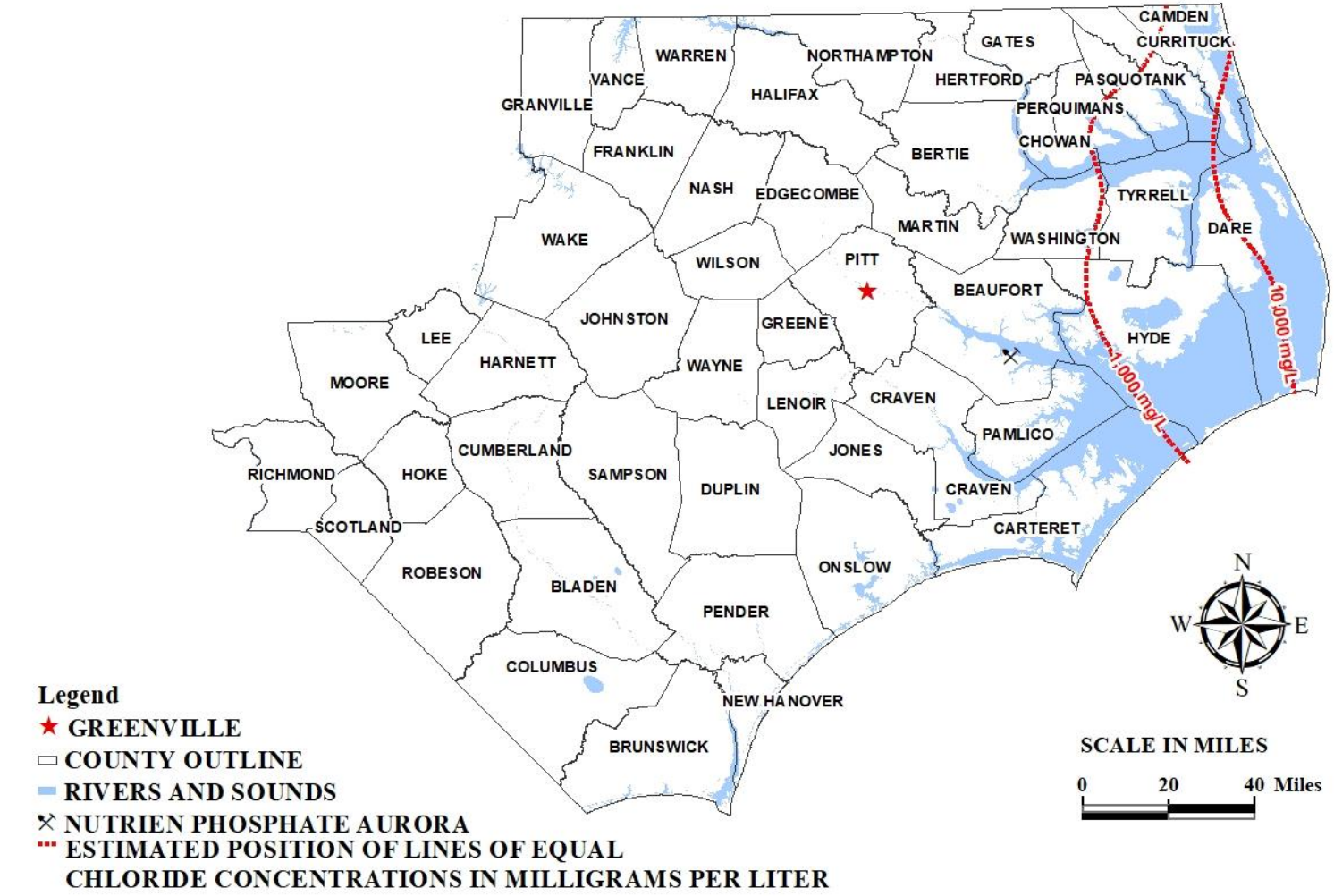

Figure 20. *Chloride concentrations at the top of the CHAS.*

3.8.6 Boundary Conditions

External model boundaries are real physical boundaries and hydraulic boundaries, which are artificial. Physical boundaries are well-defined features of geologic or hydrogeologic nature that influence the pattern of groundwater flow. Examples of physical boundaries include impermeable contacts between geologic units, faults, a contact between a large body of surface water and the porous medium or a contact between the porous medium and a man-made structure (Kresic, 2007). Physical boundaries are preferred but sometimes it is not feasible to include them in the model area, so the modeler must define hydraulic boundaries.

Hydraulic boundaries are determined from the groundwater flow net. Thus, they are termed artificial boundaries and are designated by the model designer. Examples of hydraulic boundaries include, no-flow boundaries represented by chosen streamlines because there is no flow across the streamline, or they can be boundaries with known hydraulic head and are represented by equipotential lines (Kresic, 2007). Deep, fully penetrating perennial streams are often used as ideal equipotential boundaries because there is enough flow in the river to sustain an extensive potential groundwater withdrawal from the adjacent aquifer (Kresic, 2007). The main drawback of hydraulic boundaries is that they are placed arbitrarily due to a lack of data.

This project utilizes hydraulic boundaries (known lines of hydraulic head or equipotential lines) for the western limits of the model. This type of boundary condition is a specified-head boundary and is represented in Visual MODLFOW by a constant head boundary. Under this condition, hydraulic head is maintained at a fixed value and is a function of time and position at a specified head, and groundwater flow across the boundary is proportional to the difference in hydraulic head at the boundary and in the simulated aquifer (Kelly, 2002). Locations and values

of specified-head boundaries were derived from 2017 equipotential maps, found on NCDEQ's online interactive map (https://www.ncwater.org/GWMS/openlayers/ol.php?menulist=bl).

The direction of principal groundwater flow in the system is from west to east – southeast. Therefore, no-flow boundaries were assigned to the northern and southern boundaries of the model. The upper boundary of each confined aquifer is the bottom of its associated confining layer and is treated in the model as a head-dependent flux boundary. The lateral limits for the confining layers were designated as no-flow boundaries because groundwater flow was assumed to only flow vertically in these units. The Peedee Confining Layer (PDCL) is the base of the model. According to Groundwater Management Associates (2013), the PDCL has very low vertical hydraulic conductivity, which means little water crosses this boundary. For modeling purposes, the bottom of the PDCL is designated as an impermeable boundary. Vertical groundwater flow between other confining layers and aquifers was implemented by adjusting hydraulic conductivity in the vertical direction to one tenth of the horizontal hydraulic conductivity (Hudak, 1999).

The water table is the upper boundary of the Surficial Aquifer and was simulated as a free-surface boundary across which recharge from precipitation enters the aquifers. Recharge from precipitation is the major source of water for the aquifer system. During a typical year in North Carolina, the NCCP receives approximately 50 inches of rain. According to Giese et al. (1997), of the 50 inches of annual precipitation, 33 inches is lost to evapotranspiration, 5 inches is lost to runoff, and 12 inches reaches the unconfined Surficial Aquifer but is lost by lateral seepage to streams and large bodies of water. Approximately one inch per year percolates vertically into the confined aquifer system. Recharge in the model was assigned at a rate of 1 inch per year and was adjusted during the calibration process. For this study, the recharge rate

was designed to represent the amount of water that infiltrates the confined aquifer system. Previous studies and models of the study area used this technique and achieved reasonable results (Groundwater Management Associates, 2013).

Pumped wells are internal boundaries where water is removed at a specified rate equal to the discharge of the well. Flows from these cells are recorded in the simulation budget as well discharges. In this model, one well was used to simulate the pumping conditions at the phosphate-mine, due to the close spacing of the pumping wells there. Daily pumping volumes were found here: (https://www.ncwater.org/Permits_and_Registration/Capacity_Use/Central_Coastal_Plain/ccpcuadetail.php?permit=CU1003).

A constant head boundary of 0 ft (sea level) was used to represent the Pamlico River and the Pamlico Estuary because the hydraulic head of these features is relatively constant and is a consistent source of water in the system (Groundwater Management Associates, 2013). Previous studies of this area indicate that other surface bodies of water have little influence on the flow of water in the confined aquifers throughout the model area (DeWiest, 1969). Bodies of water other than the Tar-Pamlico River System were not assigned in the model, as the confined UCH is the aquifer of interest.

3.9 Steady State Calibration

3.9.1 Manual Calibration

Calibration of the model involved a trial and error adjustment procedure where model inputs were varied in the aquifers and observed heads were compared to simulated heads under steady state conditions (Anderson and Woessner, 2002). Observed head data were acquired from

observation wells in the NCDEQ hydrogeologic framework database, the USGS monitoring well network, and from the Nutrien Phosphate-Aurora, monitoring-well network. Model head-observation wells were designated in the model and were assigned an average water level from the year 2017 (Table 4). Average water-level values were used to approximate a steady-state system. One pumping well was included in the model using average daily withdrawal rates from 2017 to simulate pumping conditions associated with the Nutrien mine.

Recharge and hydraulic conductivities of the model layers were adjusted manually until observed water levels, and those calculated by the model at the head-observation wells, were in good agreement (Figure 21). Adjustments of the model parameters were made, and new simulations performed repetitiously, until there was good agreement between the simulated water levels and the 2017 observed water levels. The steady-state manual calibration graph (Figure 21) compares the observed water levels with the simulated water levels for the 28 head-observation wells.

Error statistics were calculated to measure the goodness-of-fit of the model. Calibrating the model focused on minimizing the error statistics. The root-mean-square error (RMS) and the normalized root-mean-square error (NRMS) between observed and simulated heads, as well as the correlation coefficient, were used to assess how well the observed-head data compared to the simulated-head data. The model was considered calibrated when the RMS was less than 15 ft, the NRMS was less 10%, and the correlation coefficient was greater than 0.9 for all of the model layers. Further details regarding the error statistics of the final calibrated model are discussed in Section 3.10.

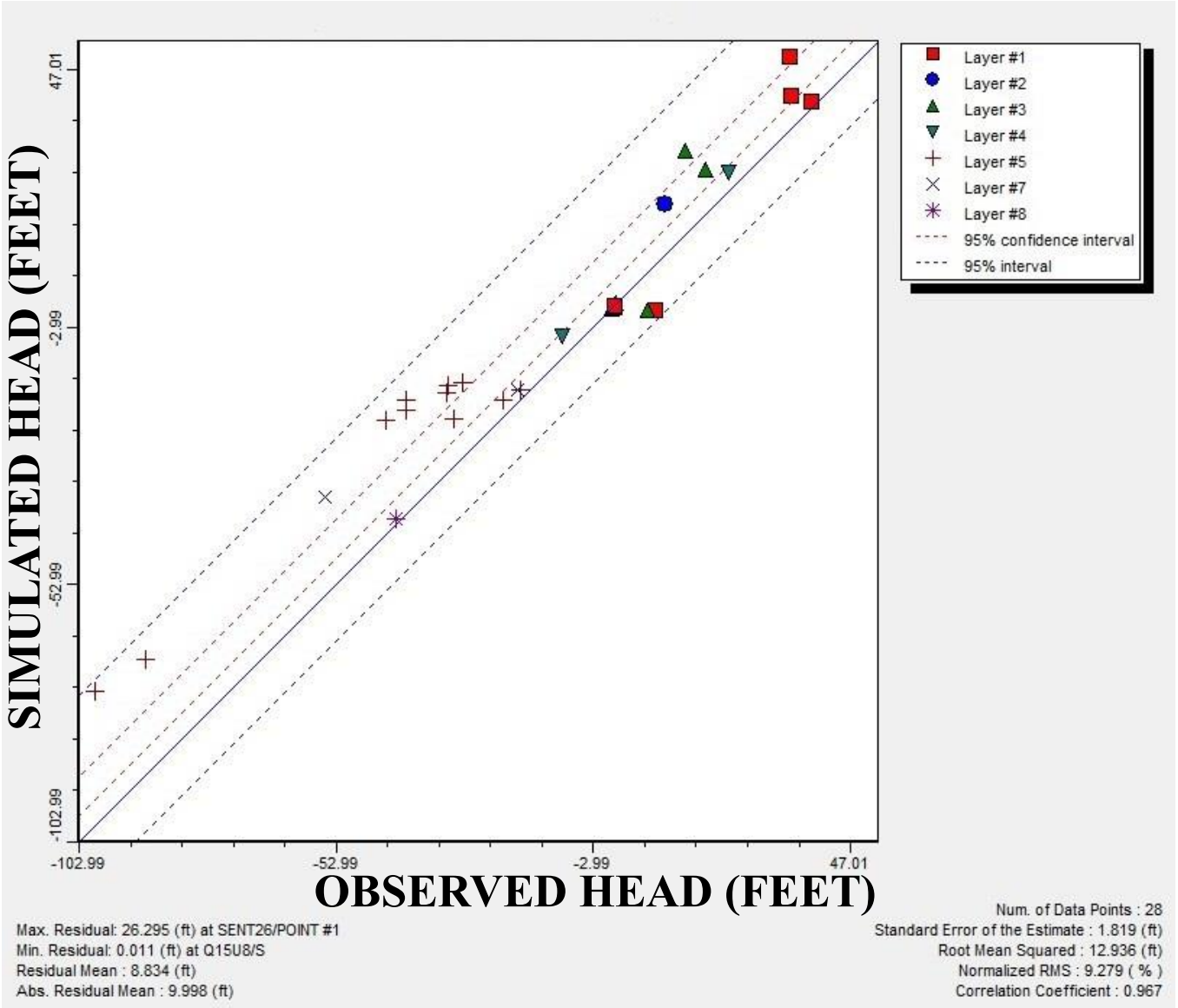

Figure 21. *Manual calibration graph.*

3.9.2 PEST Calibration

Once the model was manually calibrated, using recharge of 1 in/year and hydraulic conductivity of 200 ft /day for the UCH, Parameter Estimation (PEST) was performed. PEST is an automated trial and error algorithm that works with Visual MODFLOW. It used the manually calibrated values of recharge and hydraulic conductivity of the aquifer layers to estimate values that best fit the model and reduce model error. PEST calibration lowered the error statistics, and these statistics are as follows: the RMS is 5.856 ft, the NRMS was 4.637%, and the correlation coefficient was 0.986, for all the model layers (Figure 22). Calibration was considered acceptable for the purposes of this study when simulated water levels were within 15 feet of water levels measured in 2017 (Figure 22).

PEST produced horizontal hydraulic conductivity of 168.5 ft/day and a vertical hydraulic conductivity of 9.25 ft/day for the UCH (conductivity zone #11), as well as a recharge value of 0.8 in/year. Table 7 provides hydraulic conductivity values for each zone. Figure 23 is a three-dimensional representation of the model layers and their corresponding PEST-derived, hydraulic-conductivity zones; note that each layer can have more than one assigned conductivity zone, and not all zones are depicted.

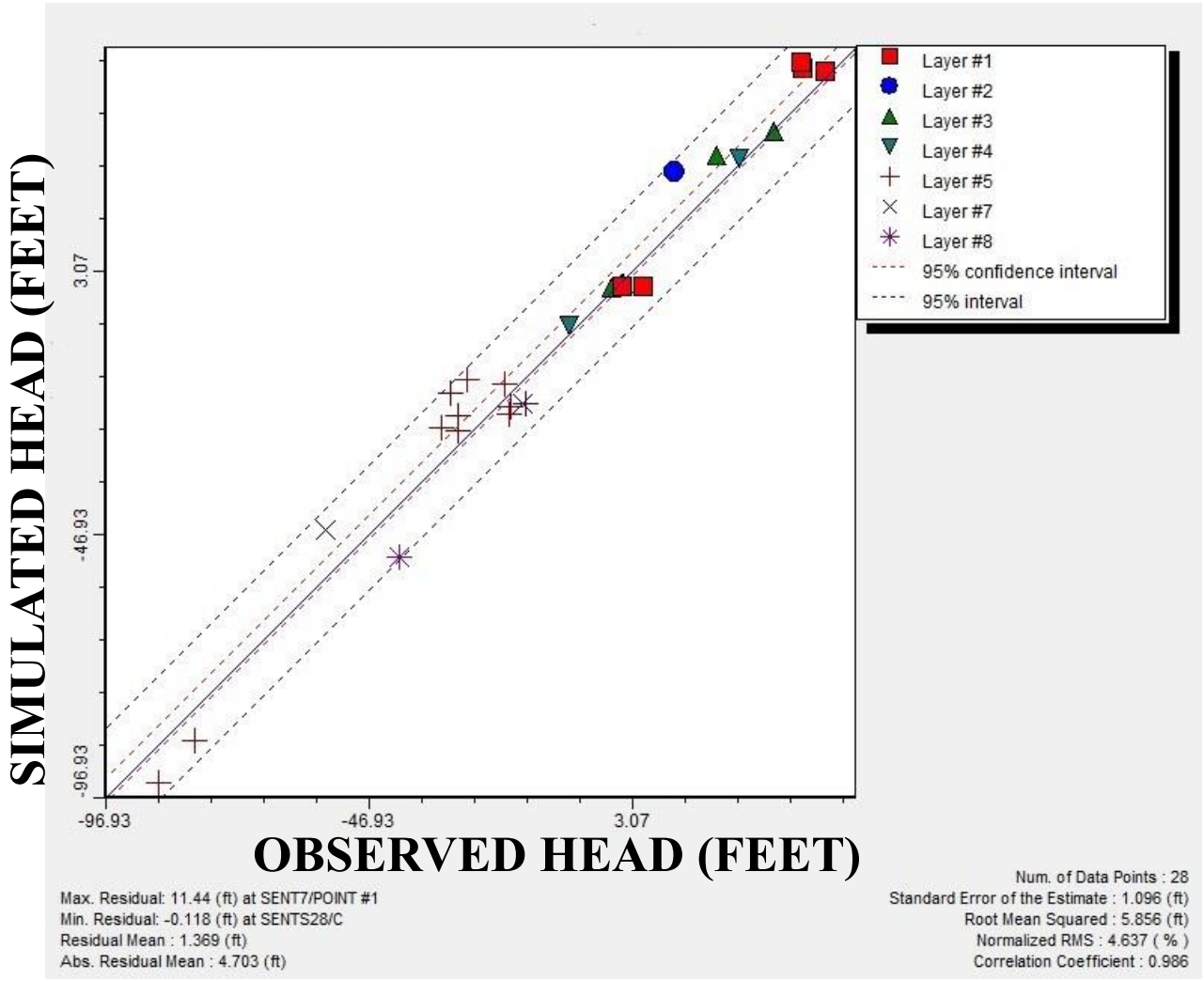

Figure 22. *PEST calibration graph.*

Table 7. Hydraulic Conductivity Zones and Corresponding Hydrogeologic Units		
Zone Number	Hydrogeologic Unit	K_x = Horizontal Hydraulic Conductivity K_v = Vertical Hydraulic Conductivity (feet/day)
Zone 1	Surficial	$K_x = 148.6$ $K_v = 1.453$
Zone 2	River Bed (layer 1)	$K_x = 11.77$ $K_v = 0.1117$
Zone 3	Yorktown Confining Layer	$K_x = 3.678$ $K_v = 0.0689$
Zone 4	River Bed (layer 2)	$K_x = 0.0308$ $K_v = 0.000303$
Zone 5	Yorktown Aquifer/Pungo River Unit	$K_x = 18.09$ $K_v = 0.179$
Zone 6	Upper Castle Hayne Confining Layer#1	$K_x = 0.00089$ $K_v = 0.00016$
Zone 7	Lower Castle Hayne Confining Layer	$K_x = 41.91$ $K_v = 21.11$
Zone 8	Lower Castle Hayne Aquifer	$K_x = 15.05$ $K_v = 6.39$
Zone 9	Beaufort Unit	$K_x = 1.43$ $K_v = 0.372$
Zone 10	Peedee Confining Layer	$K_x = 1.218\ E^{-6}$ $K_v = 1.317\ E^{-7}$
Zone 11	Upper Castle Hayne Aquifer	$K_x = 168.5$ $K_v = 9.25$
Zone 12	Upper Castle Hayne Confining Layer #2	$K_x = 0.00583$ $K_v = 1.316\ E^{-5}$

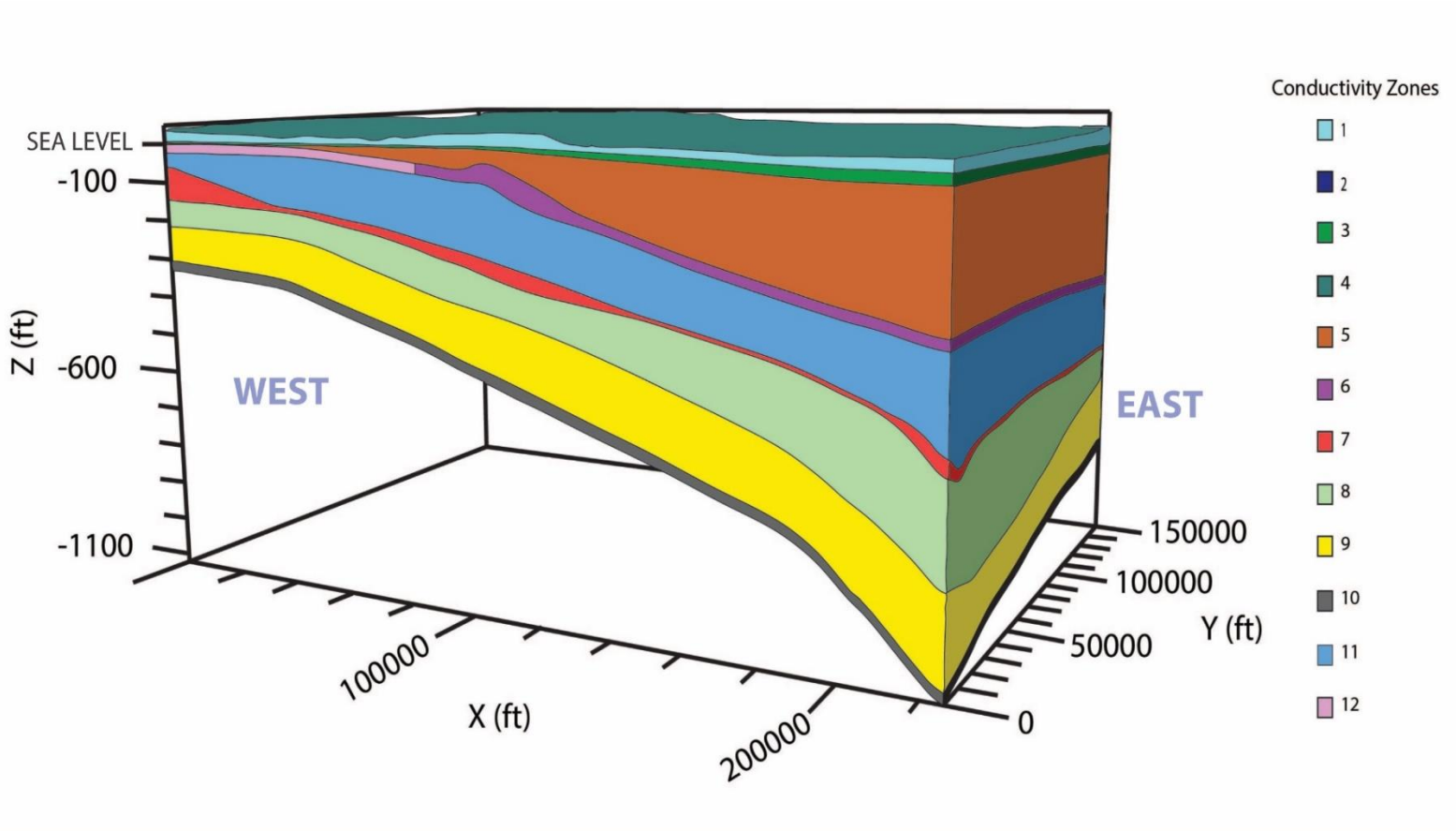

***Figure 23**. Hydraulic conductivity zones in a 3-D representation of the model.*

3.10 Error

Head-target uncertainty, or the difference between the observed head and the simulated head is expressed as a standard deviation (the square root of the average of squared differences of the values from their average value) or variance (the square of the standard deviation). It can also be expressed as the 95% confidence interval (approximately + or – two standard deviations) around the reported value (Figures 21 and 22). Residual mean is the mean difference of the residual errors, where both positive and negative differences are included and may cancel each other out. The residual mean is considered less robust than the absolute residual mean, which is the mean of the absolute values of the residuals. The absolute residual mean ensures that positive and negative values do not cancel each other out and is a better indicator of model fit than the residual mean. Root-mean-square error is the average of the squared residuals and is less robust than the normalized root-mean-square (NRMS) error, which is expressed as a percentage. Lower values of NRMS error indicate less residual variance. Table 8 provides head-target uncertainty statistics of the PEST calibrated model.

TABLE 8. ERROR STATISTICS OF THE FINAL CALIBRATED MODEL

Max. Residual	11.44 feet
Min. Residual	-0.118 feet
Residual Mean	1.369 feet
Abs. Residual Mean	4.703 feet
Standard Error of the Estimate	1.096 feet
Root Mean Squared	5.856 feet
Normalized Root Mean Squared	4.637 %
Correlation Coefficient	0.986

3.11 Sensitivity Analysis

Sensitivity analysis was conducted to evaluate the effects that recharge properties (applied to layer 1) and the hydraulic conductivity of the UCH have on the model. These factors were chosen because during the calibration process, it was determined that these properties created the most discrepancy in the observed versus simulated water levels. The focus of the sensitivity analysis was the UCH as it is the focal aquifer of this study. During the sensitivity analysis, each hydraulic property was changed by +/-90%, and +/-50%. To evaluate the effect that changes in these properties had on the model, the average head change of UCH wells was used.

Sensitivity analysis determined that hydraulic conductivity had the most significant impact on head change. Increasing hydraulic conductivity by 90% and 50% resulted in increasing average head by 2.06 feet and 1.24 feet, respectively. Decreasing hydraulic conductivity by 90% and 50% resulted in increasing average head by 26.28 feet and 25.32 feet, respectively. Decreasing the recharge by 90% and 50% resulted in average head decreases of 16.5 feet and 13.6 feet, respectively. Increasing recharge by 90% and 50% resulted in average head increases of 5.7 feet and 7.7 feet, respectively (Table 9).

	Change in Property by Percent			
Property	+90%	-90%	+50%	-50%
Hydraulic Conductivity of UCH	+2.06	+26.28	+1.24	+25.32
Recharge	+5.7	-16.5	+7.7	-13.6

Table 9. Results of sensitivity analysis of UCH. Average head change (in feet) as a result of adjusting hydraulic conductivity of the UCH and recharge to layer 1.

3.12 Particle Tracking

MODPATH is a particle-tracking, post-processing program designed to work with Visual MODFLOW (McDonald and Harbough, 1988). Output from the calibrated steady-state MODFLOW simulation was used in MODPATH to compute flowpaths, average linear velocities, and travel times for imaginary particles of water moving through the simulated groundwater system.

MODPATH's calculation for pathlines:

$$d = \frac{\bar{v} \times (\Delta t)}{n_e}$$

Where:

d = distance

$\bar{v}$ = Darcian Flux

Δt = Change in time

n_e = effective porosity

MODPATH's calculation for particle travel time:

$$travel\ time = \frac{length\ of\ flow\ line\ (ft)}{Average\ linear\ velocity\ along\ flow\ line\ (ft/day)}$$

MODPATH uses effective porosity values to calculate average linear-velocities and time markers during MODPATH simulations. MODPATH simulations can assess uncertainty in the model created by varying effective porosity values. Effective porosity refers to the amount of interconnected pore space available for fluid flow. For unconsolidated porous media and many consolidated rocks, effective porosity and total porosity are the same (Todd, 1980). There are not enough existing data to assign observed effective porosity values to all model layers, so

effective porosity values for representative geologic material were collected from the literature and previous studies and were assigned in the model. However, the UCH has been extensively studied and a range of porosity values was determined to be 15-37% (Neal et al., 2013). All confining layers were assigned an effective porosity of 50%; the Surficial Aquifer was assigned an effective porosity of 40%; the Yorktown/Pungo River aquifer, the Lower Castle Hayne aquifer, and the Beaufort unit were assigned an effective porosity of 20%. Because limestone varies widely in density, porosity, and permeability, depending on degree of consolidation and the development of permeability zones, MODPATH simulations were performed using the lowest, the medium, and the highest values of the UCH effective porosity range (i.e. 15%, 26%, and 37%, respectively). This range was applied to the model to determine the impact of increasing or decreasing effective porosity on the MODPATH-derived average linear velocities and particle travel times. Particle tracking simulations were performed by placing a ring of ten particles in the cell that contained an analyzed strontium sample. All particles were tracked backward under steady-state conditions to their original sources. MODPATH-simulated pathlines were used as a qualitative comparison tool and were applied to the results of the strontium-mixing line study conducted by Woods et al. (2000[a]).

4.0 Results

4.1 Piper Diagram

A Piper Diagram was developed to characterize hydrochemical facies of groundwater from the NCCP (Figure 24). UCH wells to the far west of the NCCP are calcium-rich and bicarbonate-rich**.** The UCH wells in the far northeastern portion of the NCCP, are alkali-rich and chloride-rich; chloride is the dominant anion of the LCH. LCH samples tend to be more chloride- rich than UCH samples from the same site. In both the UCH and LCH, chloride concentrations increase from west to east and total dissolved solids (TDS) generally increase from west to east, but the highest concentrations are in the northeast. Eastward increases of TDS are due to increased mixing of saline water. Samples from the Peedee Aquifer are calcium-bicarbonate rich. Samples from the Black Creek and Cape Fear Aquifers tend to be more sodium-chloride rich rather than calcium-bicarbonate rich, which is attributed to their non-carbonate lithologies.

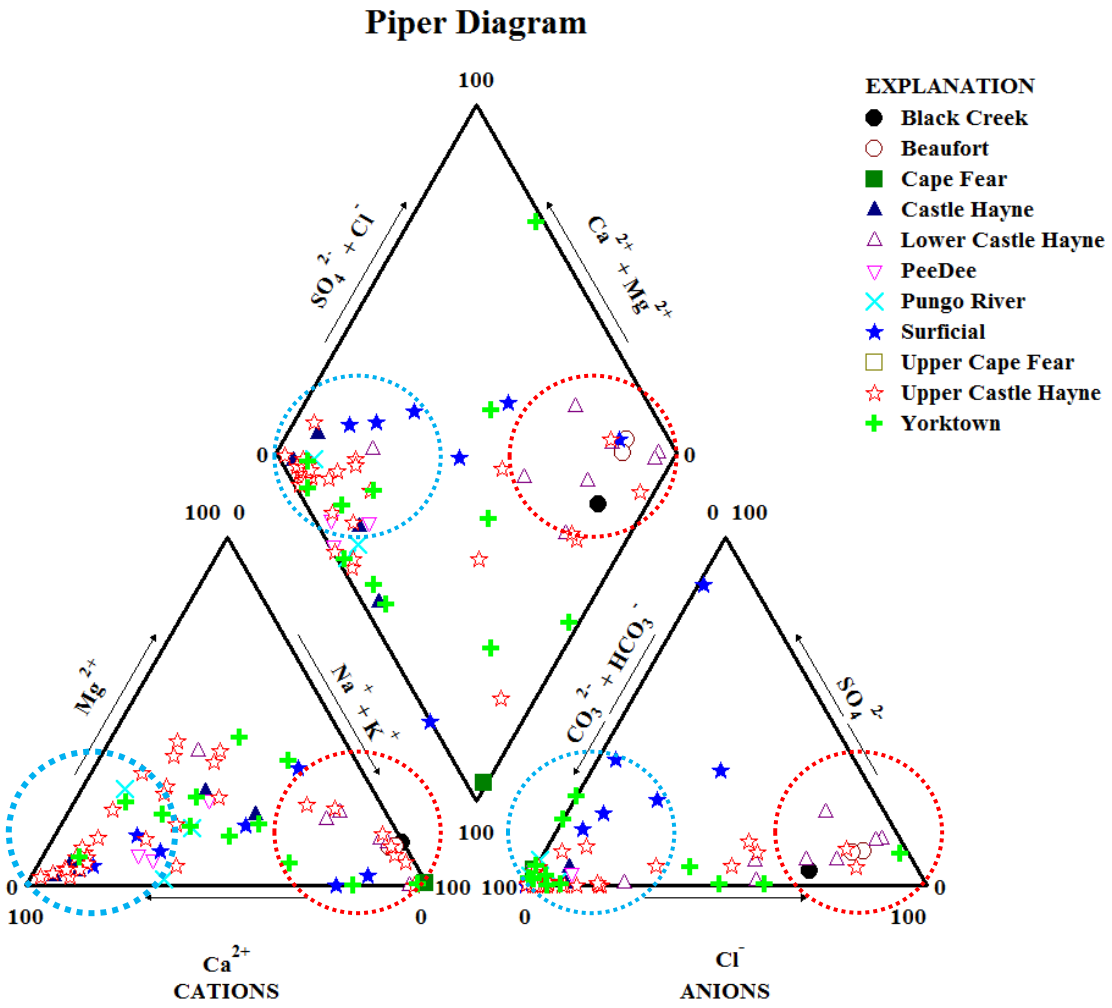

Figure 24. Piper Diagram. Blue circles indicate which wells are affected most by limestone dissolution, and the red circles are indicative of which samples are most affected by saline mixing.

4.2 Principal Component Analysis (PCA)

PCA attempts to draw straight, explanatory lines through data. Each straight line represents a principal component, or a relationship between seemingly unrelated or complexly related variables. The PCA correlation matrix is a data set derived from the original input data. From the correlation matrix, eigenvectors (lines of direction) and eigenvalues (a number, telling you how much variance there is in that direction, or magnitude of the line) are calculated. Eigenvectors and eigenvalues exist in pairs, so every eigenvector has an eigenvalue and they are ordered from highest to lowest. The eigenvectors with the highest eigenvalues are called principal components (PC; Table 10). PCA considered the 18 hydrochemical variables common to the UCH and LCH groundwater samples (Table 10).

The PC loadings in Table 10 measure the strength of the linear relationship between the variables and the individual PCs. Loadings are the coefficients of the linear combination of in-model, principal components used to approximate the original variables. The loadings equal the correlations between the original variables and the principal components, and they tell how much weight is assigned to each PC in order to explain the values of each variable. PCs with large coefficients (greater than +/- 0.5) for a variable are closely related to that variable and have a significant impact on its value. A positive correlation means that as one variable increases, the correlated variable(s) will also increase. A negative correlation means that as one variable increases, the correlated variable(s) will decrease. PC1 is the linear combination that accounts for the largest amount of variance observed in the value of the chemical parameters (variables). Successive PCs explain progressively smaller portions of the total sample variance (Table 10).

Table 10. *Principal Component Loadings from PCA*				
Variable	**PC1**	**PC2**	**PC3**	**PC4**
pH	0.007	**-0.826**	0.426	0.127
HCO_3	0.442	**-0.678**	-0.0427	**0.527**
Cl^-	**0.914**	0.383	0.0445	0.036
SO_4^{2-}	**0.867**	0.302	0.131	0.11
Na^+	**0.921**	0.325	0.113	0.099
K^+	**0.896**	0.306	0.0707	0.214
Ca^{2+}	0.394	**0.851**	-0.121	-0.188
SiO_2	-0.431	0.410	**-0.672**	0.301
F^-	**0.523**	**-0.575**	0.183	0.406
Mg^{2+}	0.292	-0.318	**-0.644**	-0.157
Sr^{2+}	**0.879**	0.379	-0.215	-0.045
$^{87}Sr/^{86}Sr$	**-0.769**	0.405	0.374	-0.168
$^{18}O/^{16}O$	**0.760**	-0.192	-0.442	-0.099
$^{13}C/^{12}C$	**0.746**	-0.244	0.372	-0.108
NH_4^+	**0.865**	0.218	0.148	0.0166
$NO_3^- + NO_2^-$	0.028	**0.583**	**0.536**	-0.190
PO_4^{3-}	**-0.503**	**0.550**	0.069	**0.607**
Fe	-0.432	**0.614**	0.066	**0.570**
% Variance	43.43%	24.31%	10.95%	8.14%
Cumulative %	43.43%	67.74%	78.70%	86.82%

Note: Significant loadings are shown in bold.

The PCA-produced scree plot (Figure 25) shows that the eigenvalues start to form a straight line after the fourth PC. This indicates that the first four PCs (those located to the left of the vertical gray line) contribute most to the observed variance in groundwater chemistry; and the other PCs account for a smaller amount of the variability and are therefore, less important (Table 10).

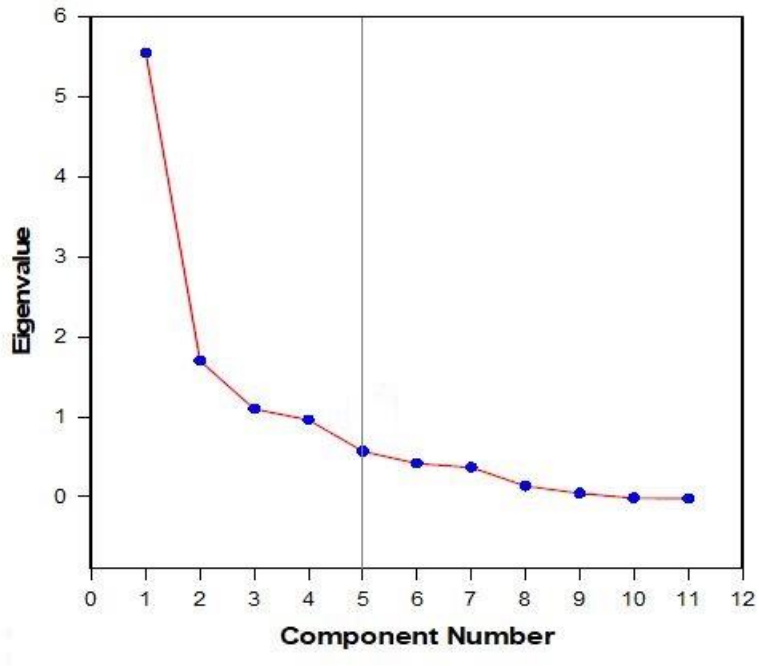

Figure 25*. Scree plot.*

PCA also produced a Component Loadings graph (Figure 26), that identifies which variables have the largest impact each PC. The axes labels show the percentage of total variance contributed by each corresponding PC. Loadings (values on the x and y-axes), if close to -1.0 or 1.0 indicate that the variable strongly influences the component. Loadings close to zero indicate that the variable has a weak influence on the component. Two variables are highly correlated if their vectors are close to pointing in the same or exactly opposite directions. Two variables are highly uncorrelated if their vectors are close to perpendicular.

The PCs are representative of specific geochemical and hydrogeologic processes, such as limestone dissolution, saline water mixing, and vertical groundwater movements between aquifers. PCs and their relation to specific processes are discussed in more detail in section 5.1.

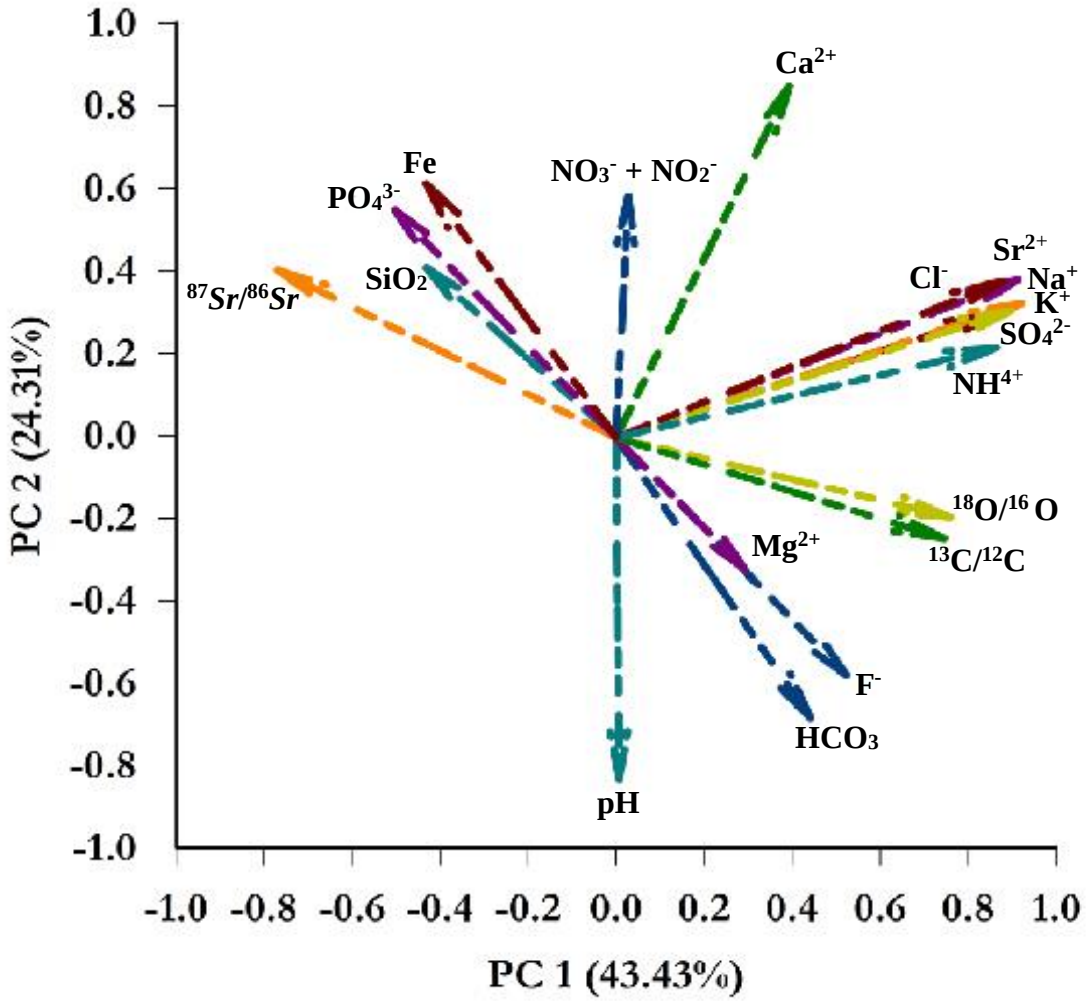

Figure 26. *Component loadings graph. The tip of the arrow for each chemical component represents the point plotted from that component's PC loadings listed in Table 10. Strong correlations can be positive or negative and are represented by arrows pointing in the same or opposite directions. Arrows that are close to perpendicular indicate variables that do not correlate well.*

4.3 Visual MODFLOW Results

The calibrated groundwater flow model provided an estimate of the conditions that exist within the groundwater system of Beaufort County, North Carolina. The model generated an equipotential map (Figure 27), that shows the effects of pumping on the shape of the UCH equipotential surface, which is representative of the known cone of depression that extends outside the model area. The cone of depression is a result of groundwater withdrawals at the mine. The natural, pre-pumping, equipotential surface for the UCH was sloping from the recharge area in the west toward the discharge areas, east of the mine. The sloping equipotential surface results in an asymmetrical shape of the equipotential surface in the vicinity of the mine. The asymmetry is further accentuated by the variable thickness of the UCH limestone and the resulting impacts on transmissivity. Figure 28 illustrates the head equipotential lines in cross-section view (row 60 from the top of the model grid). The model shows that groundwater in the UCH is moving toward the mine from all directions. The steep hydraulic gradient between the recharge area in the west and the phosphate mine indicates that groundwater flow is significantly affected by pumping at the phosphate mine.

The simulated equipotential map of the UCH (Figures 27) was compared to the observed equipotential map of 2017. The location, size, depth and shape of the cone of depression is similar to the observed equipotential maps generated from the 2017 water level data. Notable differences occur at the margins of the model to the east, north, and south, where the cone of depression approaches the model's no-flow boundaries. In these areas there is as much as 10 feet of difference. Figure 28 provides a cross-sectional view through row 60 of the model.

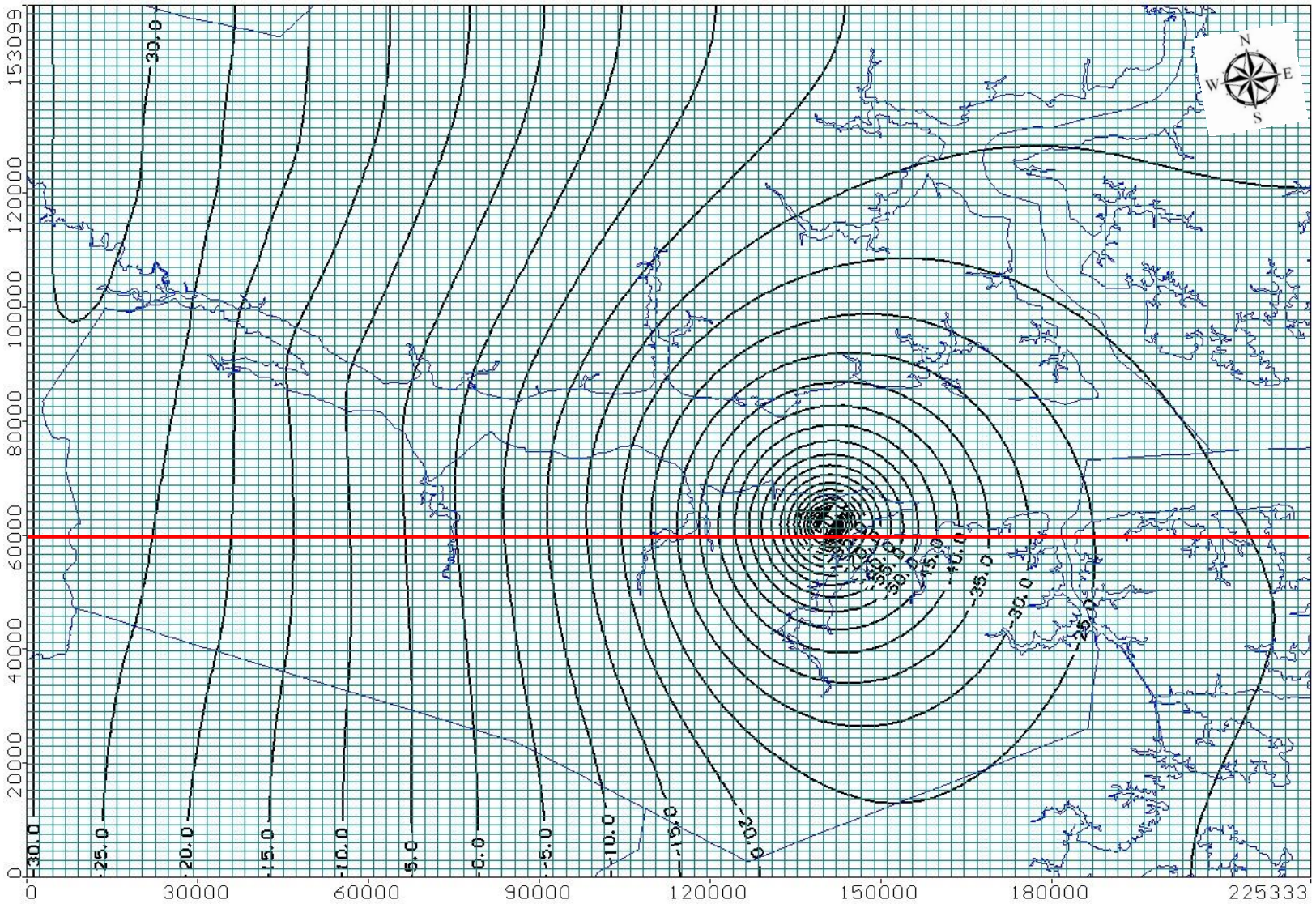

Figure 27. *Simulated head equipotential map of the Upper Castle Hayne Aquifer. Datum is sea level. Row 60 of model grid is highlighted in red. Contour interval is 5 feet.*

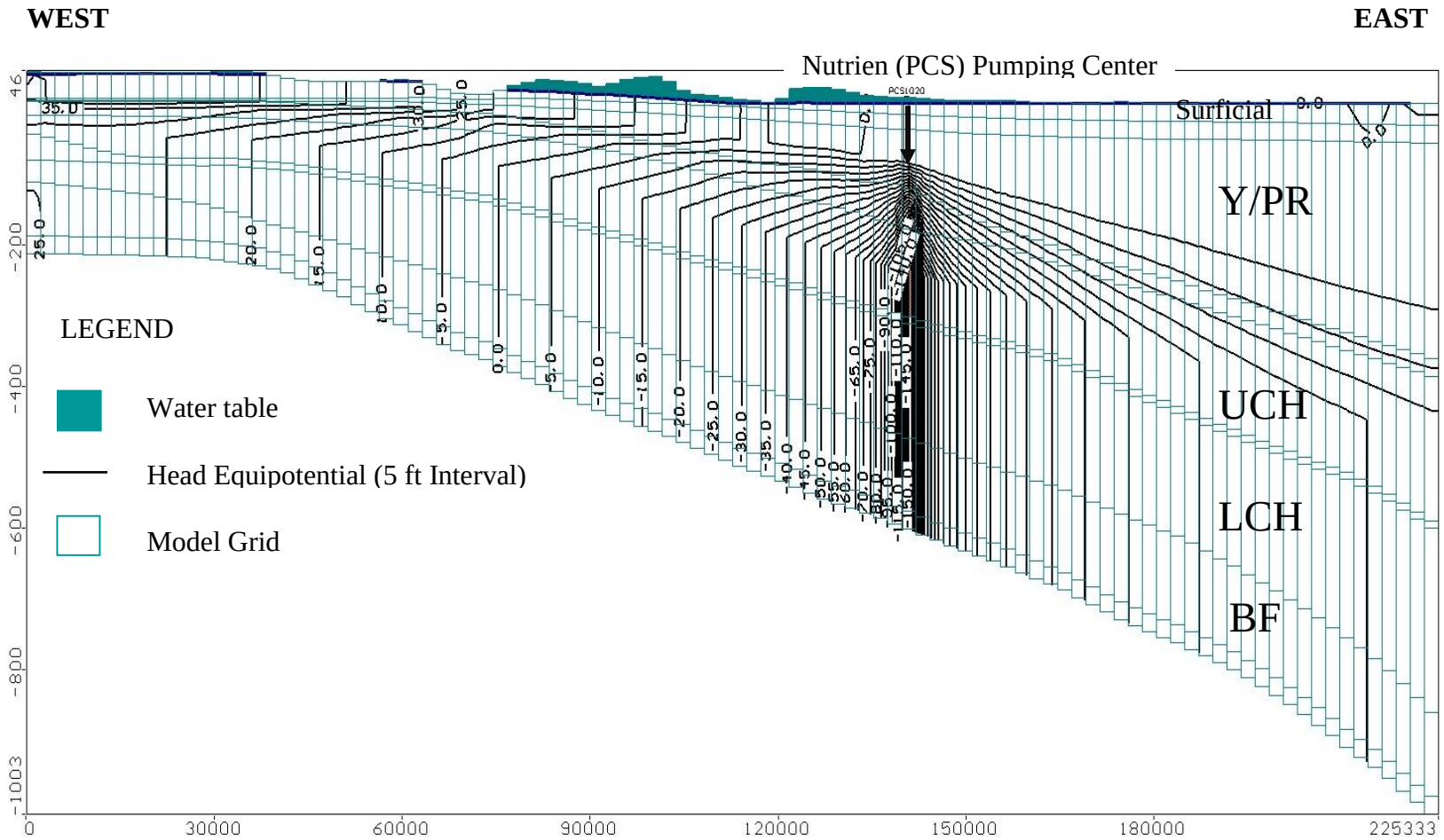

Figure 28. *Simulated head equipotential map of the Upper Castle Hayne Aquifer, cross-section through grid row 60. Datum is sea level.*

4.4 MODPATH Results

Particle tracking simulations were performed using effective porosity values of 15%, 26%, and 37% for the UCH limestone, and average values for representative geologic materials were applied to all other model layers. Simulations using varying effective porosity revealed that increasing the effective porosity results in decreasing average linear velocities (Table 11) and longer particle travel times (Table 12). During the particle tracking simulations, distances particles traveled, and sources did not vary. In other words, as effective porosity increases, groundwater moves more slowly, and groundwater particles require more time to travel the same distance, because the groundwater has more space to occupy. Thus, by applying the lowest value of effective porosity (15%) to the MODPATH simulations, the highest possible velocities and the shortest travel times of groundwater particles are calculated. For example, particles placed at the WWF2 sample location (southwestern portion of study area) had minimum total travel times of 730 years, 825 years, and 920 years with assigned effective porosities of 15%, 26% and 37 %, respectively.

Table 11. *Effects of varying effective porosity on groundwater velocity.*

	MODPATH Effective Porosity = 15%	**MODPATH Effective Porosity = 26%**	**MODPATH Effective Porosity = 37%**
Velocity Range feet/day	**0.002 - 22**	**0.0014 - 13**	**0.001 – 9.15**

Table 12. *Effects of varying effective porosity on groundwater travel time.*

Strontium Sample ID	**MODPATH Effective Porosity = 15%**	**MODPATH Effective Porosity = 26%**	**MODPATH Effective Porosity = 37%**
	Travel Time (years)	**Travel Time (years)**	**Travel Time (years)**
NUTRIEN	Min = 587	Min = 737	Min = 886
	Max = 1,262	Max = 1,773	Max = 1,920
	Avg = 1,091	Avg = 1,243	Avg = 1,400
MAS30/ P21NI	Min = 1,725	Min = 1,850	Min = 1,973
	Max = 4,738	Max = 4,872	Max = 5,006
	Avg = 3,823	Avg = 3,948	Avg = 4,072
P21K6	Min = 430	Min = 495	Min = 560
	Max = 455	Max = 525	Max = 595
	Avg = 4,440	Avg = 510	Avg = 577
WWF2	Min = 730	Min = 825	Min = 920
	Max = 790	Max = 885	Max = 980
	Avg = 757	Avg = 848	Avg = 940
TGS15	Min = 762	Min = 828	Min = 895
	Max = 783	Max = 851	Max = 919
	Avg = 771	Avg = 840	Avg = 905
O17I2	Min = 943	Min = 1,095	Min = 1,238
	Max = 961	Max = 1,118	Max = 1,284
	Avg = 950	Avg = 1,106	Avg = 1,260
O13F1	Min = 2,835	Min = 3,119	Min = 3,400
	Max = 3,942	Max = 4,260	Max = 4,580
	Avg = 3,226	Avg = 3,525	Avg = 3,825
Q15U3	Min = 2,124	Min = 2,356	Min = 2,590
	Max = 2,367	Max = 2,620	Max = 2,877
	Avg = 2,206	Avg = 2,441	Avg = 2,677
TGS11	Min = 1,687	Min = 1,838	Min = 1,985
	Max = 1,890	Max = 2,105	Max = 2,319
	Avg = 1,791	Avg = 1,973	Avg = 2,155
P1604	Min = 865	Min = 1,008	Min = 1,152
	Max = 1,266	Max = 1,406	Max = 1,545
	Avg = 1,036	Avg = 1,179	Avg = 1,323
TGS757	Min = 594	Min = 725	Min = 857
	Max = 746	Max = 907	Max = 1,069
	Avg = 642	Avg = 789	Avg = 938
TGS772	Min = 576	Min = 708	Min = 840
	Max = 628	Max = 775	Max = 923
	Avg = 602	Avg = 741	Avg = 880

All MODPATH simulations were performed under active pumping conditions. Results showed that the source of all simulated groundwater-particles is recharge infiltration from the land surface, and all flowpaths move downward into the UCH. MODPATH simulation results are provided in Appendix C. MODPATH simulations indicate that groundwater moves towards the mine from all directions (Figure 29). Vertical travel through the units overlying the UCH is much slower than horizontal travel through the UCH.

Assessment of varying effective porosity values determined that increasing the effective porosity of the UHC resulted in decreasing average linear velocities with longer travel times and decreasing the effective porosity value resulted in increasing average linear velocities with faster travel times (Tables 11 and 12). Overall, particles originating east of the mine show much longer travel times than particles that originate west of the mine (Table 12). Shorter vertical travel times for particles that originate in the west likely occur because the layers above the UCH are thinner west of the mine.

MODPATH results can only determine where groundwater particles were located at the time pumping began, about 50 years ago. Under the current influence of groundwater pumping, total travel time ranged from 430 years in the west, to 2,835 years in the east (Table 13). The minimum time required for particles to travel vertically through the units overlying the UCH, and reach the UCH is 320 years in the west and ranged up to 2,305 years in the east. Horizontal flow through the UCH ranged from 100 to 530 years. Groundwater travels through the UCH at velocities ranging from 0.02 to 0.07 miles per year (Table 13). Figure 30 presents the results of MODPATH simulations for Sr sample WWF2. Illustrations depicting the remaining Sr samples are provided in Appendix C.

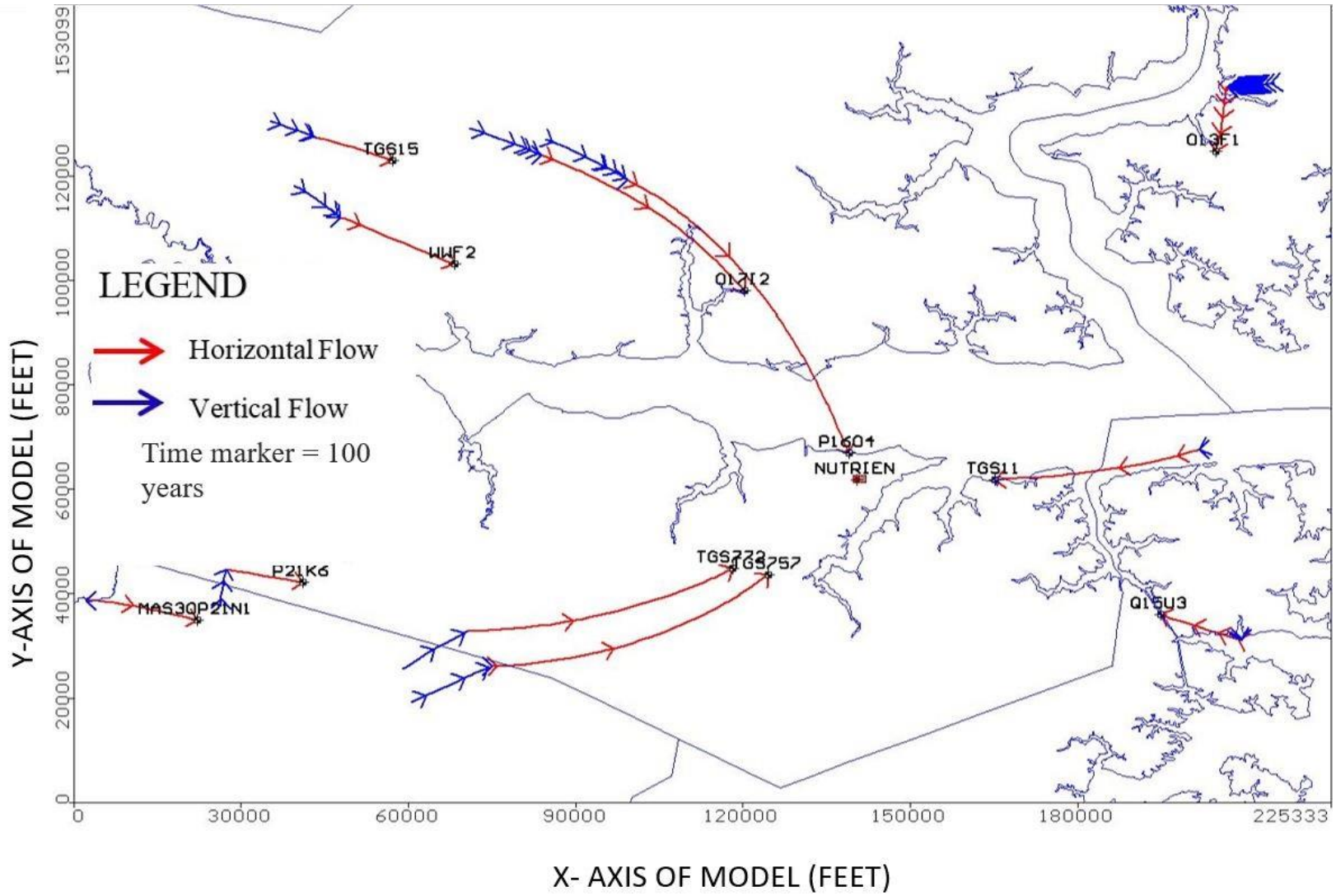

Figure 29. *Groundwater particle pathlines. The arrows are time markers, the space between each time marker represents 100 years of travel time. Blue lines indicate the particles are moving downward through units overlying the UCH, and red lines indicate the particles are travelling horizontally through the UCH.*

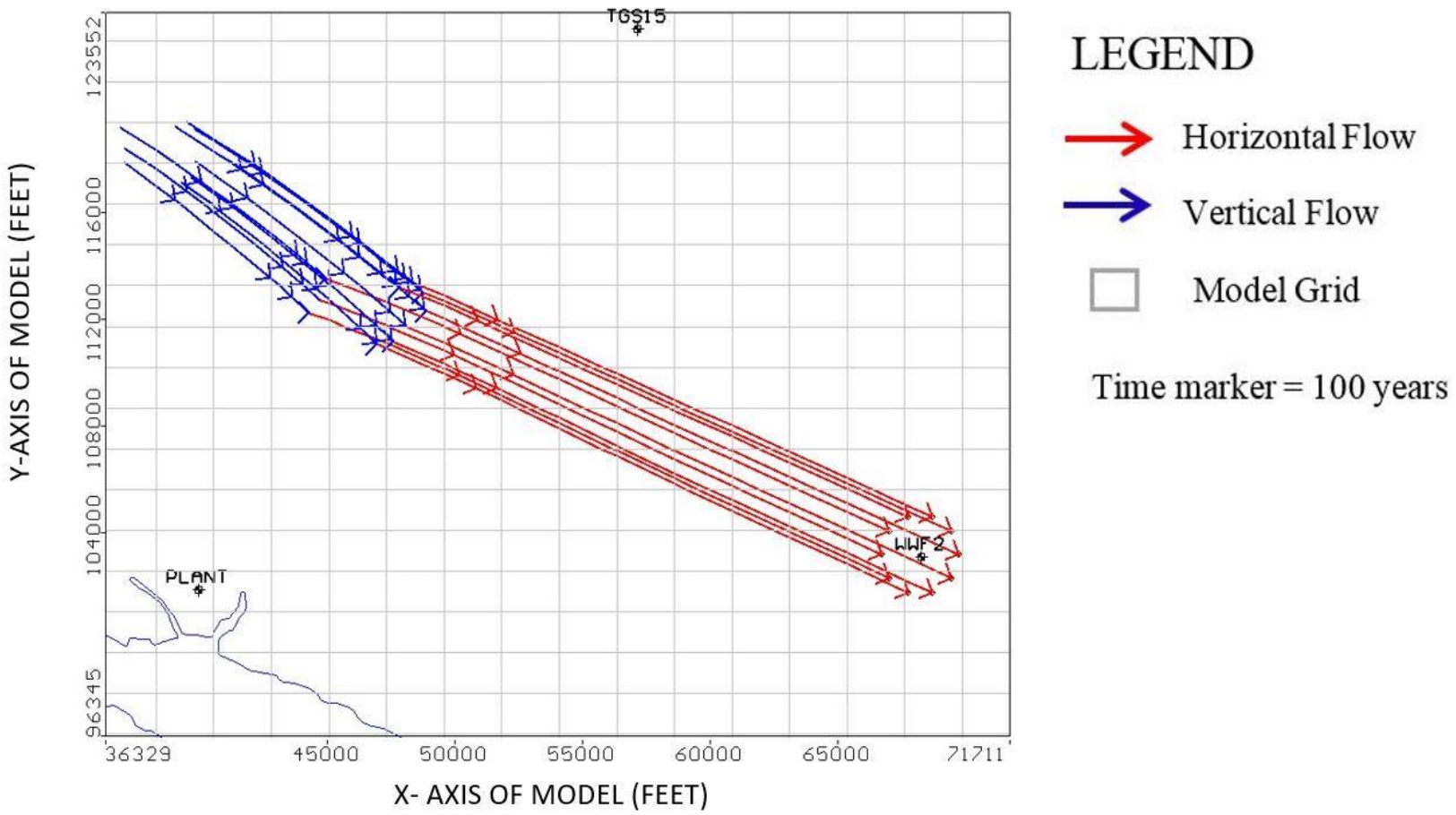

Figure 30. *Sr-sample WWF2 particle-tracking. The arrows are time markers, the space between each time marker represents 100 years of travel time. Blue lines indicate the particles are moving downward through units overlying the UCH, and red lines indicate the particles are travelling horizontally through the UCH.*

Table 13. MODPATH Simulations Under Current Pumping Conditions.

Sample ID	Total Average Travel Time in Years	Total Average Vertical Travel Time in Years	Total Average Horizontal Travel Time Through the UCH in Years	Average Rate of Horizontal Travel Through the UCH in Miles/Year
MAS30	1,725	1,525	200	0.020
P21K6	430	320	110	0.027
WWF2	730	580	150	0.027
TGS15	760	660	100	0.025
O17I2	943	573	370	0.025
O13F1	2,835	2,305	530	0.040
Q15U3	2,124	1,744	380	0.070
TGS11	1,687	1,337	350	0.020
P16O4	865	515	350	0.026
TGS757	594	394	200	0.050
TGS772	576	376	200	0.050

5.0 DISCUSSION

5.1 Piper Diagram and PCA Discussion

The chemical compositions of samples are dominated by mixed cations and bicarbonate. Statistical analyses conducted for this project confirmed the conclusions of Woods et al. (2000[b]), which indicate that the concentrations of chemical constituents in groundwater have been affected by carbonate dissolution, mineral precipitation, mixing of groundwater with saline water, recharge or leakage from other aquifers, cation exchange between water and aquifer materials, and reactions with soils before recharge. UCH wells in the western portion of the study area are calcium-rich and bicarbonate-rich (Figure 24), which indicates that dissolution of limestone is the predominant controller of groundwater chemistry in this area. UCH wells in the far northeastern portion of the NCCP are alkali-rich and chloride-rich, which suggest that mixing of freshwater with saline water is the dominant control on groundwater chemistry (Sutton, 1994). The ratio of $^{87}Sr/^{86}Sr$ for UCH groundwater steadily decreases from west to east, and strontium concentrations show a more complex pattern (Figure 12).

Principal Component Analysis determined that PC1 accounts for 43.43% of the variance in values observed for chemical parameters analyzed and shows strong positive correlations with Sr^{2+}, SO_4^{2-}, Cl^-, Na^+, and K^+, and strong negative correlation with $^{87}Sr/^{86}Sr$. As one of these variables increases, the others have a tendency to increase (Table 10). PC1 also shows a negative correlation with $^{87}Sr/^{86}Sr$. PC1 likely represents mixing of saline and fresh groundwater. Increasing ammonium (NH_4^+) with decreasing silicate $(SiO_4)^{4-}$ concentrations are also indicative of mixing between high silica/low ammonium groundwater with low silica/high ammonium saline water (Lecher, 2018).

PC2 accounts for 24.31% of variance and shows a strong correlation with Ca^{2+}, pH, and HCO_3 (Table 10). PC2 appears to be related to limestone dissolution which results in an increase in Ca^{2+}, and in a complex pattern of changes in pH and HCO_3^-.

Other correlations that provide significant insights include the negative correlation between the strontium-isotopic ratios and the ratios of carbon and oxygen isotopes, which is logical because the strontium-isotopic ratios decrease downgradient as the water incorporates more Sr, Ca^{2+}, and HCO_3^- from aquifer materials. Carbon and oxygen isotopic signatures increase eastward. The carbon-isotopic signature increases as the groundwater incorporates carbon from the limestone, which has a much higher ratio than the recharge water that originally entered the aquifer (Brown, 1999). The oxygen isotopic ratios increase eastward as the age of the groundwater increases, and it reflects the higher $^{18}O/^{16}O$ ratio of the original precipitation that recharged the aquifer during the Last Glacial Maximum (Plummer, 1993).

5.2 MODPATH Simulation Results and Strontium Mixing-Model Comparison

The objective of this study was to assess the results of a strontium-isotope-based geochemical study by analyzing groundwater flow in the CHAS. A Visual MODFLOW model was developed to simulate groundwater flow in the CHAS, and MODPATH simulations were performed to produce groundwater flowpaths. The aim was to see if strontium-isotopic analysis can reliably identify vertical groundwater movement between aquifers and their associated confining layers. Comparisons between the MODPATH simulations and the strontium study are summarized in Table 14.

Sources of strontium to UCH water, suggested by the strontium-isotopic mixing line include: the downward movement of brackish water from the Pamlico River estuary, downward

movement of brackish water from the Pungo River and Yorktown Aquifers, upward flow of water from the Lower Castle Hayne and the Beaufort Aquifers, westward movement of the freshwater-saltwater interface within the Upper Castle Hayne, and lateral migration of brackish water lenses in the UCH (Woods et al., 2000[a]).

MODPATH simulations only showed downward-directed groundwater movement, indicating many discrepancies between the MODPATH simulations and predictions of the Sr-mixing model. Therefore, the model's groundwater-flow vectors were also analyzed. Groundwater-flow vectors indicate direction of groundwater flow in the model. Groundwater direction-vector analyses show that under pumping conditions, groundwater moves vertically downward across the entire study area, and that more water is moving downward than upward. Groundwater moves vertically down from the land surface through the Surficial and overlying units and into the UCH. Direction vectors also revealed that under pumping conditions, upward flow from the LCH and BF occurs within 4,500 feet of the mine, but nowhere else in the model (Figures 31 and 32).

Table 14. Strontium-Mixing Model and MODPATH Simulation Comparison

Well ID	**Sr** (mg/L)	$^{87}Sr/^{86}Sr$	**Plot against mixing line**	**Sr prediction**	**MODPATH effective porosity = 15%** **Water Age**	**Model-Predicted Water Source**	**Good match?**
MAS30/P21N1	0.1780	0.707991	below and to the left	upward leakage from units below the UCH	minimum 1,725 years	Land surface, up-dip in UCH	no
P21K6	0.3010	0.70881	below and to the left	upward leakage from units below the UCH	minimum 430 years	Land surface, recharge originates from the south, up-dip in the UCH	no
WWF2	0.3000	0.709096	below and to the left	suggests upward leakage from units below the UCH	minimum 730 years	Land surface, recharge originates from the west, up-dip in UCH	no
TGS15	0.6320	0.709263	above and to the right	Leakage from above or a source of saline water	minimum 762 years	Land surface, recharge originates from the west, up-dip in UCH	yes

Table 14. Strontium-Mixing Model and MODPATH Simulation Comparison

Well ID	**Sr** (mg/L)	**$^{87}Sr/^{86}Sr$**	**Plot against mixing line**	**Sr prediction**	**MODPATH effective porosity = 15%** **Water Age**	**Model-Predicted Water Source**	**Good match?**
TGS11	0.7170	0.708555	on or very close to the line	little vertical movement, or movement from above and below, that cancels out the Sr-signal	minimum 1,687 years	Land surface, recharge originates from the east, down-dip in UCH	yes
P16O4	0.9000	0.708547			minimum 865 years	Land surface, recharge originates from the north, up-dip in UCH	yes
TGS757	0.6790	0.708688			minimum 594 years	Land surface, recharge originates from the southwest, up-dip in UCH	yes
TGS772	0.7000	0.708722			minimum 576 years	Land surface, recharge originates from the southwest, up-dip in UCH	yes

Table 14. Strontium-Mixing Model and MODPATH Simulation Comparison

Well ID	**Sr** (mg/L)	$^{87}Sr/^{86}Sr$	**Plot against mixing line**	**Sr prediction**	**MODPATH effective porosity = 15%** **Water Age**	**Model-Predicted Water Source**	**Good match?**
O17I2	0.958	0.708699	above and to the right	Leakage from above or a source of saline water	minimum 943 years	Land surface, recharge originates from the north, up-dip in UCH	yes
O13F1	0.824	0.708308	below and to the left	suggests upward leakage from units below the UCH	minimum 2,835 years	Land surface, recharge originates from the east, down-dip in UCH	no
Q15U3	1.118	0.708158	below and to the left	suggests upward leakage from units below the UCH	minimum 2,124 years	Land surface, recharge originates from the east, down-dip in UCH	no

MODPATH simulations support the predictions of the Sr-mixing model for Sr-samples: P16O4, TGS772, TGS757, and TGS11. These samples plot close enough to the line to suggest that the main factor influencing the groundwater at these locations is the dissolution of UCH limestone, which suggests that there is only insignificant vertical flow from above or below the UHC at these locations. MODPATH simulations did not indicate a source of water, other than initial influx from above (recharge from infiltration), followed by downgradient flow through the UCH. Also, the amount of time required for groundwater particles to travel from the land surface to the Sr-sample location ranged from 576 to 1,687 years and of the total travel time, at least 200 to 350 years is required for groundwater particles to travel horizontally through the UCH to the Sr-sample location. Therefore, this also supports the conclusions drawn from the Sr-mixing model. Furthermore, groundwater-flow vector analysis concluded that these samples (except for Sr-sample P16O4) fall outside of the 4,500 ft area of upconing at the mine, therefore upward or downward flow does not occur near theses sample locations.

MODPATH simulations also support the predictions of the Sr-mixing model for Sr-samples: TGS15 and O17I2. These samples plot above and to the right of the mixing line, which suggests a source of water has raised the $^{87}Sr/^{86}Sr$ ratio and/or the [Sr] content of these samples. The processes that could produce the Sr-signature of these samples include: the influx of high $^{87}Sr/^{86}Sr$ water from above and saline water influx. In the eastern part of the study area (Sr-sample O17I2), westward movement of the freshwater-saltwater interface could be a contributing factor. However, the freshwater-saltwater interface would not have an impact at the western location of Sr-sample TGS15. The $^{87}Sr/^{86}Sr$ of this sample could possibly be explained by an abundance of water coming from or passing through the Surficial Aquifer at a point where this

aquifer contains unusually large amounts of tecto-silicates (potassium-feldspar and mica) with abundant crystallographic sites for Rb.

Sr-samples that show discrepancy between the groundwater model and the Sr-mixing model include: WWF2, P21K6, MAS30, O13F1, and Q15U3. These samples plot below and to the left of the Sr-mixing line. Based on the pattern of change in the $^{87}Sr/^{86}Sr$ ratios observed for Coastal Plain formations, the lowered $^{87}Sr/^{86}Sr$ ratios of these samples could be a result of upward flow of water from higher $^{87}Sr/^{86}Sr$ ratio aquifers underlying the UCH. However, the positions of these samples with respect to the mixing line could also have been altered by influx of water with extremely low [Sr] that would dilute their [Sr] without changing their $^{87}Sr/^{86}Sr$ ratio. The origin of such water is very difficult to conceive unless the integrity of these well casings has been compromised and unaltered rainwater has been regularly introduced. MODPATH simulations and groundwater-flow vector analysis, under pumping conditions did not indicate any upward movement of water near these sample locations.

5.2.1 Non-pumping Simulations

Initially all MODPATH simulations were performed with an active pumping center at Nutrien, which could explain why there is not better agreement between the Sr-model and the flow-model results. To try to explain the discrepancies, non-pumping simulations were performed, and groundwater-flow vectors were analyzed.

Under non-pumping conditions, groundwater direction-vectors showed upward movement from the LCH or the BF for samples WWF2, O13F1, and Q15U3. Figure 31 illustrates predicted upward flow near Sr-sample O13F1, and Figure 32 illustrates upward flow near Sr-sample WWF2. This could indicate that prior to extensive pumping, the equipotential

surfaces of the LCH and the BF aquifers were greater than that of the UCH (simulated in Figure 33), and upward flow into the UCH occurred. This scenario provides an explanation for the Sr-signatures of samples WWF2, O13F1, and Q15U3.

MODPATH simulations and groundwater-flow vectors (pumping and non-pumping) did not confirm the Sr-model predictions for Sr-samples MAS30 and P21K6. The Sr-study suggests that samples MAS30 and P21K6 have been influenced by groundwater moving upward from below the UCH. However, MODPATH simulations with pumping active and inactive did not show this process. A plausible explanation of these samples having a low $^{87}Sr/^{86}Sr$ would be that there is more interconnectivity between the UCH and the LCH at these locations. This would occur if the confining layer between the UCH and LCH is absent.

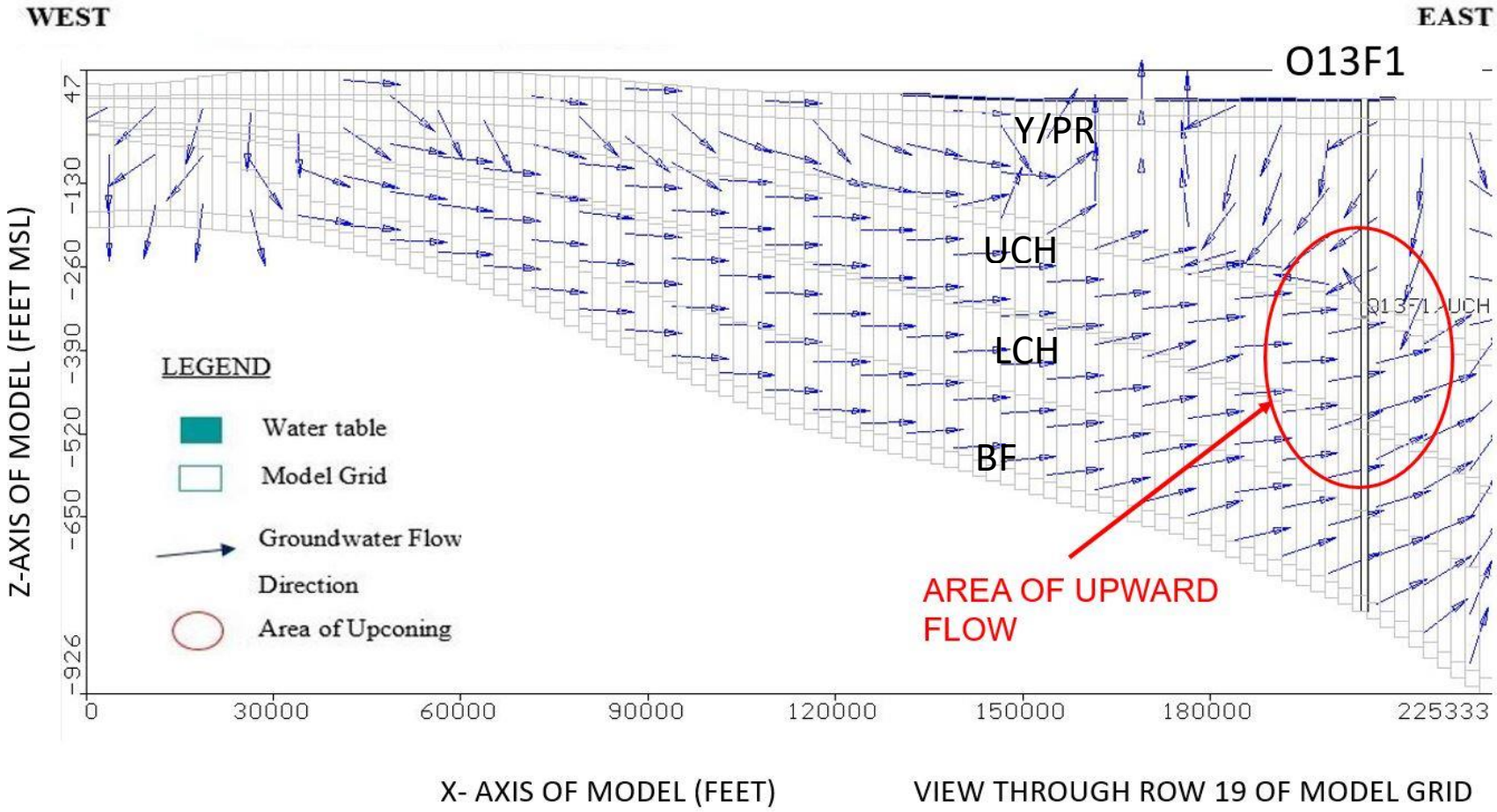

Figure 31. Non-pumping simulation Sr-sample O13F1. Datum is sea level. Area within the red circle shows upward flow from the LCH and BF aquifers to the UCH near the O13F1 Sr sample location.

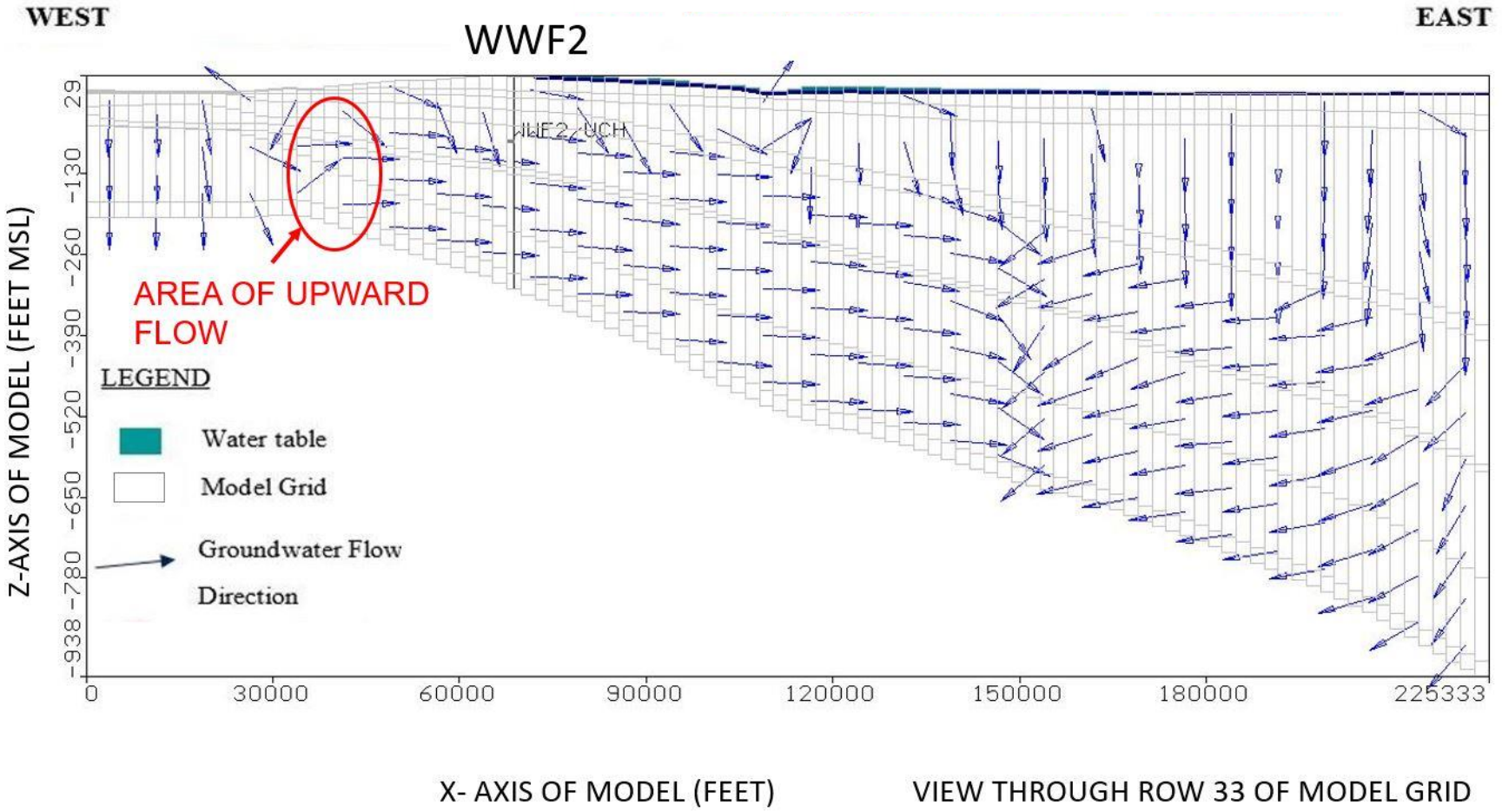

Figure 32. Non-pumping simulation Sr-sample WWF2. Datum is sea level. Area within the red circle shows upward flow from the LCH and BF aquifers to the UCH near the WWF2 Sr-sample location.

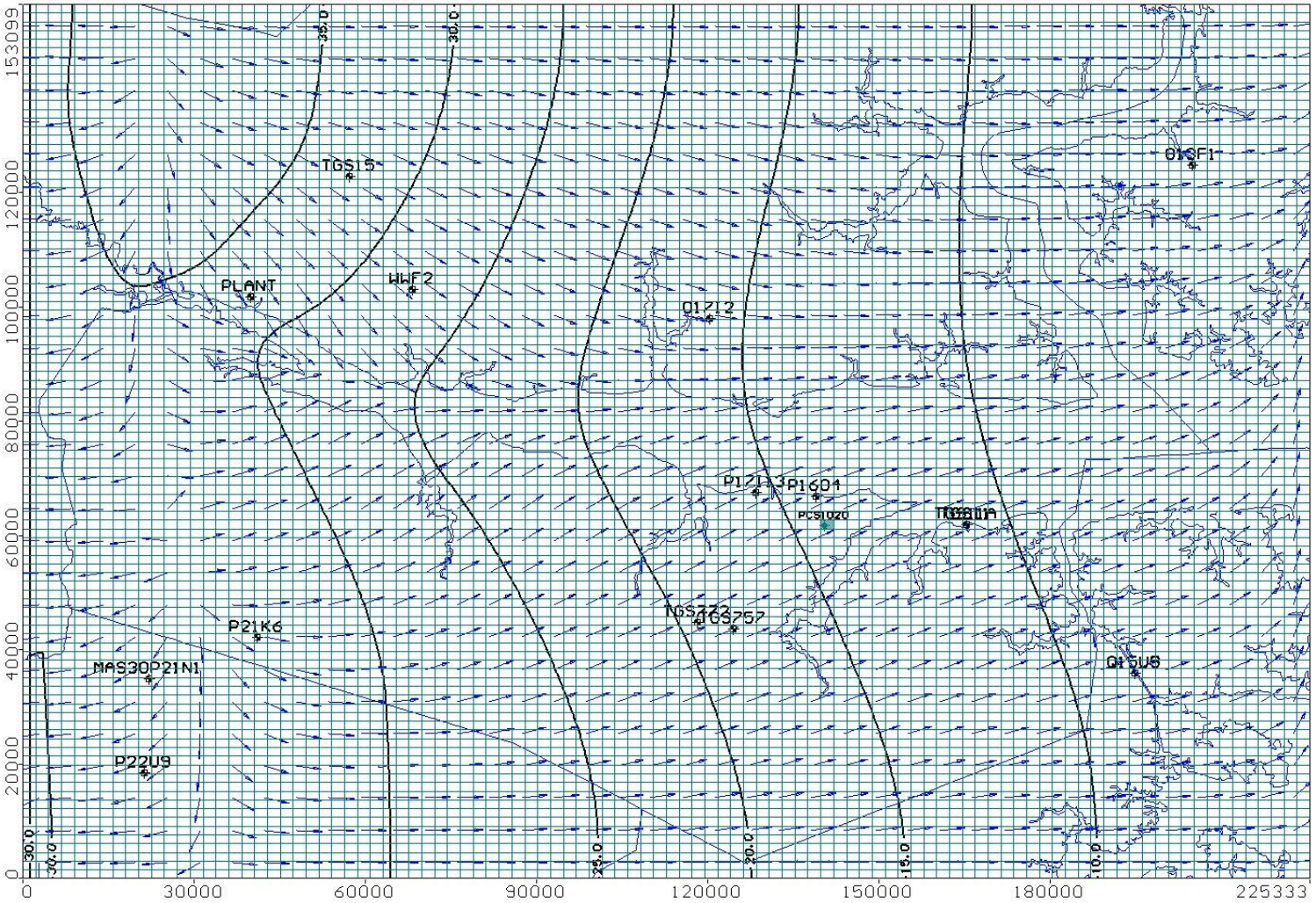

Figure 33. Non-pumping equipotential map of the Upper Castle Hayne Aquifer. Datum is sea level. Contour interval is 5 feet.

5.2.2 Additional Factors Potentially Explaining Discrepancies Between Models

Additional factors that could potentially explain the discrepancies between the groundwater model, the MODAPTH simulations, and the Sr-mixing model include:

- The Sr-composition of the Surficial Aquifer sample used to develop the mixing line, if the Sr-composition changes or differs, the position of the mixing line will shift.
- Water entering the UCH may be coming from more than one source, and a more complicated (e.g. three-component) Sr-mixing model may be required to explain deviations from the two-component mixing line.
- Flaws in well integrity, for example, a leaky casing seal could allow contribution of water from overlying units.
- Sr-residence time calculations, as well as, the evolution of $^{87}Sr/^{86}Sr$ in groundwater over time along flowpaths. If upward leakage in the western recharge areas occurred at some time prior to extensive pumping, it is possible that the Sr-signature of groundwater at these locations has only been impacted by the hydrogeologic processes that occurred prior to the 1960's, and perhaps are not being significantly influenced by pumping. Perhaps these samples are in areas where there is more interconnectivity between the UCH and the underlying LCH and BF aquifers than expected.

5.3 Model and Study Limitations

Most input parameters for this model have been well established by previous studies and existing data. However, groundwater flow models are limited by the quality and quantity of the

input data (Groundwater Management Associates, 2013), and the results of any simulation are subject to the accuracy of the simulation calibration. Head, river stage, precipitation rates, and pumping rates are variable with time, thus true steady-state conditions do not exist. However, steady-state simulations do represent long term or average flow conditions (Groundwater Management Associates, 2013). Differences between observed and simulated heads are limited by model properties and assumptions made during model development, with the most significant assumption being that the UCH is a homogeneous aquifer.

The choice of model boundaries may also contribute to the model limitations because, the western boundaries were simulated by placing specified-head boundaries (constant-head boundaries in MODFLOW) along lines of known head, or equipotential maps, using observed head data from 2017. MODFLOW does not solve for head in these cells, so the head value remains fixed at the assigned specified head value. This means that the model will supply or remove an infinite amount of water to keep the specified heads set to their assigned values. To determine the impact of constant-head boundaries on this model, another version of the model was made with head-dependent flux boundaries (general-head boundaries in MODFLOW) assigned in place of the constant-head boundaries. General-head boundaries were used to simulate the continuation of the aquifer outside the model domain where physical boundaries occur (the fall line in the west and the freshwater-saltwater interface to the east). General-head boundaries are assigned by defining a hydraulic head and a conductance value. The general-head boundary adds or removes water to adjacent cells with different hydraulic head, based on an assigned hydraulic head and a threshold conductance expressed in ft^2/day. The flow to adjacent cells is not allowed to exceed the conductance of the general head boundary (Groundwater Management Associates, 2013). To calculate the general-head boundary conductance, Visual

MODFLOW uses a default formula that is based on the distance to the hydraulic boundary to be represented, and the average hydraulic conductivity of the aquifer in which the boundary occurs.

Error statistics for the general-head boundary model are as follows: the RMS is 6.794 ft, the NRMS was 4.873%, and the correlation coefficient was 0.984, for all the model layers. The constant-head boundary model error statistics are as follows: the RMS is 5.856 ft, the NRMS was 4.637%, and the correlation coefficient was 0.986, for all the model layers. Both boundary scenarios produced a similar cone of depression, and the error statistics were similar. For example, the differences between the RMS values produced by each modeling scenario were less than 1.0 foot. Therefore, it was not possible to ascertain which boundary scenario was more favorable for the steady-state simulation. However, if the model was used to simulate a change in the system, then the type of boundary used would be more significant.

MODPATH is limited in its capabilities especially when using reverse particle tracking, as this program was designed only to track groundwater particles to their recharge sources. A more sensitive analysis, including an analysis of strontium-residence times, is required to fully understand how the strontium signatures can be supported by groundwater flow paths.

6.0 CONCLUSIONS

A previous study by Woods et al. (2000[a]) concluded that an evaluation of the strontium chemistry of groundwater from the UCH could indicate sources of Sr input to the aquifer from surface waters, dissolution of limestone, or movement from underlying/overlying aquifers.

The Piper Diagram used to characterize hydrochemical facies of UCH/LCH groundwater from the NCCP revealed that UCH wells to the far west of the NCCP are calcium-rich and bicarbonate-rich, and wells in the far northeastern portion of the NCCP are alkali-rich and chloride-rich; chloride is the dominant anion of the LCH. LCH samples tend to be more chloride-rich than UCH samples from the same site. In both the UCH and LCH, chloride concentrations increase from west to east and TDS generally increase from west to east, but the highest concentrations are in the northeast. Eastward increases of TDS are due to increased mixing of saline water. Samples from the Peedee Aquifer are calcium-bicarbonate-rich. Samples from the Black Creek and Cape Fear Aquifers tend to be more sodium-chloride rich rather than calcium-bicarbonate rich, which is attributed to their non-carbonate lithologies.

A Principal Component Analysis considering 18 typical hydrochemical variables yielded four Principal Components (PC1-PC4), which together explained 86.82% of the variance in groundwater chemistry in the UCH. The Component Loadings produced by this statistical model indicated strong correlations between:

- PC1 and Sr^{2+}, SO_4^{2-}, Cl^-, Na^+, K^+, NH_4^+, F^-, PO_4^{3-}, $^{18}O/^{16}O$, and $^{13}C/^{12}C$.
- PC2 and Ca^{+2}, pH, HCO_3^-, $NO_3^- + NO_2^-$, PO_4^{3-}, F^- and Fe.
- PC3 and SiO_2, $NO_3^- + NO_2^-$, and Mg^{2+}.
- PC4 and HCO_3^-, PO_4^{3-}, and Fe.

Based on these Component Loadings, PC1 represents influx of saline water into the UCH and PC2 represents the impact of limestone dissolution on water chemistry. The exact nature of the processes represented by PC3 and PC4 could not be determined.

The Visual MOFDFLOW model generated a simulated equipotential map that was compared to the observed equipotential map of 2017. The location, size, depth and shape of the cone of depression produced by the model is similar to the observed equipotential map generated from the 2017 water level data. The natural, pre-pumping, equipotential surface for the UCH was sloping from the recharge area in the west toward the discharge areas, east of the Nutrien mine. The pumping active model shows that groundwater in the UCH is moving toward the mine from all directions.

Most input parameters for this model have been well established by previous studies and existing data, however, differences between observed and simulated heads are limited by model properties and assumptions made during model development, with the most significant assumption being that the UCH is a homogeneous aquifer. Comparison of model results using general-head versus constant-head boundaries at the eastern and western edges of the model indicated similar cones of depression and error statistics.

Particle tracking simulations performed with MODPATH under current pumping conditions, and using effective porosities of 15%, 26% and 37 % for the UCH, yielded minimum total travel times from Earth's surface to well screens of 730 years, 825 years, and 920 years, respectively, and groundwater velocities of 0.002-22, 0.0014-13, and 0.001-9.15 (feet/day), respectively. Overall, particles originating east of the mine show much longer travel times than particles that originate west of the mine. Shorter vertical travel times for particles that originate in the west likely occur because the layers above the UCH are thinner west of the mine.

MODPATH results determined that groundwater moves downward from the land surface through overlying Surficial, Yorktown/Pungo River units and the Upper Castle Hayne Confining Layer. Upon entering the UCH, groundwater moves horizontally in the direction of the phosphate mine. For the majority of locations MODPATH simulations under pumping conditions did not indicate groundwater moving upward from the LCH and the BF into the UCH. However, when groundwater-flow vectors of the Visual MODFLOW model were assessed under pumping conditions, the model did show an area of upward flow within 4,500 feet of the mine, but nowhere else in the model.

MODPATH simulation results performed under pumping conditions often conflicted with the conclusions drawn from the Sr-model, except where the Sr-analysis indicate downward flow from the Surficial Aquifer through the overlying units.

MODPATH simulations did not indicate a source of water, other than initial influx from above (recharge from infiltration), which supports the predictions of the strontium mixing study for Sr-samples: P16O4, TGS772, TGS757, and TGS11. These samples plot close enough to the line to suggest that the main factor influencing the groundwater chemistry at these locations is the dissolution of UCH limestone, which suggests that there is no significant vertical flow from above or below the UCH at these locations.

MODPATH simulations also support the predictions of the Sr-model for Sr-samples: TGS15 and O17I2. These samples plot above and to the right of the mixing line. In the eastern part of the study area (Sr-sample O17I2), westward movement of the freshwater-saltwater interface could be a contributing factor. However, the freshwater-saltwater interface would not have an impact at the western location of Sr-sample TGS15, but the $^{87}Sr/^{86}Sr$ of this sample could be explained by an abundance of water coming from or passing through the Surficial

Aquifer at a point where this aquifer contains unusually large amounts of tecto-silicates (potassium-feldspar and mica) with abundant crystallographic sites for Rb. It is also possible that a lens of saltwater from the last sea-level transgressive event may have been trapped in the UCH (or an overlying aquifer) near this point.

The equipotential surface of the UCH produced during non-pumping simulations showed a gently sloping surface, where the principal direction of groundwater flow is from west to east. During non-pumping simulations, groundwater-flow vectors showed upward groundwater movement from the LCH and BF going into the UCH, in areas near WWF2, Q15U3, and O13F1. This means that vertical movement of water from units below the UCH could have occurred prior to pumping.

MODAPTH simulations and groundwater-flow vectors (pumping and non-pumping) did not confirm the Sr-model predictions for Sr-samples MAS30 and P21K6. The Sr-model suggests that these samples have been influenced by groundwater moving upward from units below the UCH. However, MODPATH simulations with pumping active and inactive did not show this process. A plausible explanation of these samples having a low $^{87}Sr/^{86}Sr$ would be that there is more interconnectivity between the UCH and the LCH at these locations. This would occur if the confining layer between the UCH and LCH is absent.

The model was not calibrated to conditions that existed before pumping began, as the availability of pre-pumping data is severely limited. However, a regional flow model calibrated to pre-pumping conditions is necessary to understand the natural flow patterns that existed before extensive pumping began, and changes that have occurred since. The results of this study show that prior to extensive pumping, the equipotential surfaces of the LCH and the

BF aquifers could have been greater than the UCH, which would have allowed upward flow into the UCH, thereby adding support to the conclusions drawn from the Sr-model.

7.0 REFERENCES

Akland, M., 2017, Origin and geochemical evolution of localized, high-ferrous-iron zones in the Upper Castle Hayne aquifer, Beaufort County, North Carolina [M.S. Thesis]: East Carolina University, 421 p.

Anderson, M. and W. Woessner. 2002. Applied Groundwater Modeling Simulation of Flow and Advective Transport. San Diego California: Academic Press.

Bakari, S.S, Aagaard P., Vogt, R.D., Ruden, F., Johansen, I., and Vuai, S., 2012, Delineation of groundwater provenance in a coastal aquifer using statistical and isotopic methods, Southeast Tanzania: Environmental Earth Sciences, v. 66, p. 889-902.

Bakari, S.S, Aagaard P., Vogt, R.D., Ruden, F., Johansen, I., and Vuai, S., 2013, Strontium isotopes as tracers for quantifying mixing of groundwater in the alluvial plain of a coastal watershed, south-eastern Tanzania: Journal of Geochemical Exploration, v. 130, p. 1-14.

Bales, J.D., Chapman, M.J., Oblinger, C.J., and Robbins, J.C., 2004, North Carolina District Science Plan. Science Goals for 2003-2008: U.S. Geological Survey Open-File Report 2004-1025, 1 p.

Banner, J.L., 1995, Application of the trace element and isotopic geochemistry of strontium to studies of carbonate diagenesis: Journal of Sedimentology, v. 42, p. 805-824.

Banner, J.L., Wasserburg, G.J., Dobson, P.F., Carpenter, A.B., and Moore, C.H., 1989, Isotopic and trace element constraints on the origin and evolutions of saline groundwater from central Missouri: Geochem. Cosmochim. Acta 53, p. 383-398.

Beck, E.G, 1997, Groundwater Geochemistry of the Castle Hayne Aquifer System in the North Carolina Coastal Plain [M.S. Thesis]: East Carolina University, 157 p.

Bogdon, C., 2012, http://www.novametrixgm.com/blog/what-is-modflow (accessed June 2018).

Brown, R.,1999, Groundwater Geochemistry of the Castle Hayne Aquifer [M.S. Thesis]: East Carolina University, 104 p.

Cander, H.S., 1994, An example of mixing-zone dolomite, Middle Eocene Avon Park Formation, Floridan aquifer system: Journal of Sedimentary Research A: Sedimentary Petrology & Processes, p. 615-629.

Collerson, K.D., 1988, Ground waters with unradiogenic $^{87}Sr/^{86}Sr$ ratios in the Great Artesian Basin, Australia: Geology (Boulder), v. 16, p. 59-63.

Consolvo, C.A., 1998, Hydrologic investigation and wellhead protection planning for the Castle Hayne Aquifer near Washington, North Carolina [M.S. Thesis]: East Carolina University, 140 p.

Denison, R.E., Hetherington, E.A., Bishop, B.A. and Dahl, D.A., 1993, The use of strontium isotopes in stratigraphic studies: an example from North Carolina: Southeastern Geology, v. 33, p. 53-69.

DeWiest, R.J.M., 1969, Hydrologic relationship between the Pamlico River and the Castle Hayne aquifer in Eastern North Carolina: Reston, Virginia, American Society of Civil Engineers, Annual Meeting on Water Resources Engineering Preprint 830, p. 2-19.

Driscoll, F.G., 1986, Groundwater and wells: St. Paul, Minnesota, Johnson Division, UOP Inc., 1108 p.

Faure, G., 1998, Principles and Applications of Geochemistry 2nd Edition: Upper Saddle River, N.J., Prentice Hall, 624 p.

Freethey, G.W., Spangler, L.E., and Monheiser, W.J., 1994, Determination of Hydrologic Properties Needed to Calculate Average Linear Velocity and Travel Time of Groundwater in the Principal Aquifer Underlying the South-Eastern Part of Salt Lake Valley, Utah. Geological Survey Water-Resources Investigations Report 92-4085, 11 p.

Fullagar, P.D., 2003, Personal communication.

Gamus, W.J., 1972, Analysis of Factors Controlling Groundwater Flow for Prediction of Rates of Groundwater Movement and Changes in Quality, Atlantic Coastal Plain [Ph.D. Diss.]: University of Arizona.

Giese, G.L., Eimers, J.L., and Coble, R.W., 1997, Simulation of ground-water flow in the coastal plain aquifer system of North Carolina: US Geological Survey Professional Paper, 1404-M, p. M1-M142.

Groundwater Management Associates Inc., 2013, Groundwater Model for the Depressurization of the PotashCorp Aurora Phosphate Mine, Beaufort County, North Carolina, p. 1-20.

Harned, D.A., Lloyd, O.B., Jr, and Treece, M.W.J., 1989, Assessment of hydrologic and hydrogeologic data at Camp Lejeune Marine Corps base, North Carolina., U.S. Geological Survey, Water-Resources Investigations Report 89-4096, 64 p.

Heath, R., 1983, Basic Ground-Water Hydrology. U.S. Geological Survey Water-Supply Paper 2220, p. 1-8.

Hudak, P., 1999, Principles of Hydrogeology, Second Edition: Boca Raton, Florida, CRC Press, 40 p.

Jacobson, A.D. and Wasserburg. G.J., 2005, Anhydrite and the Sr isotope evolution of groundwater in a carbonate aquifer: Chemical Geology, v. 214, p. 331-350.

Johnson, P.K., 2007, Characterization of Surface water/groundwater interactions along a coastal plain river [M.S. Thesis]: East Carolina University, 215 p.

Katz, B.G. and Bullen, T.D., 1996, The combined use of $^{87}Sr/^{86}Sr$ and carbon and water isotopes to study the hydrochemical interaction between groundwater and lake water in mantled karst: Geochem. Cosmochim., Acta 60, p. 5075-5087.

Kelly, B.P., 2002, Ground-water flow simulation and chemical and isotopic mixing equation analysis to determine source contributions to the Missouri River alluvial aquifer in the vicinity of the Independence, Missouri, Well Field: U.S. Geological Survey Water-Resources Investigations Report 2002-4208, 31 p.

Kresic, N., 2007, Hydrogeology and Groundwater Modeling: Boca Raton, Florida, CRC Press, 600 p.

Lautier, J.C., 2001, Hydrogeologic Framework and Ground Water Conditions in the North Carolina Central Coastal Plain, North Carolina Department of Environment and Natural Resources, Division of Water Resources, p. 1-38.

Leahy, P.P., and Martin, M., 1993, Geohydrology and Simulation of Ground-Water Flow in the Northern Atlantic Coastal Plain Aquifer System: U.S. Geological Survey Professional Paper 1404-K, p. K1

Lecher, A., 2018, Quantifying Processes Governing Nutrient Concentrations in a Coastal Aquifer via Principal Component Analysis: Hydrology, v. 5, p. 15.

Lohman, S.W., 1972, Definitions of selected groundwater terms-revisions and conceptual refinements: U.S. Geological Survey Water-Supply Paper 1988, 21 p.

Lyke, W.L. and Treece, M.W. Jr., 1988, Hydrogeology and effects of ground-water withdrawals in the Castle Hayne aquifer in coastal North Carolina, in Lyke and Hoban (eds.), Proceedings of the AWRA Symposium on Coastal Water Resources, Wilmington, N.C., May 22-25, 1988: Bethesda, Md., American Water Resources Association, p. 469-478.

McDonald, M.G., and Harbaugh, A.W., 1988, A modular three-dimensional finite-difference ground-water flow model: U.S. Geological Survey, Techniques of Water-Resources Investigations, v. 06-A1, p. 567.

Meisler, Harold, 1989, The Occurrence and Geochemistry of Salty Groundwater in the North Atlantic Coastal Plain: U.S. Geological Survey Professional Paper, v. 1404 D, 13 p.

McNutt, R.H., Frape, S.K., Fritz, P., Jones, M.G., and MacDonald, I.M., 1990, The $^{87}Sr/^{86}Sr$ values of Canadian Shield brines and fracture minerals with applications to groundwater mixing, fracture history, and geochronology: Geochim. Cosmochim, Acta 54, p. 205-215.

North Carolina Geological Survey (NCGS), 1985, Geologic map of North Carolina: North Carolina Geological Survey, General Geologic Map, scale 1:500000.

North Carolina Department of Water and Air Resources; W.F. Guyton and Associates; Legette, Brashers and Graham; Harshbarger and Associates; and W.C. Walton, 1971, Report on Hydrogeology and Effects of Pumping from Castle Hayne Aquifer System Beaufort County, North Carolina, p. 1-52.

Piper, A.M., 1944, A graphic procedure in the geochemical interpretation of water-analyses: Transactions - American Geophysical Union, v. 25, p. 914-928.

Neal, D.W., Simms, C.S., and Barr, J., 2013, Porosity of the Eocene Castle Hayne Limestone, Central Coastal Plain, NC: Geological Society of America Abstracts with Programs, v. 45, no. 2, p.13.

Plummer, N.L., 1993, Stable isotope enrichment in paleo waters of the Southeast Atlantic Coastal Plain, United States: Science, v. 262, 5 p.

Pollock, D.W., 1994, User's Guide for MODPATH/MODPAT-PLOT, Version 3- A particle-tracking post-processing package for MODFLOW, the U.S. Geological Survey finite-difference groundwater flow model: U.S. Geological Survey, Open-File Report 94-464, p. 3.

Reynolds, J.W., 1992, Aquifer depressurization for mining at Texasgulf, Inc.: Evaluation and modeling of hydrogeologic impacts and potential mitigative strategies [M.S. Thesis]: East Carolina University, 140 p.

Reynolds, J.W., and Spruill, R.K., 1995, Ground-water flow simulation for the management of a regulated aquifer system: A case study in the North Carolina Coastal Plain: Groundwater, v. 33, p. 741-748.

Sherwani, J. K., 1980, Public policy for the management of groundwater in the Coastal Plain of North Carolina: University of North Carolina Water Resources Research Institute Report No. 129, 63 p.

Sirtariotis, N., 1998, Application of isotopes to the study of regional ground waters in the Coastal Plain of North Carolina [M.S. Thesis]: University of North Carolina at Wilmington.

Sprinkle, C.L., 1989, Geochemistry of the Floridan aquifer system in Florida and in parts of Georgia, South Carolina, and Alabama: U.S. Geological Survey Professional Paper, v. 1403 I, 105 p.

Stueber, A.M., Walter, L.M., Huston, T.J., and Pushkar, P., 1993, Formation waters from Mississippian-Pennsylvanian reservoirs, Illinois basin, USA: Chemical and isotopic constraints on evolution and migration. Geochem. Cosmochim., Acta 57, p. 763-784.

Sutton, L.C., and Woods, T.L., 1995, Geochemistry of groundwater from the Castle Hayne Aquifer in northeastern North Carolina: Southeastern Geology, v. 35, p. 93-119.

Sutton, L.C., 1994, Groundwater Geochemistry of the Castle Hayne Aquifer in Capacity Use Area No. 1, Northeastern North Carolina [M.S. Thesis]: East Carolina University, 148 p.

Todd, D.K., 1980, Groundwater Hydrology 2nd Edition: New York, John Wiley and Sons, Inc., 535 p.

U.S. Geological Survey, 2010, Regional Groundwater Availability Studies Geospatial Data: https://water.usgs.gov/ogw/gwrp/activities/gspdata/Studies/NSCCoastal.html (accessed May 2018).

Veizer, J., 1989, Strontium isotopes in seawater through time: Annual Review of Earth and Planetary Sciences, v .17, p. 141-167.

Villegas, P., 2013, Assessing the hydrochemistry of the Urabá Aquifer, Colombia by principal component analysis: Journal of Geochemical Exploration, v. 134, p. 120-129.

Waddell, K.M., Seiler, R.L., Santini, M., and Soloman, D.K., 1987, Groundwater conditions in Salt Lake Valley, Utah, 1969-1983, and predicted effects of increased withdrawals from wells: Utah Department of Natural Resources Technical Publication No. 87, 69 p.

Warner, D., 1993, Hydrogeologic study of the Castle Hayne aquifer system: northern Beaufort County, N.C.: verification of well field design [M.S. Thesis]: East Carolina University, p. 1-55.

Winner, M.D. and Coble, R.W., 1996, Hydrogeologic Framework of the North Carolina Plain: U.S. Geological Survey Professional Paper 1404-I, p. I7-I46.

Winston, R.B., 2000, Graphical User Interface for MODFLOW, Version 4: U.S. Geological Survey Open-File Report 00-315, 27 p.

Woods, T.L., Beck, E.G., Tolen-Mehlhop, D.L., Troiano, R., and Whitley, J.K., 2000[a], Geochemical tracers of ground water movement between the Castle Hayne and associated Coastal Plain aquifers. Report 328, Raleigh, North Carolina, 237 p.

Woods, T.L., Fullagar, P.D., Spruill, R.K., and Sutton, L.C., 2000[b], Strontium Isotopes and Major Elements as Tracers of Ground Water Evolutions: Example from the Upper Castle Hayne Aquifer of North Carolina: Ground Water, v. 38, p. 762-771.

8.0 APPENDICES

APPENDIX A

CHEMICAL ANALYSES FROM PREVIOUS STUDIES

Well ID	T˚ C	Aquifer	Date Sampled	F^- (ppm)	S^{2-} (ppm)	$NO_3^- + NO_2^-$ (ppm)	PO_4^{3-} (ppm)	Fe^{2+} (ppm)	Source
K17a5	17.9	UCH	5/23/1993	0.55	0.122	0	0.009	0.212	Sutton and Woods (1995)
L10a3	22.2	UCH	5/11/1993	1.33	ND	0.001	0.012	7.6	Sutton and Woods (1995)
L10a5	21.22	LCH	5/11/1993	1.17	0.056	0	0.016	1.26	Sutton and Woods (1995)
L13i1	18.06	UCH	5/7/1993	1.96	ND	0.001	0.064	0.317	Sutton and Woods (1995)
L13i5	19.8	LCH	5/7/1993	1.29	ND	0.001	0.017	0.261	Sutton and Woods (1995)
M12l1	19.7	UCH	7/9/1993	3.20	1.55	0.004	0.009	0.191	Sutton and Woods (1995)
M12l4	20.1	LCH	5/5/1993	1.31	ND	0.0025	0.000	3.12	Sutton and Woods (1995)
M12l4	21.5	LCH	7/9/1993	1.35	2.35	0.0055	0.003	0.673	Sutton and Woods (1995)
N15y5	19.57	LCH	5/10/1993	1.19	0.021	0.002	0.015	2.94	Sutton and Woods (1995)
O10w3	20.3	UCH	5/6/1993	1.20	ND	0.002	0.023	0.816	Sutton and Woods (1995)
O13f1	19.5	UCH	5/10/1993	1.49	0.056	0.002	0.039	1.61	Sutton and Woods (1995)
O13f1	20	UCH	7/8/1993	1.52	0.47	0.004	0.012	0.153	Sutton and Woods (1995)
O17i2	18.1	UCH	5/17/1993	0.60	0.0115	0.002	0.004	0.78	Sutton and Woods (1995)
P16o3	21	LCH	5/24/1993	0.75	7.1	0.001	0.015	0.252	Sutton and Woods (1995)
P16o4	19.5	UCH	5/27/1993	0.58	0.031	0	0.028	0.218	Sutton and Woods (1995)
P21k6	16.27	CH	5/17/1993	0.27	0.0082	0.002	0.086	4.75	Sutton and Woods (1995)
Q15u3	20.2	UCH	5/18/1993	1.11	2.6	0	0.040	0.188	Sutton and Woods (1995)
Q15u5	20.5	LCH	5/27/1993	1.65	1.1	0.002	0.017	0.294	Sutton and Woods (1995)
S15y3	22.5	LCH	5/18/1993	0.75	2.6	0.004	0.003	0.396	Sutton and Woods (1995)
S15y4	18.67	UCH	5/18/1993	0.56	0.57	0	0.006	0.191	Sutton and Woods (1995)
TGCW11A	18	UCH	5/20/1993	0.61	5.8	0.002	0.023	0.483	Sutton and Woods (1995)
TGCW14	23.2	UCH	6/21/1993	0.29	0.0245	0.001	0.004	0.71	Sutton and Woods (1995)
TGS11	20	UCH	6/21/1993	0.70	0.275	0.002	0.004	1.08	Sutton and Woods (1995)
TGS11A	22	BF	6/21/1993	1.71	0.0068	0.005	0.003	0.432	Sutton and Woods (1995)
TGS15	17.1	UCH	5/20/1993	0.19	0.0145	0.006	0.042	9.29	Sutton and Woods (1995)

ND: No Data Available

Well ID	T˚ C	Aquifer	Date Sampled	F^- (ppm)	S^{2-} (ppm)	$NO_3^- + NO_2^-$ (ppm)	PO_4^{3-} (ppm)	Fe^{2+} (ppm)	Source
TGS18	22	UCH	6/21/1993	1.01	0.0415	0.005	0.003	0.23	Sutton and Woods (1995)
TGS28	18	UCH	6/22/1993	0.23	0.014	0.002	0.004	3.3	Sutton and Woods (1995)
WWF1	17	UCH	5/2/1993	0.15	ND	0	0.076	2.93	Sutton and Woods (1995)
WWF2	16.9	UCH	5/26/1993	0.19	0	0.003	0.025	2.89	Sutton and Woods (1995)
WWF3	16.66	UCH	5/25/1993	0.40	0	0.001	0.037	1.2	Sutton and Woods (1995)
WWF4	16.55	UCH	5/22/1993	0.27	0.013	0	0.025	1.13	Sutton and Woods (1995)
AA39V1	18	PD	12/10/1996	ND	ND	ND	ND	ND	Beck (1997) and Sirtariotis (1998)
AA39V4	19	BC	12/9/1996	ND	ND	ND	ND	ND	Beck (1997) and Sirtariotis (1998)
CC38B5	18	S	12/5/1996	ND	ND	ND	ND	ND	Beck (1997) and Sirtariotis (1998)
CC38B6	18	PD	12/5/1996	ND	ND	ND	ND	ND	Beck (1997) and Sirtariotis (1998)
CC38B7	??	CF	12/1992	ND	ND	ND	ND	ND	Beck (1997) and Sirtariotis (1998)
CC38B8	19	BC	12/4/1996	ND	ND	ND	ND	ND	Beck (1997) and Sirtariotis (1998)
DD33y1	18	PD	7/17/1995	0.08	0	0.002	0.013	1.0	Beck (1997) and Sirtariotis (1998)
EE36K2	19	CF	12/9/1996	ND	ND	ND	ND	ND	Beck (1997) and Sirtariotis (1998)
EE36K3	18	PD(S)	12/1/1996	ND	ND	ND	ND	ND	Beck (1997) and Sirtariotis (1998)
EE36K4	19.5	PD/BC	12/9/1996	ND	ND	ND	ND	ND	Beck (1997) and Sirtariotis (1998)
EE36K5	21	BC	12/9/1996	ND	ND	ND	ND	ND	Beck (1997) and Sirtariotis (1998)
EE36K7	19	PD(S)	12/9/1996	ND	ND	ND	ND	ND	Beck (1997) and Sirtariotis (1998)
FF32y1	19	PD(S)	7/18/1995	0.14	0	0.001	0.02	4.0	Beck (1997) and Sirtariotis (1998)
FF32Y2	19	S	11/13/1996	ND	ND	ND	ND	ND	Beck (1997) and Sirtariotis (1998)
FF33D1	18.5	PD	11/13/1996	ND	ND	ND	ND	ND	Beck (1997) and Sirtariotis (1998)
GG32t4	20	PD	7/17/1995	0.18	0	0.002	0.013	0.7	Beck (1997) and Sirtariotis (1998)
SPPW002	20	CH	6/17/1996	0.13	0	< 0.001	0.043	0.3	Beck (1997) and Sirtariotis (1998)
SPPW003	20	CH	6/17/1996	0.13	0	< 0.001	0.045	0.4	Beck (1997) and Sirtariotis (1998)

ND: No Data Available

Well ID	T˚ C	Aquifer	Date Sampled	F^- (ppm)	S^{2-} (ppm)	$NO_3^- + NO_2^-$ (ppm)	PO_4^{3-} (ppm)	Fe^{2+} (ppm)	Source
BCPW2	17.5	CHPD	6/18/1996	0.09	0	< 0.001	0.158	3.0	Beck (1997) and Sirtariotis (1998)
BCPW5	19	CHPD	6/18/1996	0.12	0	< 0.001	0.161	2.0	Beck (1997) and Sirtariotis (1998)
BCPW7	19	CHPD	6/18/1996	0.12	0	< 0.001	0.134	2.0	Beck (1997) and Sirtariotis (1998)
BCPW15	19	CHPD	6/18/1996	0.09	0	< 0.001	0.13	2.0	Beck (1997) and Sirtariotis (1998)
BCPW18	19	CHPD	6/18/1996	0.12	0	< 0.001	0.145	2.0	Beck (1997) and Sirtariotis (1998)
SFOW1	18	CH	2/13/1996	0.26	0.0	< 0.001	0.00	0.6	Beck (1997) and Sirtariotis (1998)
SFOW2	18.5	CH	2/12/1996	0.26	0.0	0.001	0.00	0.5	Beck (1997) and Sirtariotis (1998)
SFOW3	19	CH	1/27/1996	0.60	4.5	0.001	0.01	0.2	Beck (1997) and Sirtariotis (1998)
SFOW4	18	CH	2/12/1996	0.21	0.0	< 0.001	0.01	7	Beck (1997) and Sirtariotis (1998)
HPW2	19	CH	3/5/1996	0.11	0.0	0.002	0.12	0.9	Beck (1997) and Sirtariotis (1998)
HPW3	18.5	CH	3/5/1996	0.08	0.1	0.001	0.11	0.8	Beck (1997) and Sirtariotis (1998)
HOW5	18	CH	2/27/1996	0.19	0.0	0.001	0.10	1	Beck (1997) and Sirtariotis (1998)
Y25Q1	18.5	CH	3/5/1996	0.12	0.00	0.027	0.22	4	Beck (1997) and Sirtariotis (1998)
ABPW5	19	UCH	6/20/1996	0.26	0.0	< 0.001	0.01	0.1	Beck (1997) and Sirtariotis (1998)
ABPW6	21	UCH	6/20/1996	0.37	0.0	< 0.001	0.01	0.1	Beck (1997) and Sirtariotis (1998)
BBPW2	20	UCH	6/21/1996	0.37	0.1	< 0.001	0.01	0.1	Beck (1997) and Sirtariotis (1998)
BBPW5	19	UCH	6/21/1996	0.24	1.5	< 0.001	0.01	0.3	Beck (1997) and Sirtariotis (1998)
BBPW7	21	UCH	6/21/1996	0.19	0.1	< 0.001	0.01	0.1	Beck (1997) and Sirtariotis (1998)
Pe72	19	CH	6/20/1996	0.17	0.0	< 0.001	0.11	0.7	Beck (1997) and Sirtariotis (1998)
K17a4	19.5	BF	3/27/1997	1.37	0.0	0.004	0.019	0.2	Brown (1999)
K17a4d	19.5	BF	3/27/1997	1.37	0.0	0.007	0.021	0.2	Brown (1999)
K17a5	19	UCH	3/27/1997	0.69	0.2	0.007	0.008	0.1	Brown (1999)
K17a6	19	LCH	3/27/1997	0.61	0.0	0.007	0.008	0.6	Brown (1999)
L13i1	18	UCH	4/30/1997	2.11	0.0	0.007	0.058	0.1	Brown (1999)
L13i1(d)	18	UCH	4/30/1997	2.11	0.0	0.008	0.058	0.1	Brown (1999)

ND: No Data Available

Well ID	T˚ C	Aquifer	Date Sampled	F^- (ppm)	S^{2-} (ppm)	$NO_3^- + NO_2^-$ (ppm)	PO_4^{3-} (ppm)	Fe^{2+} (ppm)	Source
L13i2	17	Y	4/30/1997	0.32	0.0	0.007	0.07	4.5	Brown (1999)
L13i5	19.5	LCH	5/9/1997	1.42	0.2	0.007	0.018	0.1	Brown (1999)
M12l1	20.5	UCH	4/3/1997	1.42	5.0	0.007	0.032	0.1	Brown (1999)
M12l4	21	LCH	4/3/1997	1.46	0.0	0.008	0.009	0.8	Brown (1999)
M12l4(d)	21	LCH	4/3/1997	1.48	0.0	0.009	0.009	0.8	Brown (1999)
M12l6	ND	Y	4/3/1997	0.27	0.0	0.005	0.167	2.9	Brown (1999)
O10w1	18	Y	4/21/1997	0.38	1.0	0.007	0.022	0.3	Brown (1999)
O10w1(d)	18	Y	4/21/1997	0.38	1.0	0.007	0.021	0.3	Brown (1999)
O10w3	21	UCH	4/21/1997	1.27	3.0	0.007	0.029	0.1	Brown (1999)
P16o3	20	LCH	3/20/1997	0.84	0.0	0.007	0.013	0.3	Brown (1999)
P16o3(d)	20	LCH	3/20/1997	0.85	0.0	0.005	0.013	0.3	Brown (1999)
P16o4	19	UCH	3/20/1997	0.66	0.0	0.006	0.009	0.3	Brown (1999)
P21k6	17	CH	3/19/1997	0.3	0.0	0.004	0.257	5.7	Brown (1999)
P21k7	18	PD	5/10/1997	0.71	0.0	0.004	0.006	0.2	Brown (1999)
P21k7(d)	18	PD	5/10/1997	0.7	0.0	0.004	0.006	0.2	Brown (1999)
Q15u3	20	UCH	5/6/1997	1.2	4.0	0.010	0.024	0.1	Brown (1999)
Q15u5	21	LCH	5/6/1997	1.77	1.0	0.009	0.019	0.2	Brown (1999)
Q15u5(d)	21	LCH	5/6/1997	1.82	1.0	0.012	0.024	0.2	Brown (1999)
Q15u6	19	Y	5/6/1997	0.24	0.0	0.005	0.042	7.7	Brown (1999)
S15y1	18	Y	5/8/1997	0.12	0.0	0.005	0.094	8.8	Brown (1999)
S15y3	21	LCH	5/8/1997	0.85	4.0	0.005	0.024	0.2	Brown (1999)
S15y4	19	UCH	5/8/1997	0.61	1.0	0.005	0.009	0.2	Brown (1999)
S15y4(d)	19	UCH	5/8/1997	0.62	1.0	0.005	0.013	0.2	Brown (1999)
S18u3	ND	Y	4/25/1997	0.18	0.0	0.005	0.092	0.7	Brown (1999)
S18u5	ND	CH	3/29/1997	0.67	2.0	0.002	0.016	0.2	Brown (1999)

ND: No Data Available

Well ID	T˚ C	Aquifer	Date Sampled	F^- (ppm)	S^{2-} (ppm)	$NO_3^- + NO_2^-$ (ppm)	PO_4^{3-} (ppm)	Fe^{2+} (ppm)	Source
S18u6	19	UCH	3/22/1997	0.5	0.0	0.005	0.006	0.0	Brown (1999)
S18u7	18	PR	3/22/1997	0.19	0.0	0.005	0.167	0.2	Brown (1999)
TGS15	17	UCH	5/9/1997	0.22	0.0	0.005	0.626	16.4	Brown (1999)
Plant	17	UCH	3/11/1997	0.24	0.0	0.007	0.125	2.4	Brown (1999)
Slatestone	18	UCH	3/13/1997	0.13	0.0	0.007	0.195	4.0	Brown (1999)
Far East	ND	UCH	3/13/1997	0.36	0.2	0.005	0.013	0.0	Brown (1999)
Far East(d)	ND	UCH	3/13/1997	0.36	0.2	0.005	0.013	0.0	Brown (1999)
WWF9	23	S	10/26/1995	0.089	0.00	1.006	0.129	0.1	Woods et al (2000[b])
F22b3	17	S	11/31/95	0.03	0.00	2.027	0.010	0.2	Woods et al (2000[b])
WWF9	18	Y	10/26/1995	0.215	0.00	0.050	0.115	4.4	Woods et al (2000[b])
O17I1	17	Y	10/17/1995	0.161	0.00	0.063	0.026	6.2	Woods et al (2000[b])
K2e4	18	Y	11/7/1995	0.068	0.15	0.003	0.038	9.6	Woods et al (2000[b])
L13I2	18	Y	7/25/1995	0.207	0.00	0.000	0.010	3.7	Woods et al (2000[b])
Hyde Plant	17	Y	11/8/1995	0.185	0.00	0.011	0.134	1.2	Woods et al (2000[b])
Columbia	16	Y	1/24/1996	0.111	0.00	0.000	0.024	2.3	Woods et al (2000[b])
Belhaven	18	Y	6/27/1996	0.253	0.10	0.001	0.015	0.0	Woods et al (2000[b])
Plant Yorktown	23	Y	8/31/1995	0.061	0.00	0.000	0.061	0.0	Woods et al (2000[b])
Waves	22.5	Y	8/2/1996	1.465	0.00	0.024	0.065	0.0	Woods et al (2000[b])
Plant	19	PR	8/31/1995	0.151	0.00	0.015	0.065	7.0	Woods et al (2000[b])
WWF9	18	PR	9/1/1995	0.129	0.00	0.017	0.332	3.1	Woods et al (2000[b])
WWF9	18	UCH	9/1/1995	0.169	0.10	0.001	0.015	0.0	Woods et al (2000[b])
Plant	17	UCH	8/31/1995	0.11	0.00	0.000	0.038	4.7	Woods et al (2000[b])
R26n5	19	PD	9/12/1995	0.095	0.00	0.001	0.017	0.4	Woods et al (2000[b])
P21k5	21	BC	7/24/1995	3.838	0.00	0.018	0.408	0.0	Woods et al (2000[b])
P26n1	19	PD	10/17/1995	0.185	0.00	0.027	0.015	0.0	Woods et al (2000[b])

ND: No Data Available

Well ID	T˚ C	Aquifer	Date Sampled	F^- (ppm)	S^{2-} (ppm)	$NO_3^- + NO_2^-$ (ppm)	PO_4^{3-} (ppm)	Fe^{2+} (ppm)	Source
J13d4	18	PD	11/7/1995	0.452	0.05	0.001	0.024	5.3	Woods et al (2000[b])
Chinq1	19	PD	6/28/1996	0.173	0.00	0.001	0.051	0.0	Woods et al (2000[b])
Chinq2	19	PD	6/28/1996	0.139	0.00	0.012	0.022	0.0	Woods et al (2000[b])
RoseHill	ND	PD	5/24/1996	0.111	0.00	0.013	0.180	0.0	Woods et al (2000[b])
PinkHill	ND	PD	5/24/1996	0.062	0.00	0.000	0.040	0.0	Woods et al (2000[b])
Wallace (Ann)	ND	PD	6/14/1996	0.13	0.00	0.012	0.040	0.0	Woods et al (2000[b])
Wallace (Res)	18.5	PD	6/14/1996	0.114	0.00	0.000	0.047	0.0	Woods et al (2000[b])
C15s5	18	CF	9/21/1995	3.078	0.00	0.010	0.245	0.0	Woods et al (2000[b])
G19b3	17	UCF	11/2/1995	0.638	0.00	0.001	0.033	0.0	Woods et al (2000[b])
MAS5	18.8	CH	10/29/2002	0.17	ND	0.06	0.06	3.0	Fullagar (2003)
MAS10	18.9	CH	10/30/2002	0.17	ND	0.16	0.02	0.0	Fullagar (2003)
MAS12	21.9	CH	9/11/2002	0.1	ND	0.05	0.1	1.2	Fullagar (2003)
MAS13	20.3	CH	9/11/2002	0.09	ND	0.05	0.11	1.0	Fullagar (2003)
MAS14	19.1	CH	9/18/2002	0.26	ND	0.05	0.02	0.2	Fullagar (2003)
MAS21	17.8	CH	9/12/2002	0.28	ND	0.05	0.2	0.4	Fullagar (2003)
MAS25	20.7	CH	10/2/2002	0.17	ND	0.06	0.02	1.2	Fullagar (2003)
MAS30	18.4	UCH	9/12/2002	0.1	ND	0.05	0.03	2.1	Fullagar (2003)
CR533	17.4	UCH	10/31/2002	0.17	ND	0.06	0.02	2.7	Fullagar (2003)
CR543	17.5	CH	10/30/2002	0.17	ND	0.06	0.33	1.6	Fullagar (2003)
JO064	15.8	CH	11/13/2002	0.17	ND	0.08	0.17	1.6	Fullagar (2003)
ON267	18.7	S	11/14/2002	0.17	ND	11.4	0.02	3.2	Fullagar (2003)
BO-419	17.5	UCH	8/14/2003	0.2	ND	0.06	0.01	1.7	Fullagar (2003)
BO-358	17.2	UCH	5/6/2003	0.32	ND	0.06	0.05	4.3	Fullagar (2003)
BO-384	18.1	UCH	8/11/2003	0.6	ND	0.06	0.02	1.3	Fullagar (2003)
BR-082	20	CH	5/27/2003	0.2	ND	0.06	0.04	0.6	Fullagar (2003)

ND: No Data Available

Well ID	T˚C	Aquifer	Date Sampled	F^- (ppm)	S^{2-} (ppm)	$NO_3^- + NO_2^-$ (ppm)	PO_4^{3-} (ppm)	Fe^{2+} (ppm)	Source
BR-112	17.9	PD(S)	3/26/2003	0.14	ND	0.06	0.02	5.4	Fullagar (2003)
CT-153	20.5	CH	8/18/2003	0.3	ND	0.06	0.09	1.7	Fullagar (2003)
DU-128	18.9	CH	8/19/2003	0.2	ND	0.06	0.09	2.1	Fullagar (2003)
DU-134	17.7	CH	6/2/2003	0.3	ND	0.06	0.2	6.9	Fullagar (2003)
MAS4	18.1	CH	2/12/2003	0.05	ND	0.06	0.04	0.3	Fullagar (2003)
MAS15	17.3	CH	1/9/2003	0.97	ND	0.06	0.02	0.0	Fullagar (2003)
MAS26	17.5	CH	1/14/2003	0.3	ND	0.06	0.02	1.1	Fullagar (2003)
MAS13B	17.7	CH	1/15/2003	0.18	ND	0.06	0.15	2.0	Fullagar (2003)
MAS12B	18.5	CH	2/6/2003	0.18	ND	0.06	0.1	0.3	Fullagar (2003)
MAS5B	17.7	CH	3/12/2003	0.14	ND	0.06	0.03	3.0	Fullagar (2003)
CR-626	18	CH	8/13/2003	0.2	ND	0.06	0.03	2.9	Fullagar (2003)
PI-612	17.8	CH	8/12/2003	0.2	ND	0.06	0.4	9.1	Fullagar (2003)
PI-613	18.3	CH	8/12/2003	0.9	ND	0.06	0.02	0.1	Fullagar (2003)
WS-108	18.4	UCH	5/7/2003	0.58	ND	0.06	0.02	3.8	Fullagar (2003)

ND: No Data Available

Well ID	Aquifer	T °C	pH	TDS (ppm)	HCO_3^- (ppm)	Cl^- (ppm)	SO_4^{2-} (ppm)	Na^+ (ppm)	K^+ (ppm)	Ca^{2+} (ppm)	SiO_2 (ppm)	Mg^{2+} (ppm)	Source
K17a5	UCH	17.9	7.387	970	395.28	243	37.3	164	23	49.2	17.6	37	Sutton and Woods (1995)
L10a3	UCH	22.2	7.37	4693	600	1769	336	1688	81.9	53.9	14.8	1.27	Sutton and Woods (1995)
L10a5	LCH	21.22	7.313	8652	498	3625	793	3134	1.24	129	10.6	3.18	Sutton and Woods (1995)
L13i1	UCH	18.06	8.051	1294	783	55	87.9	305	22.1	7.04	16.3	12.4	Sutton and Woods (1995)
L13i5	LCH	19.8	7.665	1833	642	508	88.7	471	35.7	19.8	17.7	37.5	Sutton and Woods (1995)
M12l1	UCH	19.7	7.44	2087	688	524	182	562	38.6	20.6	16.8	40.7	Sutton and Woods (1995)
M12l4	LCH	20.1	7.328	10934	468	5502	1608	3194	103	131	17.3	2.51	Sutton and Woods (1995)
M12l4	LCH	21.5	7.03	10613	468	5100	1119	3355	121	140	17.8	2.73	Sutton and Woods (1995)
N15y5	LCH	19.57	7.459	2087	517	762	116	547	37.4	30.1	17.4	49	Sutton and Woods (1995)
O10w3	UCH	20.3	7.375	3728	574	1791	161	977	54.1	41.2	18.1	95.9	Sutton and Woods (1995)
O13f1	UCH	19.5	7.67	1703	570	470	113	454	27.2	17.7	20.2	25.3	Sutton and Woods (1995)

NA: No Data Available

Well ID	Aquifer	T °C	pH	TDS (ppm)	HCO_3^- (ppm)	Cl^- (ppm)	SO_4^{2-} (ppm)	Na^+ (ppm)	K^+ (ppm)	Ca^{2+} (ppm)	SiO_2 (ppm)	Mg^{2+} (ppm)	Source
O13f1	UCH	20	7.57	1715	556	469	108	478	29.4	19.3	19.5	28.5	Sutton and Woods (1995)
O17i2	UCH	18.1	7.145	622	393	54	0	28.4	11.2	73.6	32.2	24.7	Sutton and Woods (1995)
P16o3	LCH	21	7.234	1380	478	376	14.4	323	25.5	70.8	25.3	51.7	Sutton and Woods (1995)
P16o4	UCH	19.5	7.178	593	407	34.7	0	19.2	12.7	56.9	31	28.5	Sutton and Woods (1995)
P21k6	CH	16.27	7.27	374	242	6.7	0	10	1	76.6	22.8	4.08	Sutton and Woods (1995)
Q15u3	UCH	20.2	7.414	954	503	134	34.8	170	18.3	29.4	26.4	31.6	Sutton and Woods (1995)
Q15u5	LCH	20.5	7.489	3661	542	1385	612	918	40.1	41.3	20.3	80.3	Sutton and Woods (1995)
S15y3	LCH	22.5	6.888	2435	452.5	1034	142	561	31.3	83.5	26	95.9	Sutton and Woods (1995)
S15y4	UCH	18.67	7.172	637	444	27.3	0	22	11.8	63.1	27.8	38	Sutton and Woods (1995)
TGCW11A	UCH	18	7.087	531	370.88	8.79	0	10.8	4.23	81.2	37.1	9.2	Sutton and Woods (1995)
TGCW14	UCH	23.2	7.27	379	263.52	6.1	0	8.52	1.4	69	20.8	4.72	Sutton and Woods (1995)
TGS11	UCH	20	7.21	610	414.8	23.9	0	39	16.2	50.6	29.3	30.5	Sutton and Woods (1995)

NA: No Data Available

Well ID	Aquifer	T °C	pH	TDS (ppm)	HCO_3^- (ppm)	Cl^- (ppm)	SO_4^{2-} (ppm)	Na^+ (ppm)	K^+ (ppm)	Ca^{2+} (ppm)	SiO_2 (ppm)	Mg^{2+} (ppm)	Source
TGS11A	BF	22	7.29	4901	531.92	2256	382	1465	58.2	56.8	18.5	102	Sutton and Woods (1995)
TGS15	UCH	17.1	6.923	516	346	13.2	0	14.6	2.49	82.4	37.4	7.33	Sutton and Woods (1995)
TGS18	UCH	22	7.41	493	329.4	4.74	0	42.9	12.9	49.1	29.1	19.4	Sutton and Woods (1995)
TGS28	UCH	18	7.03	530	361.12	7.01	0	10.2	3.64	103	32.6	5.89	Sutton and Woods (1995)
WWF1	UCH	17	7.34	315	215	6.99	1.75	6.5	1.15	58.7	17.3	1.32	Sutton and Woods (1995)
WWF2	UCH	16.9	7.34	363	249	3.6	0	9.69	1.28	62.9	27.8	3.16	Sutton and Woods (1995)
WWF3	UCH	16.66	7.298	380	273	8.32	0	6.95	1.47	61.5	21.2	4.53	Sutton and Woods (1995)
WWF4	UCH	16.55	7.198	393	273	4.77	0	9.01	2.1	64.6	32.3	4.49	Sutton and Woods (1995)
AA39V1	PD	18	7.52	331	213.6	21.1	3.8	8.5	3.2	62.5	ND	1.7	Beck (1997) and Sirtariotis (1998)
AA39V4	BC	19	8.13	242	151.3	16.8	1.4	7	5.8	38	ND	6.8	Beck (1997) and Sirtariotis (1998)
CC38B5	S	18	6.97	482	291.7	48.8	7.2	21.2	4.8	93.8	ND	2.8	Beck (1997) and Sirtariotis (1998)
CC38B6	PD	18	9.4	244	151.3	22	0.5	8.4	11	33.5	ND	7.2	Beck (1997) and Sirtariotis (1998)

NA: No Data Available

Well ID	Aquifer	T °C	pH	TDS (ppm)	HCO_3^- (ppm)	Cl^- (ppm)	SO_4^{2-} (ppm)	Na^+ (ppm)	K^+ (ppm)	Ca^{2+} (ppm)	SiO_2 (ppm)	Mg^{2+} (ppm)	Source
CC38B7	CF	??	ND	ND	ND	ND	ND	ND	ND	ND	ND	ND	Beck (1997) and Sirtariotis (1998)
CC38B8	BC	19	8.93	404	263.6	36.1	3.1	80	8.4	2.3	ND	0.6	Beck (1997) and Sirtariotis (1998)
DD33y1	PD	18	7.3	333	215	21	13	8	4	66	3	2	Beck (1997) and Sirtariotis (1998)
EE36K2	CF	19	9.14	11722	145.8	7945	0	3333.6	176	19.5	ND	101.2	Beck (1997) and Sirtariotis (1998)
EE36K3	PD(S)	18	ND	ND	ND	ND	ND	ND	ND	ND	ND	ND	Beck (1997) and Sirtariotis (1998)
EE36K4	PD/BC	19.5	8.07	4929	7.3	3192.1	9.9	772.5	49.7	833.7	ND	9.9	Beck (1997) and Sirtariotis (1998)
EE36K5	BC	21	7.77	5115	9.8	3234.5	8	1673.7	84.5	70.5	ND	15.9	Beck (1997) and Sirtariotis (1998)
EE36K7	PD(S)	19	7.28	514	322.2	30.4	1.6	17.8	6.3	110.2	ND	2.9	Beck (1997) and Sirtariotis (1998)
FF32y1	PD(S)	19	6.9	567	371	29	22	20	8	94	16	3	Beck (1997) and Sirtariotis (1998)
FF32Y2	S	19	5.5	67	24.2	23.5	8.3	4.2	0.6	1.5	ND	1.1	Beck (1997) and Sirtariotis (1998)
FF33D1	PD	18.5	7.34	473	299	24.9	6.7	11.5	4	110.6	ND	1.9	Beck (1997) and Sirtariotis (1998)
GG32t4	PD	20	7.4	487	268	71	8	40	17	66	8	8	Beck (1997) and Sirtariotis (1998)

NA: No Data Available

Well ID	Aq.	T ˚C	pH	TDS (ppm)	HCO_3^- (ppm)	Cl^- (ppm)	SO_4^{2-} (ppm)	Na^+ (ppm)	K^+ (ppm)	Ca^{2+} (ppm)	SiO_2 (ppm)	Mg^{2+} (ppm)	Source
SPPW002	CH	20	7.5	409	203	76	4	31	10	71	9	4	Beck (1997) and Sirtariotis (1998)
SPPW003	CH	20	7.5	387	217	50	3	26	8	66	12	4	Beck (1997) and Sirtariotis (1998)
BCPW2	CHPD	17.5	7.1	484	325	24	5	16	6	86	15	3	Beck (1997) and Sirtariotis (1998)
BCPW5	CHPD	19	7.26	376	244	22	5	14	5	71	9	3	Beck (1997) and Sirtariotis (1998)
BCPW7	CHPD	19	7.25	384	249	25	4	15	5	72	10	2	Beck (1997) and Sirtariotis (1998)
BCPW15	CHPD	19	7.1	474	320	21	9	16	6	88	10	2	Beck (1997) and Sirtariotis (1998)
BCPW18	CHPD	19	7.14	501	337	21	4	16	5	90	22	3	Beck (1997) and Sirtariotis (1998)
SFOW1	CH	18	7.4	399	266	19	0.3	12	7	77	13	4	Beck (1997) and Sirtariotis (1998)
SFOW2	CH	18.5	7.4	377	243	20	0.2	12	8	76	13	4	Beck (1997) and Sirtariotis (1998)
SFOW3	CH	19	7.2	853	395	250	11	50	27	81	24	9	Beck (1997) and Sirtariotis (1998)
SFOW4	CH	18	6.8	467	290	25	20	15	9	77	17	6	Beck (1997) and Sirtariotis (1998)
HPW2	CH	19	7.2	387	245	31	3	12	5	80	8	2	Beck (1997) and Sirtariotis (1998)

NA: No Data Available

Well ID	Aquifer	T °C	pH	TDS (ppm)	HCO_3^- (ppm)	Cl^- (ppm)	SO_4^{2-} (ppm)	Na^+ (ppm)	K^+ (ppm)	Ca^{2+} (ppm)	SiO_2 (ppm)	Mg^{2+} (ppm)	Source
HPW3	CH	18.5	7.35	340	210	31	3	11	5	70	7	2	Beck (1997) and Sirtariotis (1998)
HOW5	CH	18	7.28	373	244	24	1	9	5	78	9	2	Beck (1997) and Sirtariotis (1998)
Y25Q1	CH	18.5	7.3	413	253	31	7	15	4	70	24	4	Beck (1997) and Sirtariotis (1998)
ABPW5	UCH	19	7.14	487	317	26	4	13	13	90	17	6	Beck (1997) and Sirtariotis (1998)
ABPW6	UCH	21	7.1	545	358	28	4	16	15	90	20	13	Beck (1997) and Sirtariotis (1998)
BBPW2	UCH	20	7.23	454	293	28	4	14	10	85	14	5	Beck (1997) and Sirtariotis (1998)
BBPW5	UCH	19	7.18	846	288	360	13	40	20	100	13	10	Beck (1997) and Sirtariotis (1998)
BBPW7	UCH	21	7.14	536	343	31	3	18	19	89	20	12	Beck (1997) and Sirtariotis (1998)
Pe72	CH	19	7.36	342	200	33	5	16	6	67	8	6	Beck (1997) and Sirtariotis (1998)
K17a4	BF	19.5	7.81	3883.85	585.6	1927	327.49	886.59	64.18	20.76	6.95	63.91	Brown (1999)
K17a4d	BF	19.5	7.81	3898.67	586	1908	357.09	890	66.11	20.37	6.34	63.39	Brown (1999)
K17a5	UCH	19	7.37	734.42	402.6	55.2	36.36	94.28	25.87	61.78	19.81	37.83	Brown (1999)
K17a6	LCH	19	7.46	513.42	300	56.1	2.01	25.87	23.26	54.59	17.04	33.94	Brown (1999)
L13i1	UCH	18	7.82	1123.34	789	47.3	83.68	150.05	24.59	7.24	6.47	12.9	Brown (1999)
L13i1(d)	UCH	18	7.82	1129.2	789	45.9	82.48	158.8	25.12	7.24	5.65	12.9	Brown (1999)
L13i2	Y	17	7.15	386.063	284.26	7.44	ND	7.57	0.893	65.52	15.91	4.15	Brown (1999)

NA: No Data Available

Well ID	Aquifer	T ˚C	pH	TDS (ppm)	HCO_3^- (ppm)	Cl^- (ppm)	SO_4^{2-} (ppm)	Na^+ (ppm)	K^+ (ppm)	Ca^{2+} (ppm)	SiO_2 (ppm)	Mg^{2+} (ppm)	Source
L13i5	LCH	19.5	7.6	1542.74	659	434	63.64	250.98	55.87	21.24	18.34	38.25	Brown (1999)
M12l1	UCH	20.5	7.66	1549.76	682	443	107.9	199.46	42.4	19.58	15.75	38.25	Brown (1999)
M12l4	LCH	21	7.29	8322.34	480	4700	839.47	1785.75	142.72	124.16	16.05	232.73	Brown (1999)
M12l4(d)	LCH	21	7.29	8353.88	480	4700	849.18	1800.88	148.18	124.86	16.05	233.25	Brown (1999)
M12l6	Y	ND	7.15	636.4	447	24.4	1.77	35.95	5.98	80.75	22.04	18.24	Brown (1999)
O10w1	Y	18	7.46	837.65	280	241	1.65	130.74	58.56	49.84	8.99	66.49	Brown (1999)
O10w1(d)	Y	18	7.46	867.24	280	297	1.77	130.44	54.42	29.26	9.03	64.94	Brown (1999)
O10w3	UCH	21	7.34	3187.25	577	1795	97.75	460.14	69.79	63.86	10	112.44	Brown (1999)
P16o3	LCH	20	7.2	1445.04	478	592	19.29	167.5	27.52	89.8	23.12	46.97	Brown (1999)
P16o3(d)	LCH	20	7.2	1454.01	481	596	19.53	166.72	28.84	91.21	22.79	47.07	Brown (1999)
P16o4	UCH	19	7.29	609.26	400.2	45.7	1.77	20.88	12.97	68.68	26.24	32.16	Brown (1999)
P21k6	CH	17	7.18	397.04	253.8	13.5	12.25	8.14	1.26	83.78	19.73	4.28	Brown (1999)
P21k7	PD	18	7.4	467.53	290	18.7	8.53	43.53	11.86	55.74	18.76	19.7	Brown (1999)
P21k7(d)	PD	18	7.4	581.32	290	21.8	7.09	43.53	120.85	58.95	18.91	19.49	Brown (1999)
Q15u3	UCH	20	7.37	886.19	497.8	128	66.95	65.01	31	41.95	20.39	33.89	Brown (1999)
Q15u5	LCH	21	7.23	2834.42	542	1395	153.53	531.73	48.79	56.85	16.06	88.69	Brown (1999)
Q15u5(d)	LCH	21	7.23	2851.21	545	1396	161.4	534.95	50.23	58.95	14.69	88.17	Brown (1999)
Q15u6	Y	19	6.98	454.256	280	0.906	ND	20.02	5.48	123.15	19.14	5.32	Brown (1999)
S15y1	Y	18	7.15	393.49	272	23.7	ND	10.52	0.84	69.25	13.76	3.3	Brown (1999)
S15y3	LCH	21	7.09	2058.51	446	1020	74.8	269.3	31.56	108.04	19.79	88.17	Brown (1999)
S15y4	UCH	19	7.06	649.58	444	21.6	1.53	21.17	11.74	86.37	25.37	37.19	Brown (1999)
S15y4(d)	UCH	19	7.06	648.19	445	20.3	1.53	20.98	12.64	85.07	24.76	37.29	Brown (1999)
S18u3	Y	ND	7.66	226.28	150	1.17	1.77	5.23	7.08	39.08	13.1	8.67	Brown (1999)
S18u5	CH	ND	7.12	654.72	430	27	1.89	54.46	19.84	77.29	14	29.57	Brown (1999)
S18u6	UCH	19	7.25	514.66	358.9	10.9	1.65	9.36	15.48	68.39	25.61	23.87	Brown (1999)
S18u7	PR	18	7.36	283.44	190	9	1.65	4.84	4.95	39.65	21.88	11.28	Brown (1999)

ND: No Data Available

Well ID	Aquifer	T °C	pH	TDS (ppm)	HCO_3^- (ppm)	Cl^- (ppm)	SO_4^{2-} (ppm)	Na^+ (ppm)	K^+ (ppm)	Ca^{2+} (ppm)	SiO_2 (ppm)	Mg^{2+} (ppm)	Source
TGS15	UCH	17	6.9	510.68	344	12.3	ND	14.07	26.35	70.98	34.19	8.57	Brown (1999)
Plant	UCH	17	7.45	387.31	262.3	1.17	ND	8	1.98	64.08	45.1	4.44	Brown (1999)
Slatestone	UCH	18	7.34	352.67	248.9	1.45	10.5	6.49	1.23	64.08	17.93	1.96	Brown (1999)
Far East	UCH	ND	7.41	429.686	305	0.726	1.53	8.83	5.18	65.8	29.05	13.21	Brown (1999)
Far East(d)	UCH	ND	7.41	431.31	305	1.17	1.53	8.79	6.08	66.38	28.89	13.11	Brown (1999)
WWF9	S	23	5.06	88.939	24	13.21	17.87	8.96	3.61	3.15	13.74	4.31	Woods et al (2000[b])
F22b3	S	17	5.7	41.87	20	0	0.02	6	3	2	10.82	0	Woods et al (2000[b])
WWF9	Y	18	7.03	426.715	215	0	39.52	47.32	7.22	67.31	26.66	23.47	Woods et al (2000[b])
O17I1	Y	17	6.7	663.191	450	0	6.97	44	31	84	30.06	17	Woods et al (2000[b])
K2e4	Y	18	7	14079.3	360	10000	1400	510	590	600	19.22	600	Woods et al (2000[b])
L13I2	Y	18	7	599.602	440	0	6.72	21	23	77	27.675	4	Woods et al (2000[b])
Hyde Plant	Y	17	7.1	920.175	620	22.17	0	107	44	78	23.82	25	Woods et al (2000[b])
Columbia	Y	16	7.2	763.321	330	130.55	24.18	140	47	73	9.48	9	Woods et al (2000[b])
Belhaven	Y	18	7.2	735.559	500	0	23.12	71	39	80	6.186	16	Woods et al (2000[b])
Plant Yorktown	Y	23	5.7	58.661	22	0	5.86	9	2	2	17.74	0	Woods et al (2000[b])
Waves	Y	22.5	7.9	1649.66	740	403.55	5.23	430	45	9	14.41	1	Woods et al (2000[b])
Plant	PR	19	6.5	388.051	250	0	15.94	21	24	59	16.96	1	Woods et al (2000[b])
WWF9	PR	18	6.82	255.989	183	0	4	10.92	6.6	19.54	27.46	4.34	Woods et al (2000[b])
WWF9	UCH	18	7.12	493.919	342	0	0.9	22.37	25.84	60.87	29.98	11.79	Woods et al (2000[b])
Plant	UCH	17	6.86	371.5	244	0	7.63	19	25.89	52.35	19.32	3.2	Woods et al (2000[b])
R26n5	PD	19	7.76	194.925	85	0	0.76	14.68	24.28	58.8	7.48	3.83	Woods et al (2000[b])
P21k5	BC	21	8.3	1757.5	498	741.3	63.05	397.48	17.75	1.41	5.12	29.55	Woods et al (2000[b])
P26n1	PD	19	7.1	330.955	210	0	7.08	9	27.57	64	8.12	5	Woods et al (2000[b])
J13d4	PD	18	7.3	ND	ND	8900	1120	3600	220	91	5.18	290	Woods et al (2000[b])
Chinq1	PD	19	8.3	260.233	195	0	0.42	45	5	5	5.64	4	Woods et al (2000[b])

ND: No Data Available

Well ID	Aquifer	T ˚C	pH	TDS (ppm)	HCO_3^- (ppm)	Cl^- (ppm)	SO_4^{2-} (ppm)	Na^+ (ppm)	K^+ (ppm)	Ca^{2+} (ppm)	SiO_2 (ppm)	Mg^{2+} (ppm)	Source
RoseHill	PD	ND	7.73	266.171	190	0	1.64	9	22	33	8.42	2	Woods et al (2000[b])
PinkHill	PD	ND	8.29	215.132	136	0	1.73	13	11	45	5.34	3	Woods et al (2000[b])
Wallace (Ann)	PD	ND	7.8	260.72	180	0	1.73	38	14	16	6.86	4	Woods et al (2000[b])
Wallace (Res)	PD	18.5	7.86	307.224	214	0	1.53	32.68	19.89	25.89	8.56	4.56	Woods et al (2000[b])
C15s5	CF	18	8.61	1032.15	704	0	26.03	277.04	16.09	0	5.34	0.57	Woods et al (2000[b])
G19b3	UCF	17	7.9	ND	ND	0	1.13	108.05	17.81	11.03	8.02	7.75	Woods et al (2000[b])
MAS5	CH	18.8	7.2	381.5	244	22.3	4.8	7.12	0.82	89	11.3	1.99	Fullagar (2003)
MAS10	CH	18.9	8.2	150.945	110	2.7	3.1	2.24	2.01	29	1.25	0.475	Fullagar (2003)
MAS12	CH	21.9	7.5	251.07	166	10	0.5	6.04	0.68	57.7	8.32	1.73	Fullagar (2003)
MAS13	CH	20.3	7.3	311.15	212	8.47	0.2	5.32	0.73	70.4	12.4	1.54	Fullagar (2003)
MAS14	CH	19.1	7.5	365.89	234	6.38	0.1	7.21	4.77	68.3	41.3	3.57	Fullagar (2003)
MAS21	CH	17.8	7.3	276.54	160	9.19	11.9	6.07	2.04	71.2	13.8	2.06	Fullagar (2003)
MAS25	CH	20.7	7.3	384.2	262	7.53	0.4	7.6	1.3	83.4	19.9	1.9	Fullagar (2003)
MAS30	UCH	18.4	7.5	291.96	190	3.83	0.3	5.14	1.21	59.2	30.4	1.78	Fullagar (2003)
CR533	UCH	17.4	7.5	394.73	248	7.22	21.7	5.39	0.64	86.8	23.2	1.61	Fullagar (2003)
CR543	CH	17.5	7.2	511.79	366	4.45	0.2	3.3	1.01	122	12.5	2.16	Fullagar (2003)
JO064	CH	15.8	7	311.59	217	5.68	0.2	3.59	0.78	68.2	14.4	1.57	Fullagar (2003)
ON267	S	18.7	6	100.07	37	27.7	0.1	10.2	2.04	4.95	6.21	11.7	Fullagar (2003)
BO-419	UCH	17.5	7.4	316.47	200	6.54	0.9	8.16	2.21	61	35.3	2.16	Fullagar (2003)
BO-358	UCH	17.2	7.3	371.41	240	6.14	0.2	9.78	1.18	64.8	45.9	3.09	Fullagar (2003)
BO-384	UCH	18.1	7.2	670.3	393	49.9	0.3	33.2	11.9	86.2	68.9	26.3	Fullagar (2003)
BR-082	CH	20	7.4	430.96	275	14.2	0.2	11.2	1.83	79.8	45.4	3.13	Fullagar (2003)
BR-112	PD(S)	17.9	7.1	549.63	364	14.9	0.2	13.2	1.42	107	46.4	2.37	Fullagar (2003)

ND: No Data Available

Well ID	Aq.	T °C	pH	TDS (ppm)	HCO_3^- (ppm)	Cl^- (ppm)	SO_4^{2-} (ppm)	Na^+ (ppm)	K^+ (ppm)	Ca^{2+} (ppm)	SiO_2 (ppm)	Mg^{2+} (ppm)	Source
CT-153	CH	20.5	7.3	481.03	322	11.3	0.2	10.1	6.05	83.2	42.2	5.68	Fullagar (2003)
DU-128	CH	18.9	7.3	388.14	259	7.1	0.2	3.03	1.38	77.2	38.3	1.73	Fullagar (2003)
DU-134	CH	17.7	7.1	417.48	287	5.12	0.2	7.4	1	91.6	22.6	2.26	Fullagar (2003)
MAS4	CH	18.1	7.5	249.27	166	5.52	0.6	4.93	0.54	62.9	7.24	1.49	Fullagar (2003)
MAS15	CH	17.3	8.2	650.84	381	50.8	4.4	144	11.7	17.6	35.9	4.47	Fullagar (2003)
MAS26	CH	17.5	7.4	338.72	229	7.19	0.2	7.32	2.07	71	20.2	1.44	Fullagar (2003)
MAS13B	CH	17.7	7.4	341.37	226	8.74	0.2	7.34	0.94	73.2	22.9	1.87	Fullagar (2003)
MAS12B	CH	18.5	8.1	181.97	83	11.9	27.2	7.21	0.9	40	9.87	1.71	Fullagar (2003)
MAS5B	CH	17.7	7	601.26	307	10.5	118	6.75	2.16	145	7.53	4.18	Fullagar (2003)
CR-626	CH	18	7.3	340.21	212	4.68	0.2	8.85	1.28	66	45	2	Fullagar (2003)
PI-612	CH	17.8	7	522.43	349	6.57	0.2	7	1.49	106	49.5	2.47	Fullagar (2003)
PI-613	CH	18.3	7.8	365.04	249	4.54	1.8	40.8	12.2	28.9	16	10.9	Fullagar (2003)
WS-108	UCH	18.4	7.6	579.18	365	45.9	1.6	36.2	21.4	47.3	27.2	34	Fullagar (2003)

ND: No Data Available

APPENDIX B

MODFLOW SURFACES

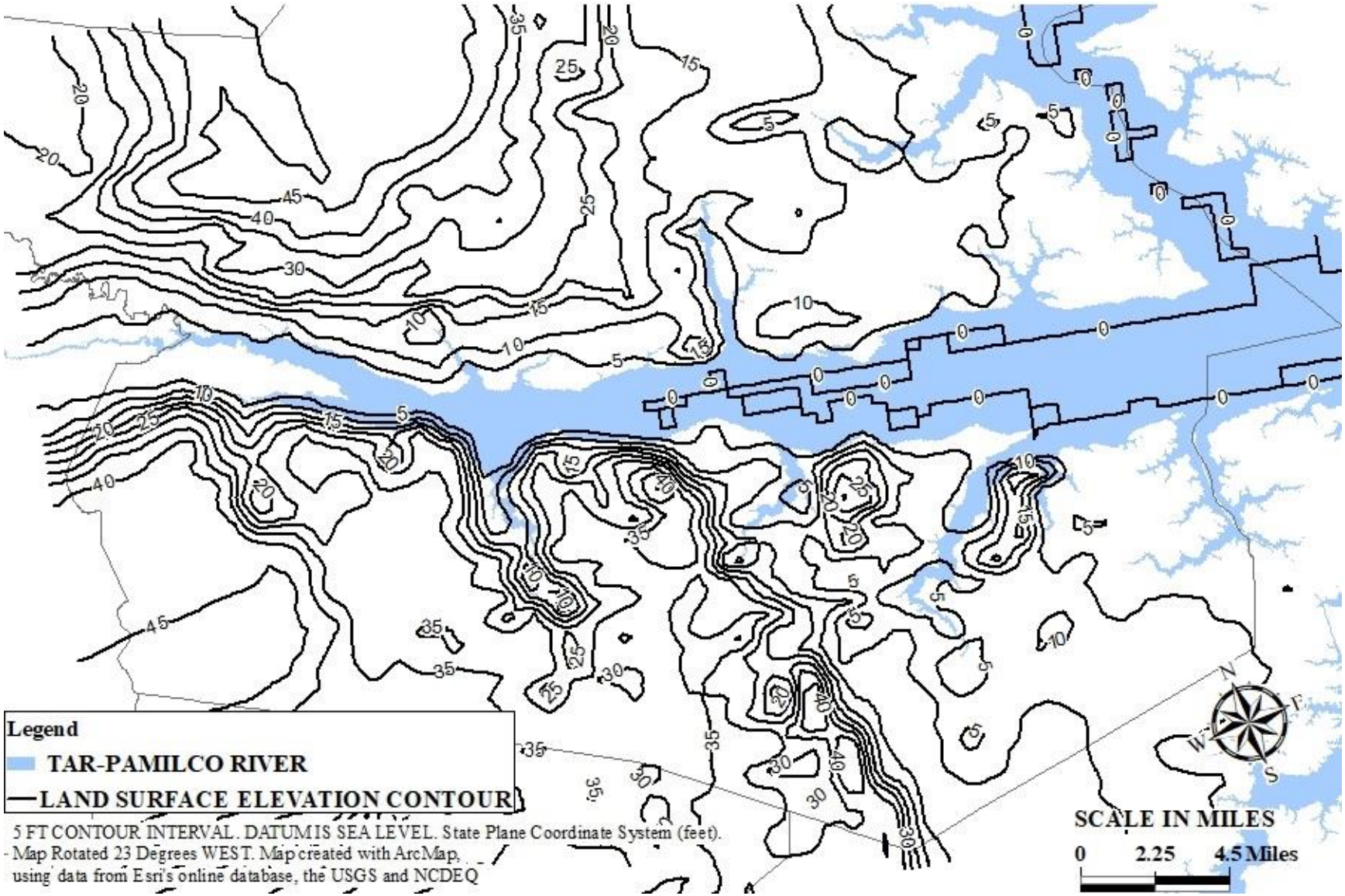

Land surface elevation.

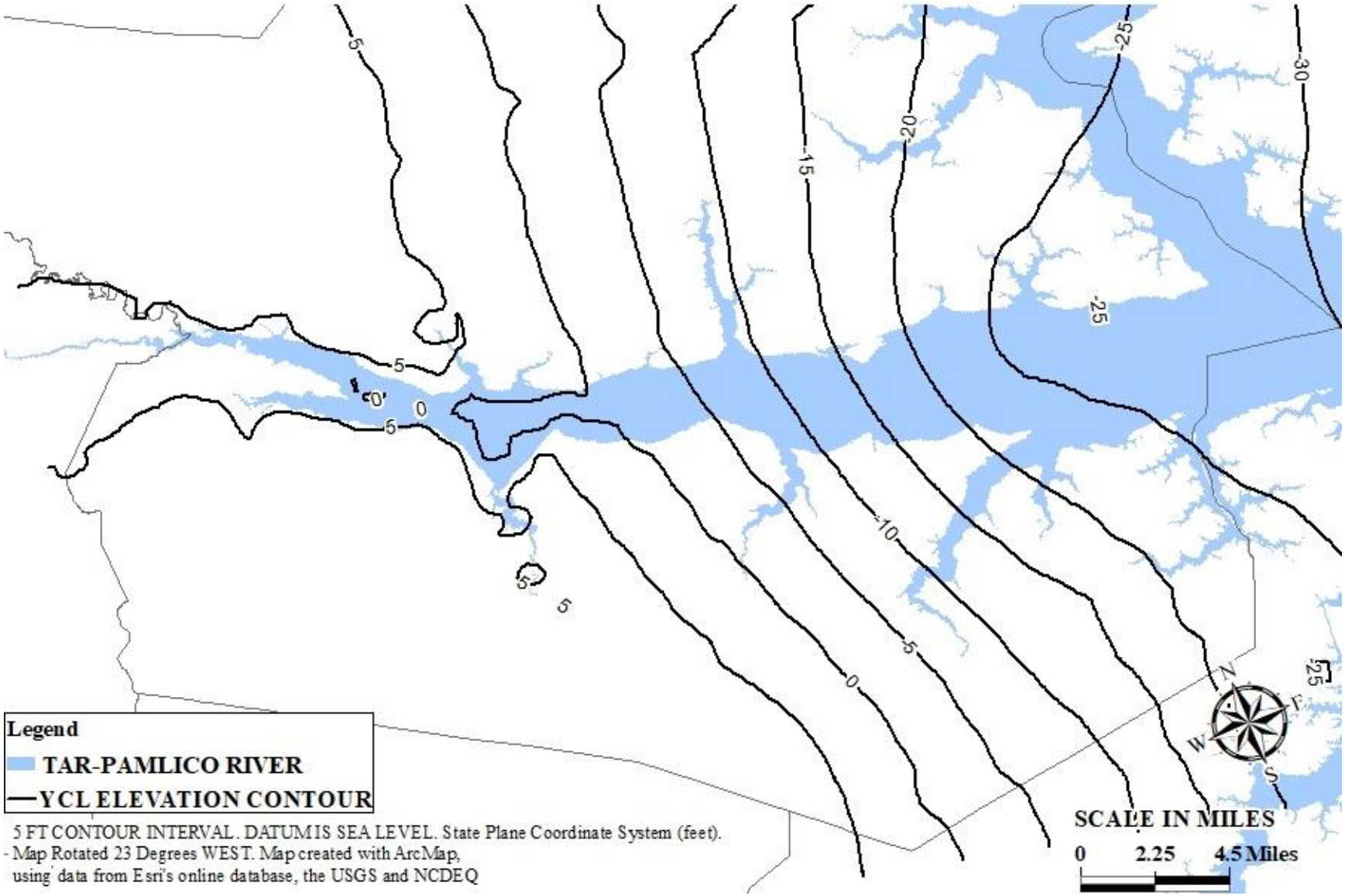

Top of the Yorktown Confining Layer.

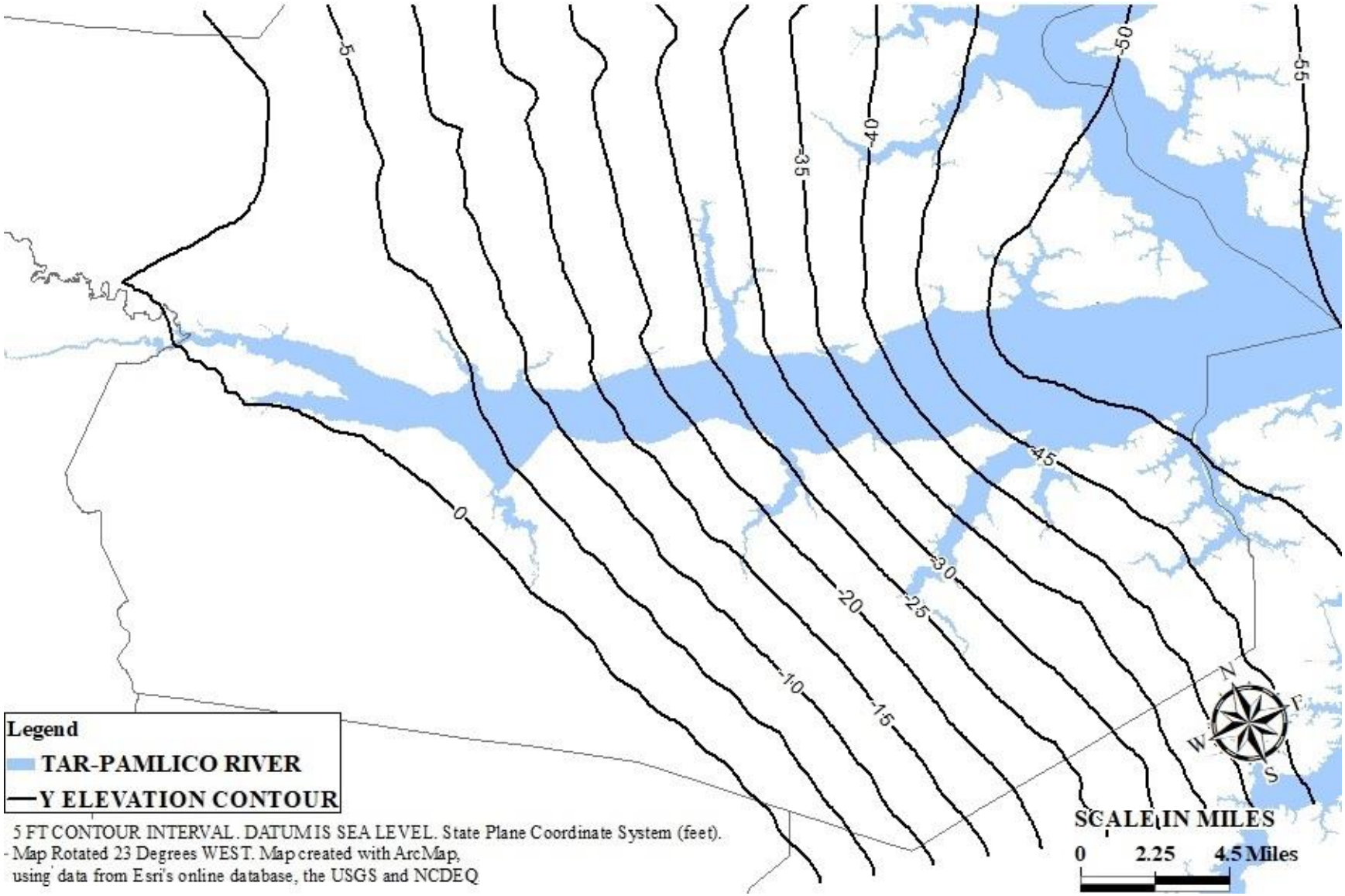

Top of the Yorktown Aquifer.

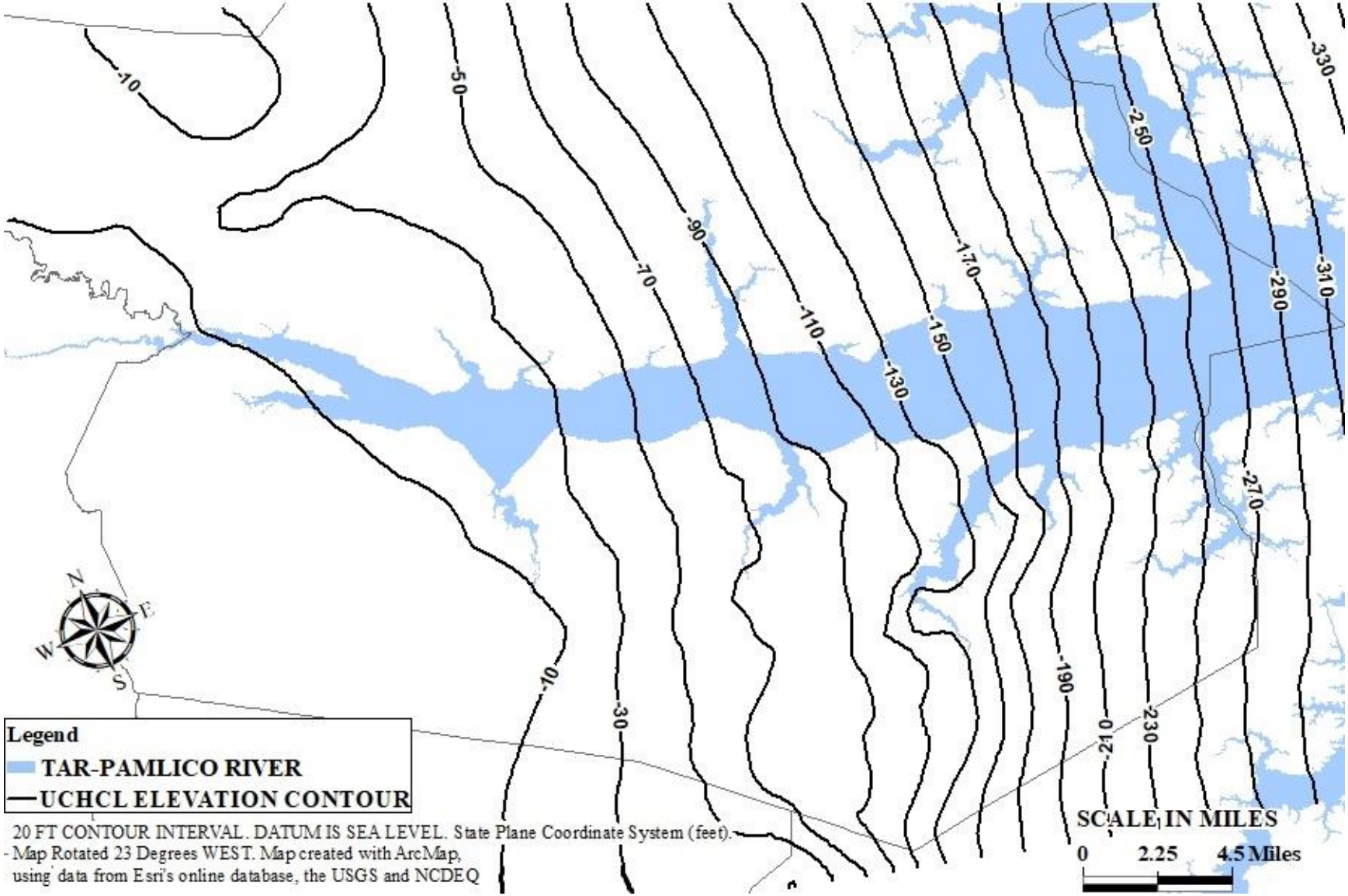

Top of the Upper Castle Hayne Confining Layer.

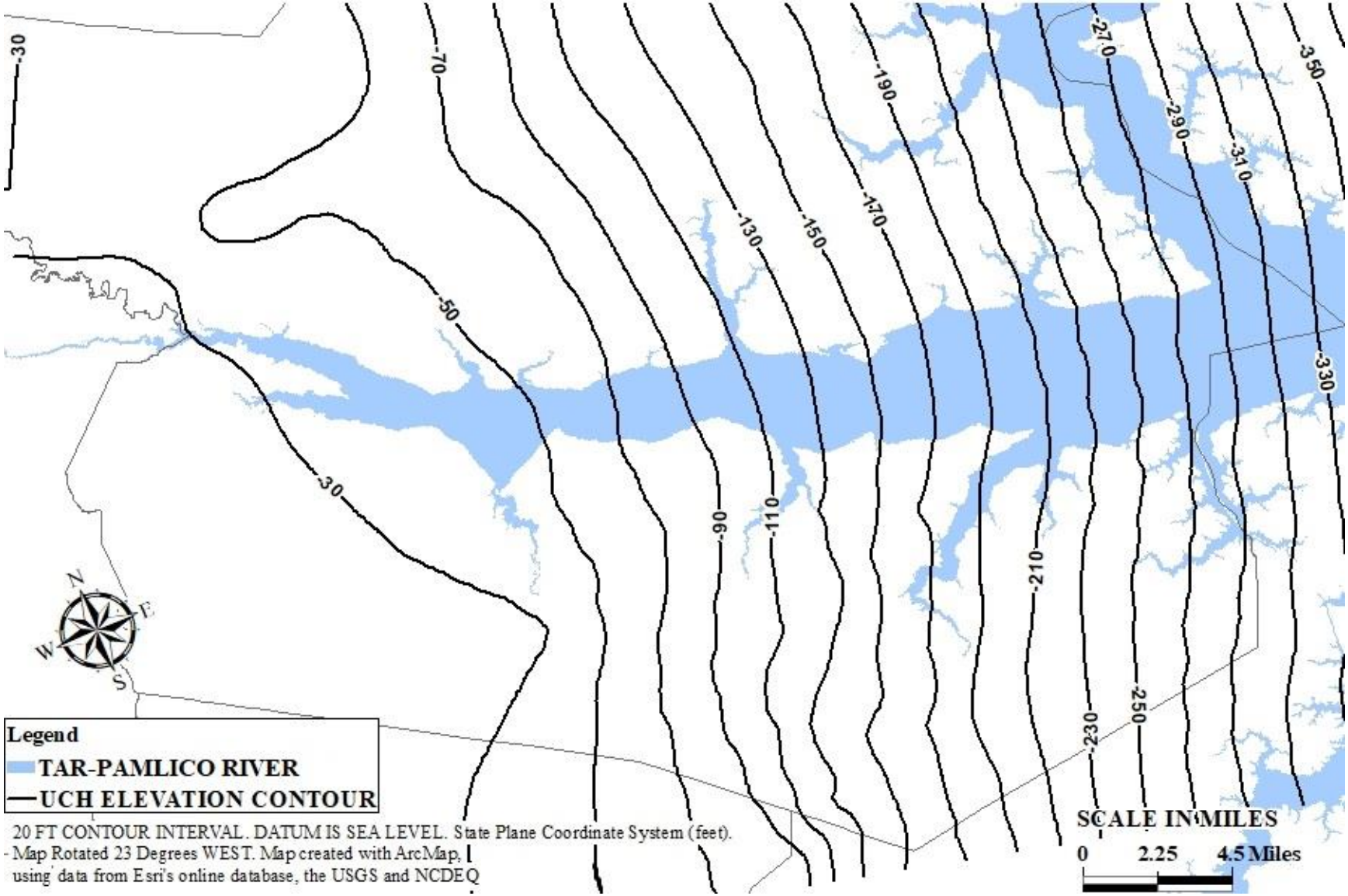

Top of the Upper Castle Hayne Aquifer.

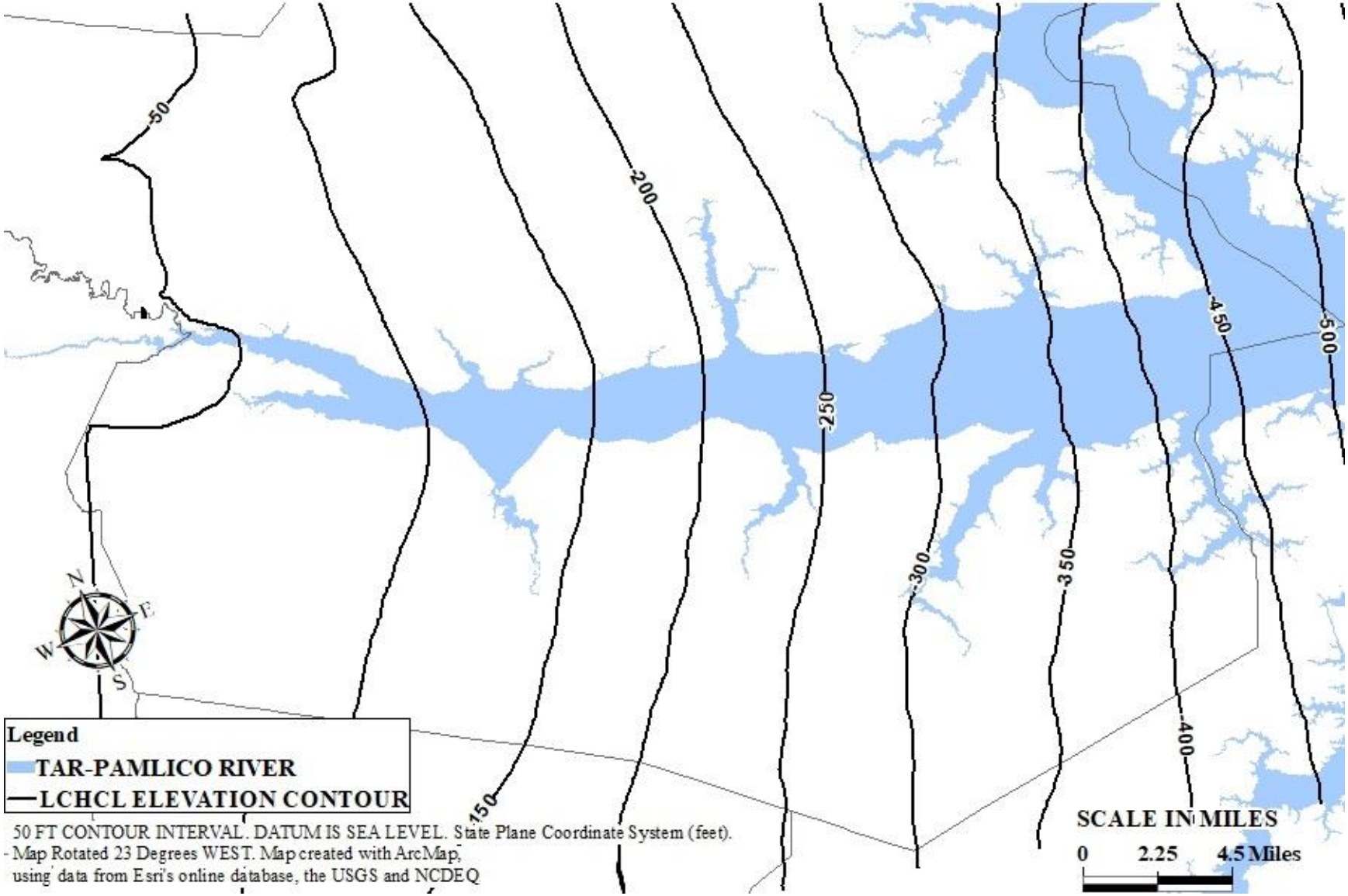

Top of the Lower Castle Hayne Confining Layer.

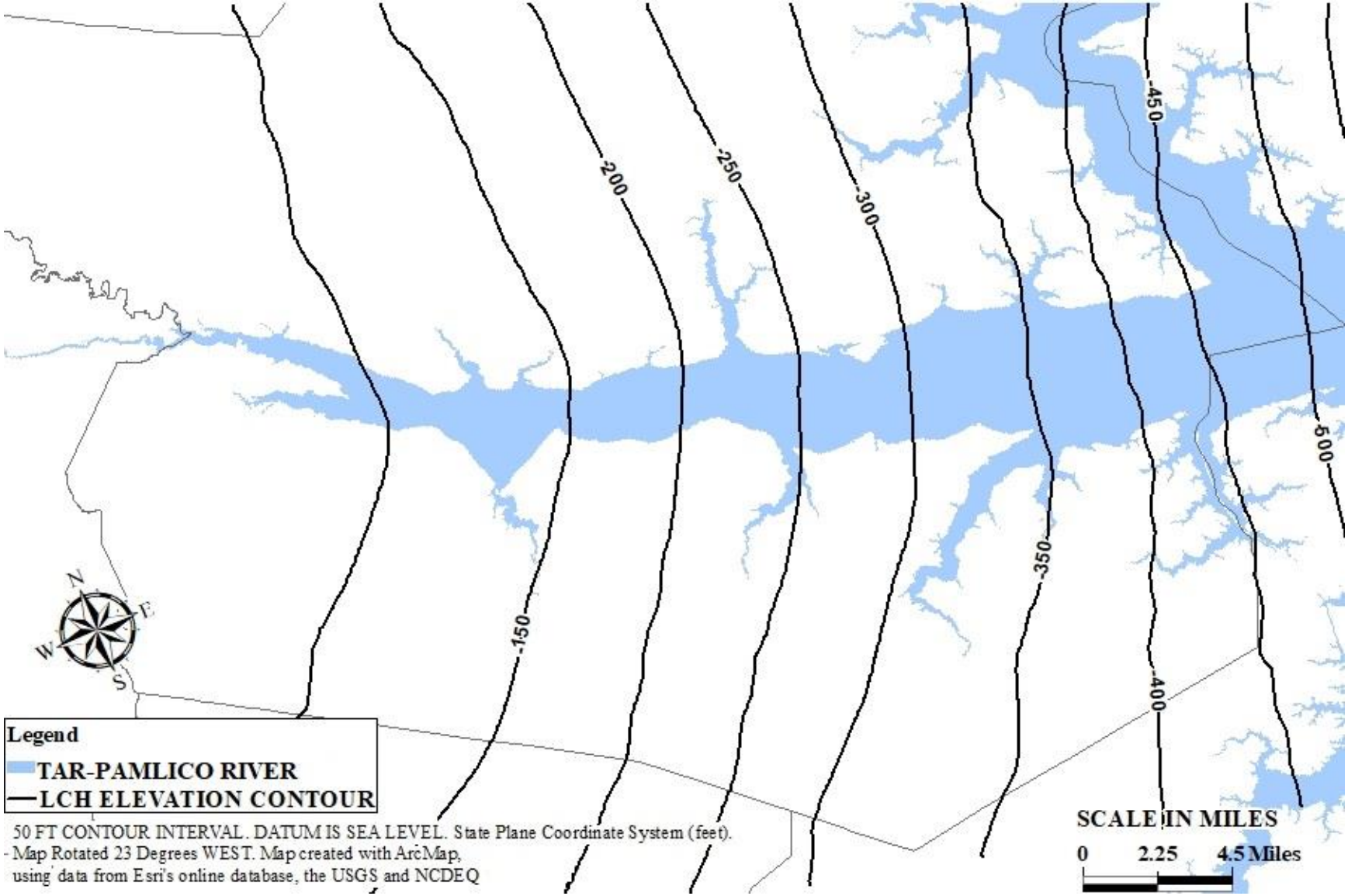

Top of the Lower Castle Hayne Aquifer.

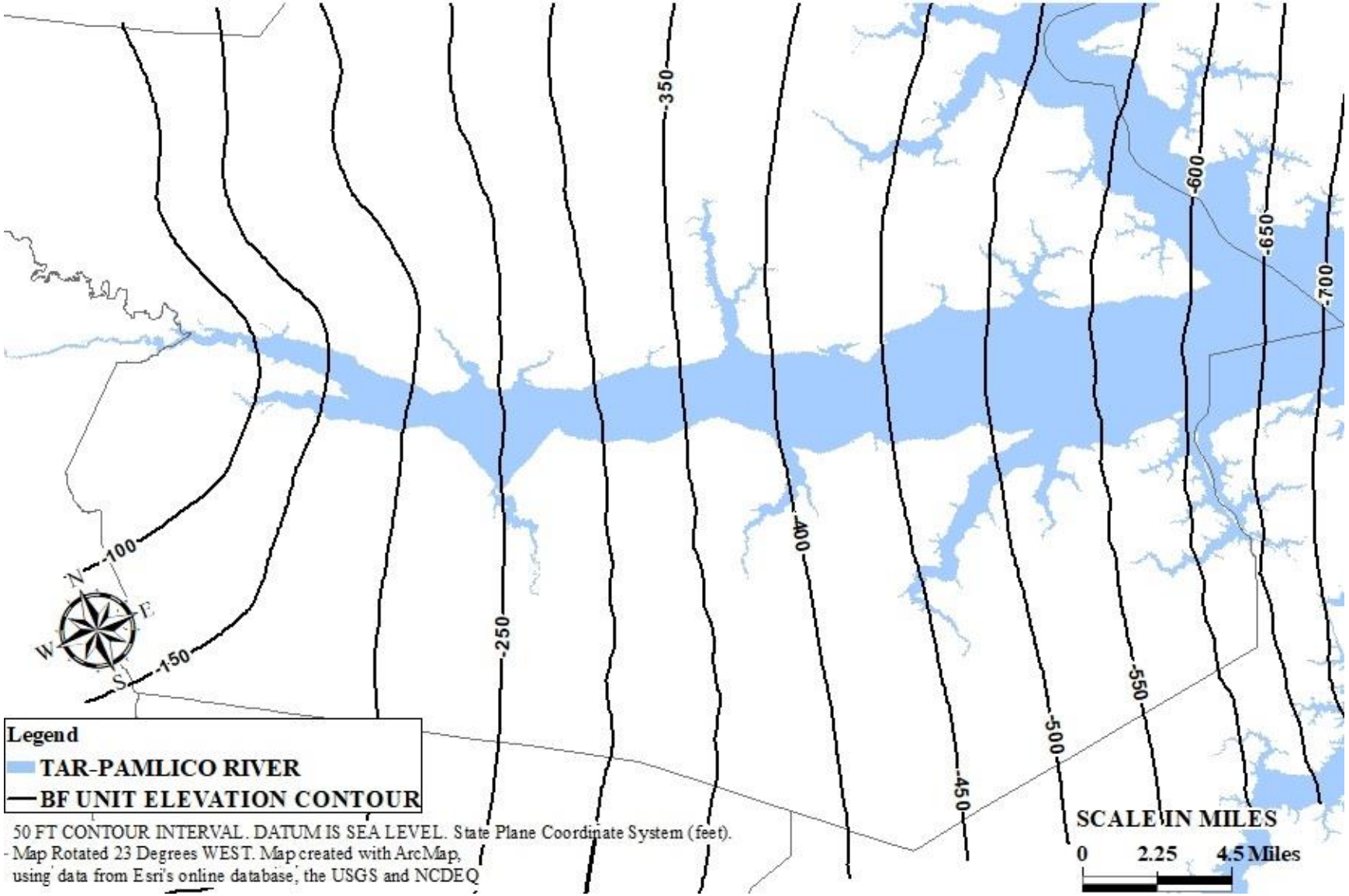

Top of the Beaufort Unit.

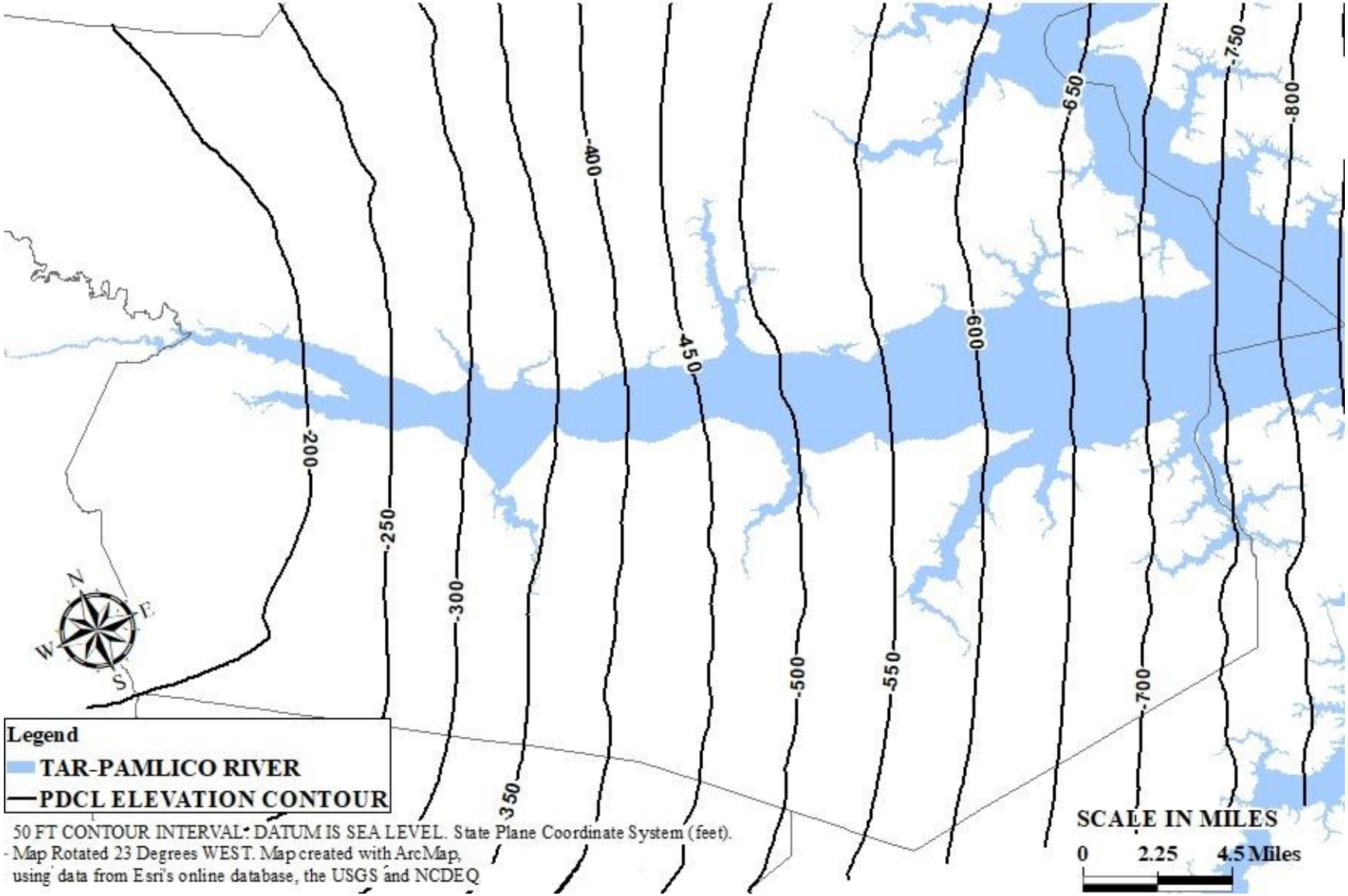

Top of the Peedee Confining Layer.

APPENDIX C

MODPATH SIMULATIONS

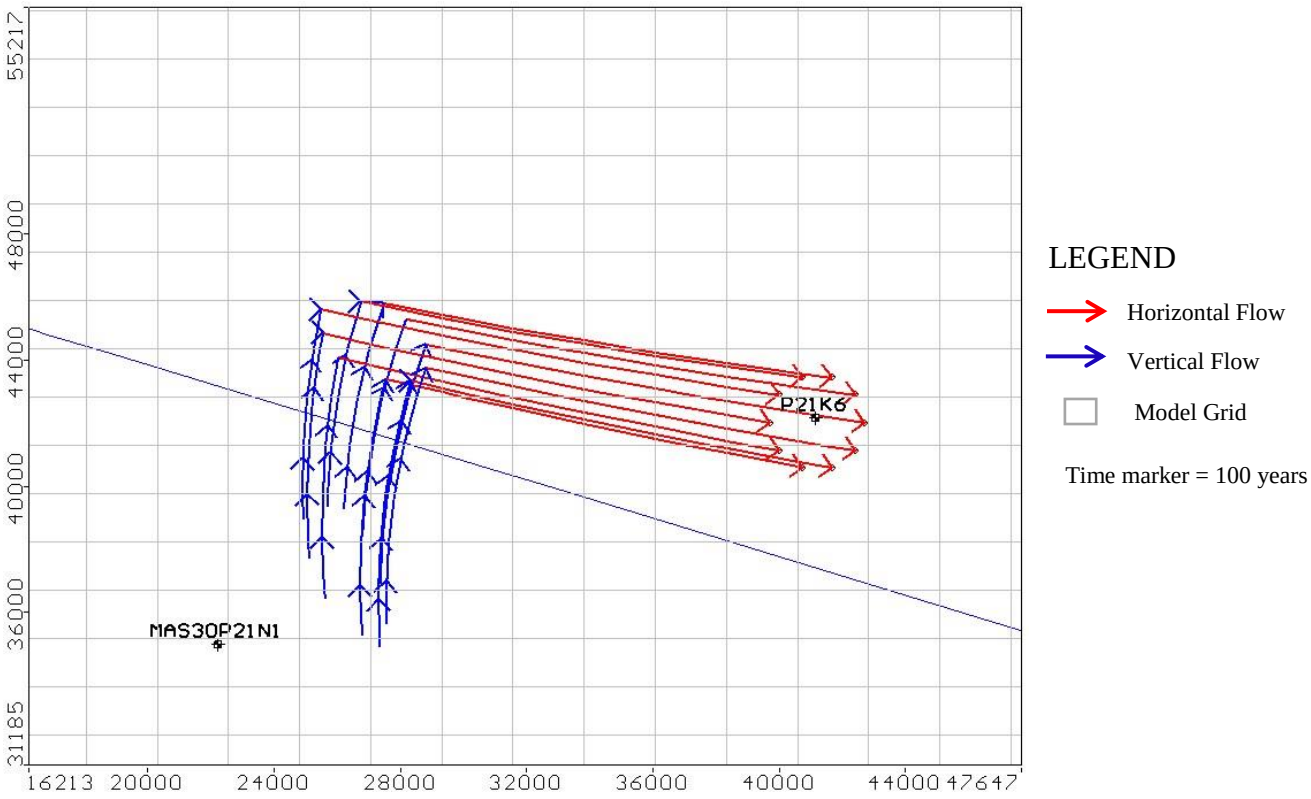

Sample P21K6 particle tracking. Travel time marker = 100 years.

MODPATH results indicate that the source of these groundwater particles comes from recharge infiltration. Under the current influence of groundwater pumping, it would take a minimum total travel time of 430 years for groundwater particles to travel from their source to the sample location. The minimum time required for particles to travel vertically through the units overlying the UCH is 320 years. Horizontal flow through the UCH (3 miles) requires approximately 110 years. Horizontal flow through the UCH occurs at an average rate of 0.027 miles/year.

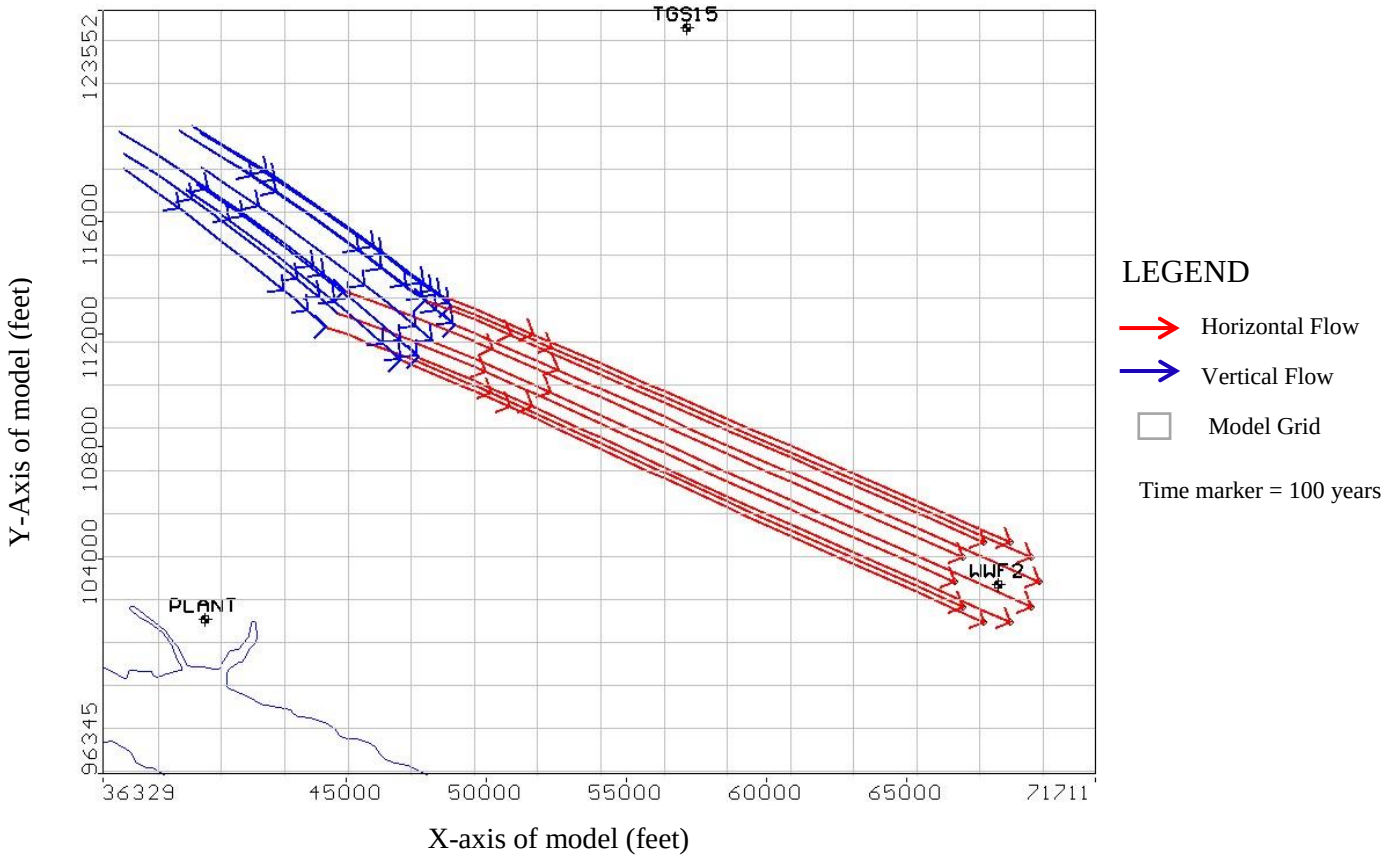

Sample WWF2 particle tracking. Travel time marker = 100 years.

MODPATH results indicate that the source of these groundwater particles comes from recharge infiltration. Under the current influence of groundwater pumping, it would take a minimum total travel time of 730 years for groundwater particles to travel from their source to the sample location. The minimum time required for particles to travel vertically through the units overlying the UCH is 580 years. Horizontal flow through the UCH (4 miles) requires approximately 150 years. Horizontal flow through the UCH occurs at an average rate of 0.027 miles/year.

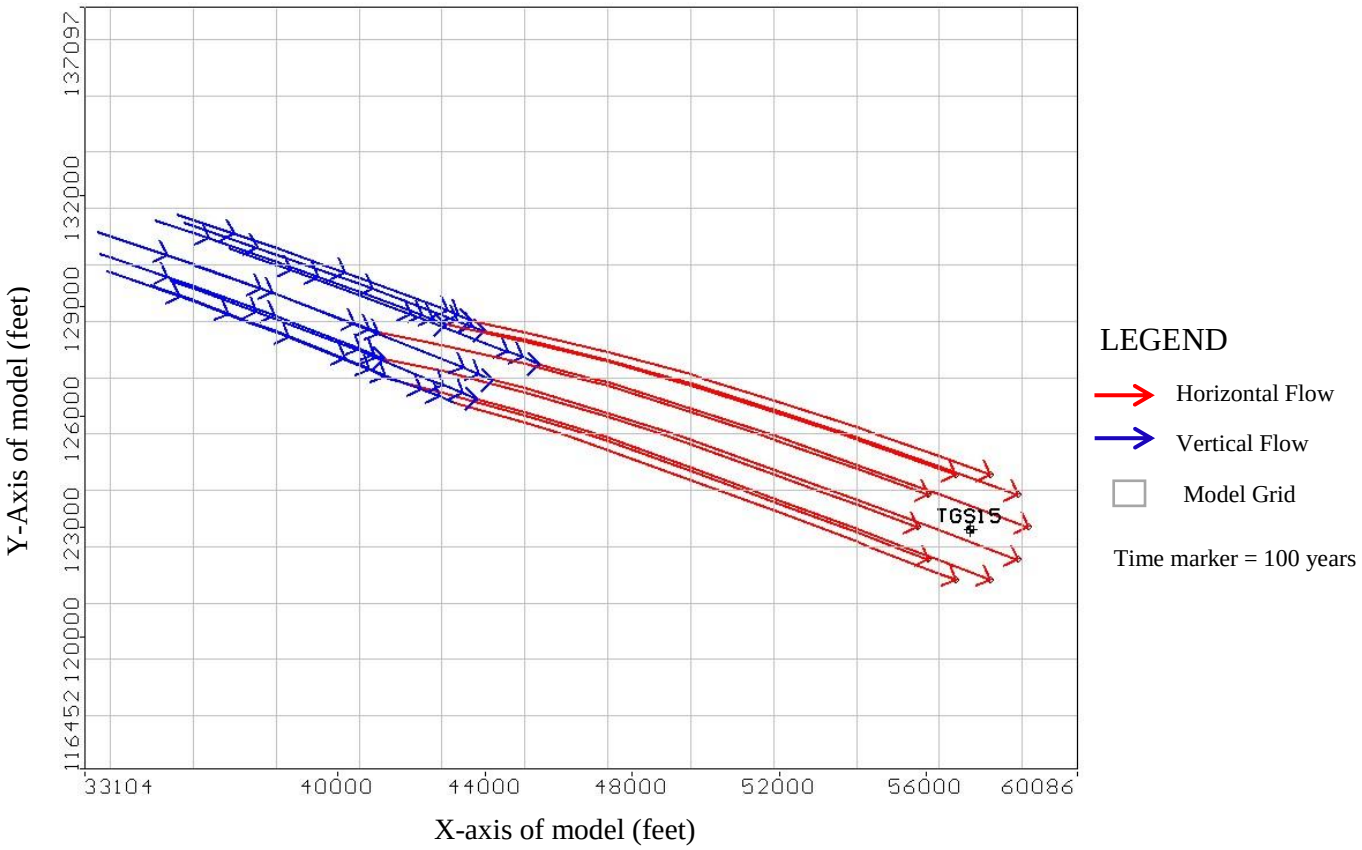

Sample TGS15 particle tracking. Travel time marker = 100 years.

MODPATH results indicate that the source of these groundwater particles comes from recharge infiltration. Under the current influence of groundwater pumping, it would take a minimum total travel time of 760 years for groundwater particles to travel from their source to the sample location. The minimum time required for particles to travel vertically through the units overlying the UCH is 660 years. Horizontal flow through the UCH (2.5 miles) requires approximately 100 years. Horizontal flow through the UCH occurs at an average rate of 0.025 miles/year.

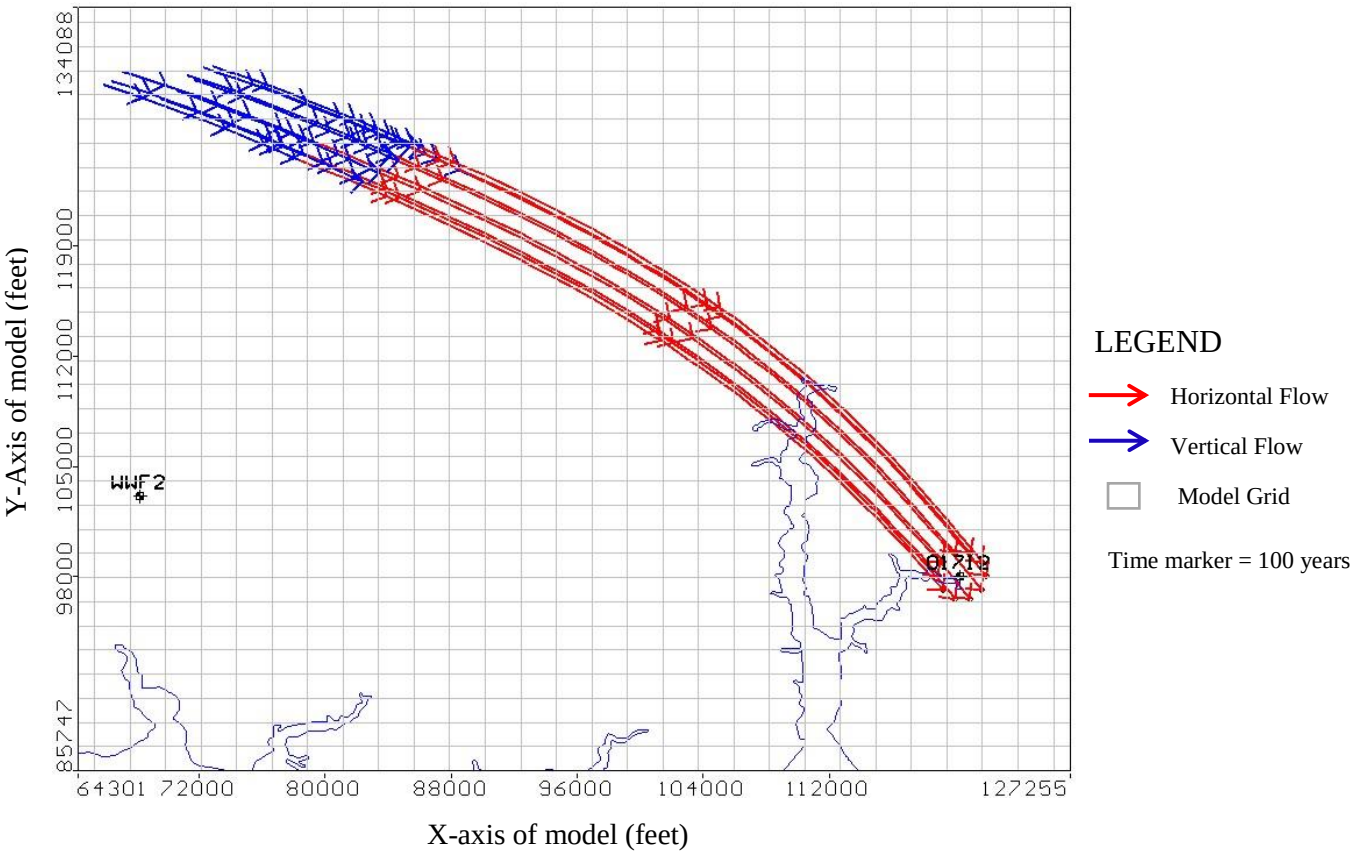

Sample O17I2 particle tracking. Travel time marker = 100 years.

MODPATH results indicate that the source of these groundwater particles comes from recharge infiltration. Under the current influence of groundwater pumping, it would take a minimum total travel time of 943 years for groundwater particles to travel from their source to the sample location. The minimum time required for particles to travel vertically through the units overlying the UCH is 573 years. Horizontal flow through the UCH (9.5 miles) requires approximately 370 years. Horizontal flow through the UCH occurs at an average rate of 0.025 miles/year.

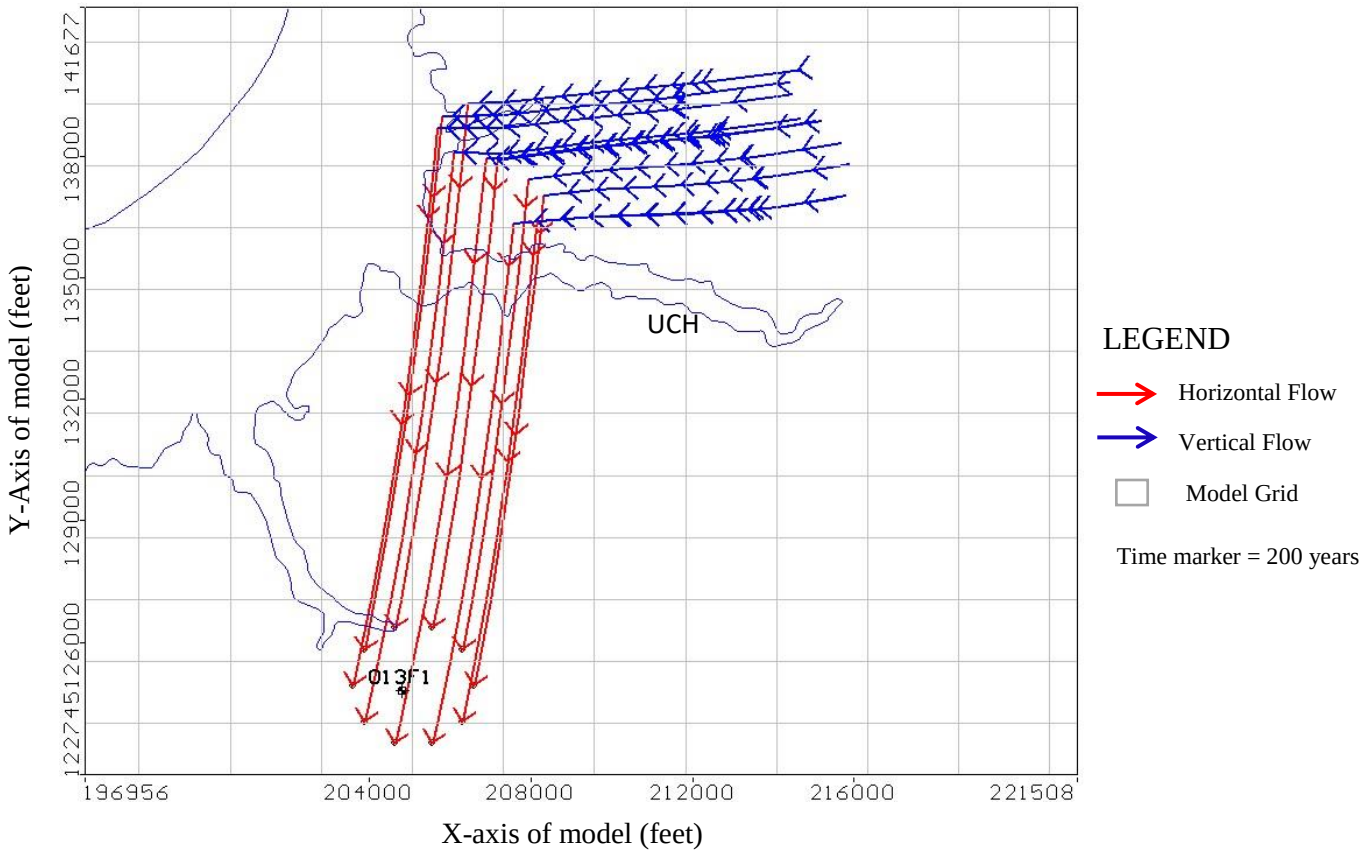

Sample O13F1 particle tracking. Travel time marker = 200 years.

MODPATH results indicate that the source of these groundwater particles comes from recharge infiltration. Under the current influence of groundwater pumping, it would take a minimum total travel time of 2,835 years for groundwater particles to travel from their source to the sample location. The minimum time required for particles to travel vertically through the units overlying the UCH is 2,305 years. Horizontal flow through the UCH (2 miles) requires approximately 530 years. Horizontal flow through the UCH occurs at an average rate of 0.004 miles/year.

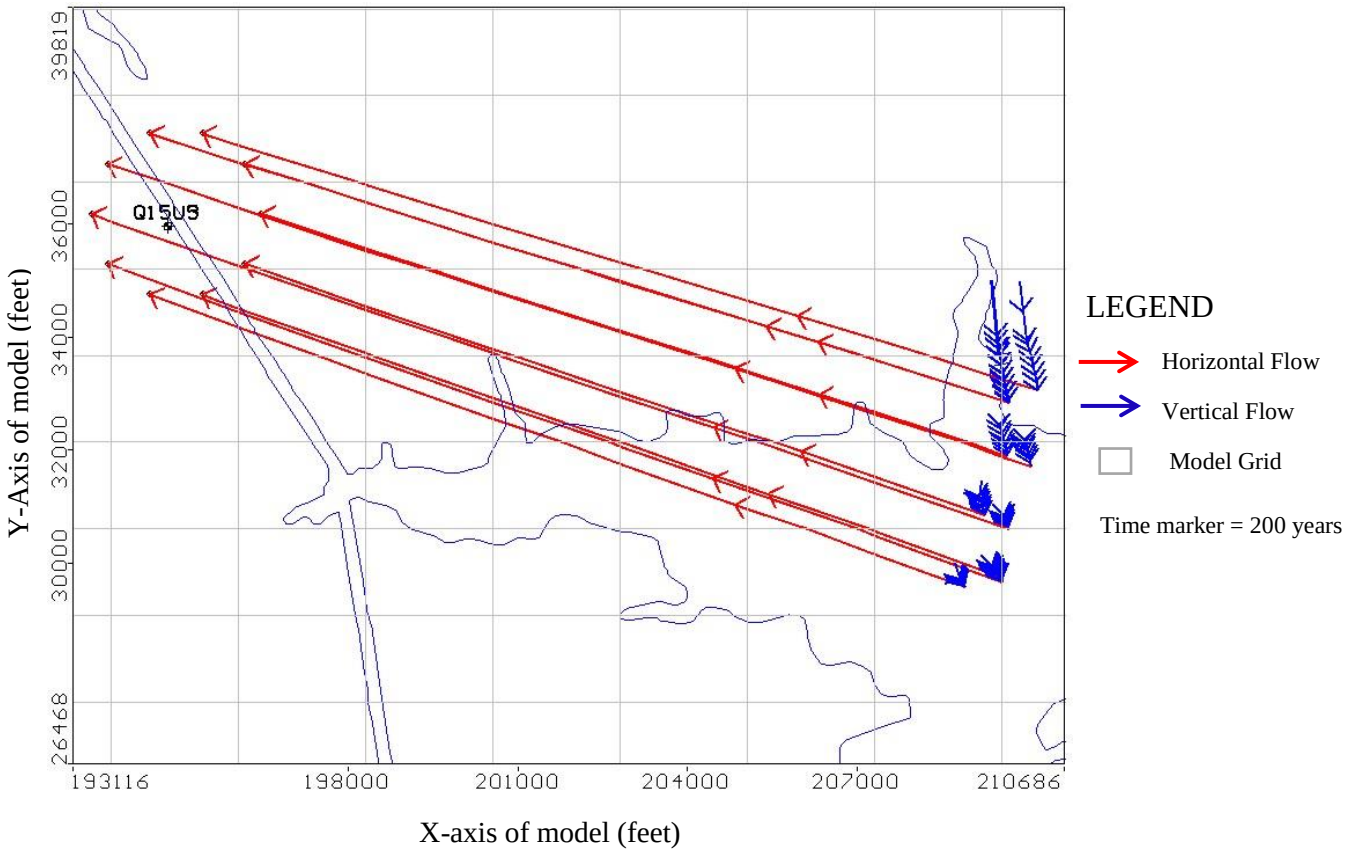

Sample Q15U3 particle tracking. Travel time marker = 200 years.

MODPATH results indicate that the source of these groundwater particles comes from recharge infiltration. Under the current influence of groundwater pumping, it would take a minimum total travel time of 2,124 years for groundwater particles to travel from their source to the sample location. The minimum time required for particles to travel vertically through the units overlying the UCH is 1,744 years. Horizontal flow through the UCH (2.5 miles) requires approximately 380 years. Horizontal flow through the UCH occurs at an average rate of 0.007 miles/year.

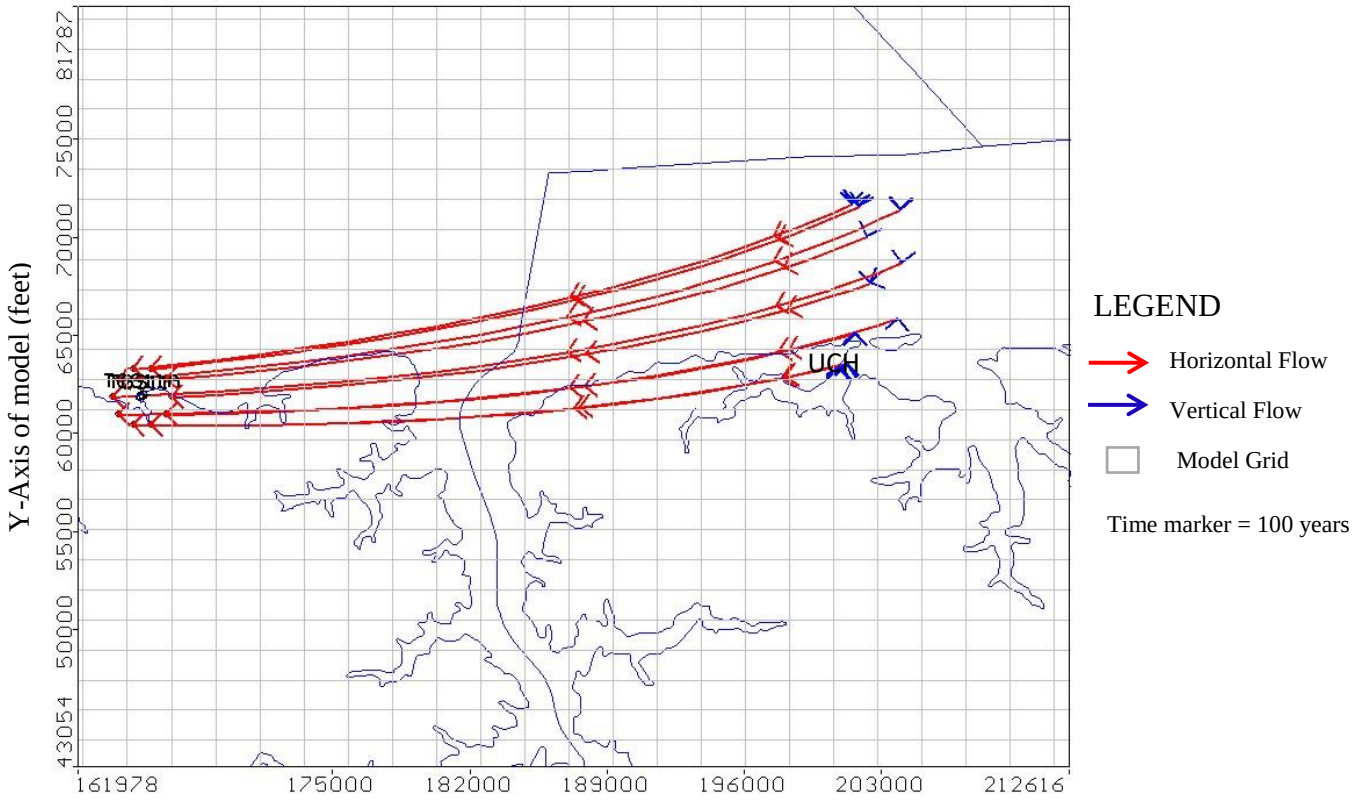

Sample TGS11 particle tracking. Travel time marker = 100 years.

MODPATH results indicate that the source of these groundwater particles comes from recharge infiltration. Under the current influence of groundwater pumping, it would take a minimum total travel time of 1,687 years for groundwater particles to travel from their source to the sample location. The minimum time required for particles to travel vertically through the units overlying the UCH is 1,337 years. Horizontal flow through the UCH (7 miles) requires approximately 350 years. Horizontal flow through the UCH occurs at an average rate of 0.02 miles/year.

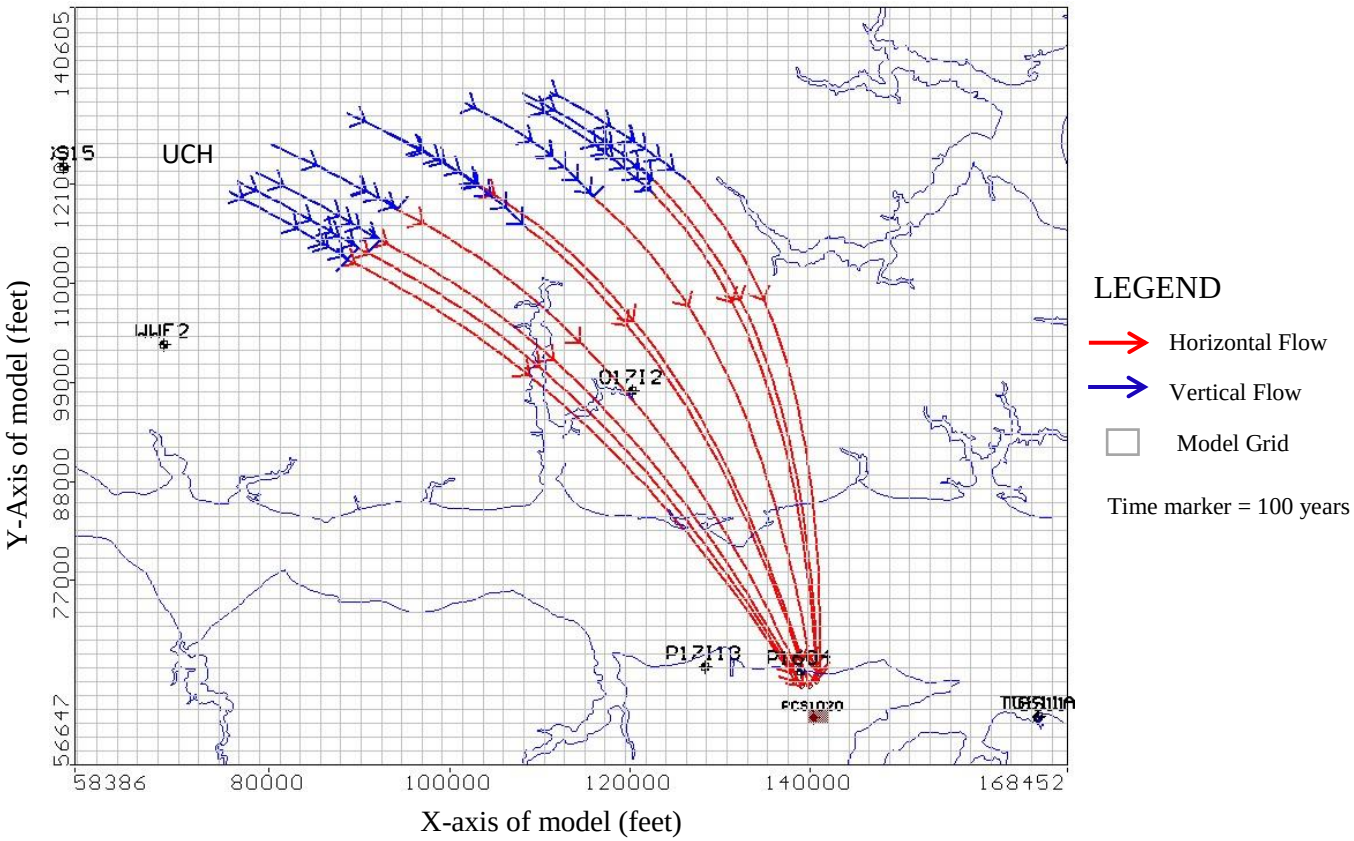

Sample**.** P16O4 particle tracking. Travel time marker = 100 years.

MODPATH results indicate that the source of these groundwater particles comes from recharge infiltration. Under the current influence of groundwater pumping, it would take a minimum total travel time of 865 years for groundwater particles to travel from their source to the sample location. The minimum time required for particles to travel vertically through the units overlying the UCH is 515 years. Horizontal flow through the UCH (9 miles) requires approximately 350 years. Horizontal flow through the UCH occurs at an average rate of 0.026 miles/year.

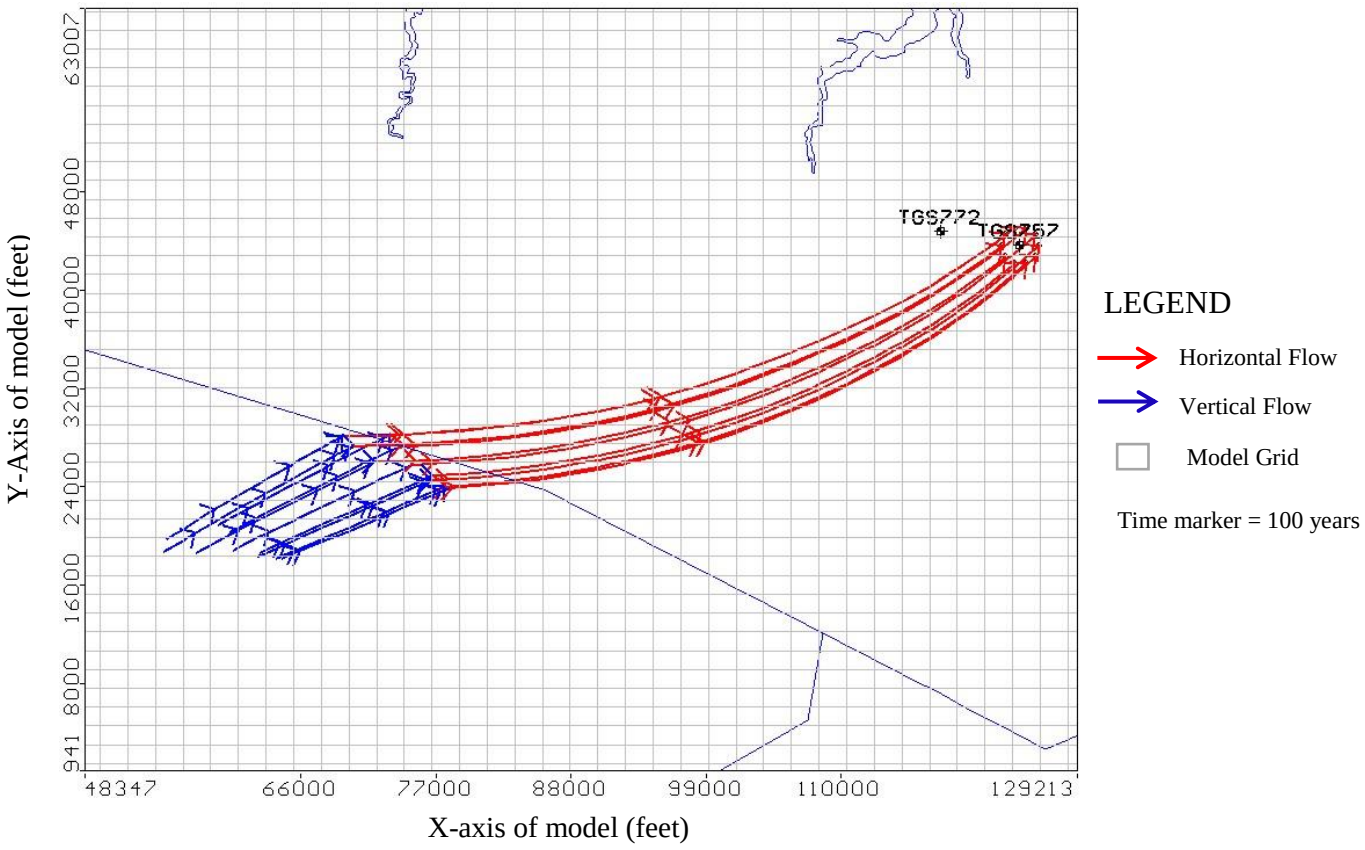

Sample TGS757 particle tracking. Travel time marker = 100 years.

MODPATH results indicate that the source of these groundwater particles comes from recharge infiltration. Under the current influence of groundwater pumping, it would take a minimum total travel time of 594 years for groundwater particles to travel from their source to the sample location. The minimum time required for particles to travel vertically through the units overlying the UCH is 394 years. Horizontal flow through the UCH (10 miles) requires approximately 200 years. Horizontal flow through the UCH occurs at an average rate of 0.05 miles/year.

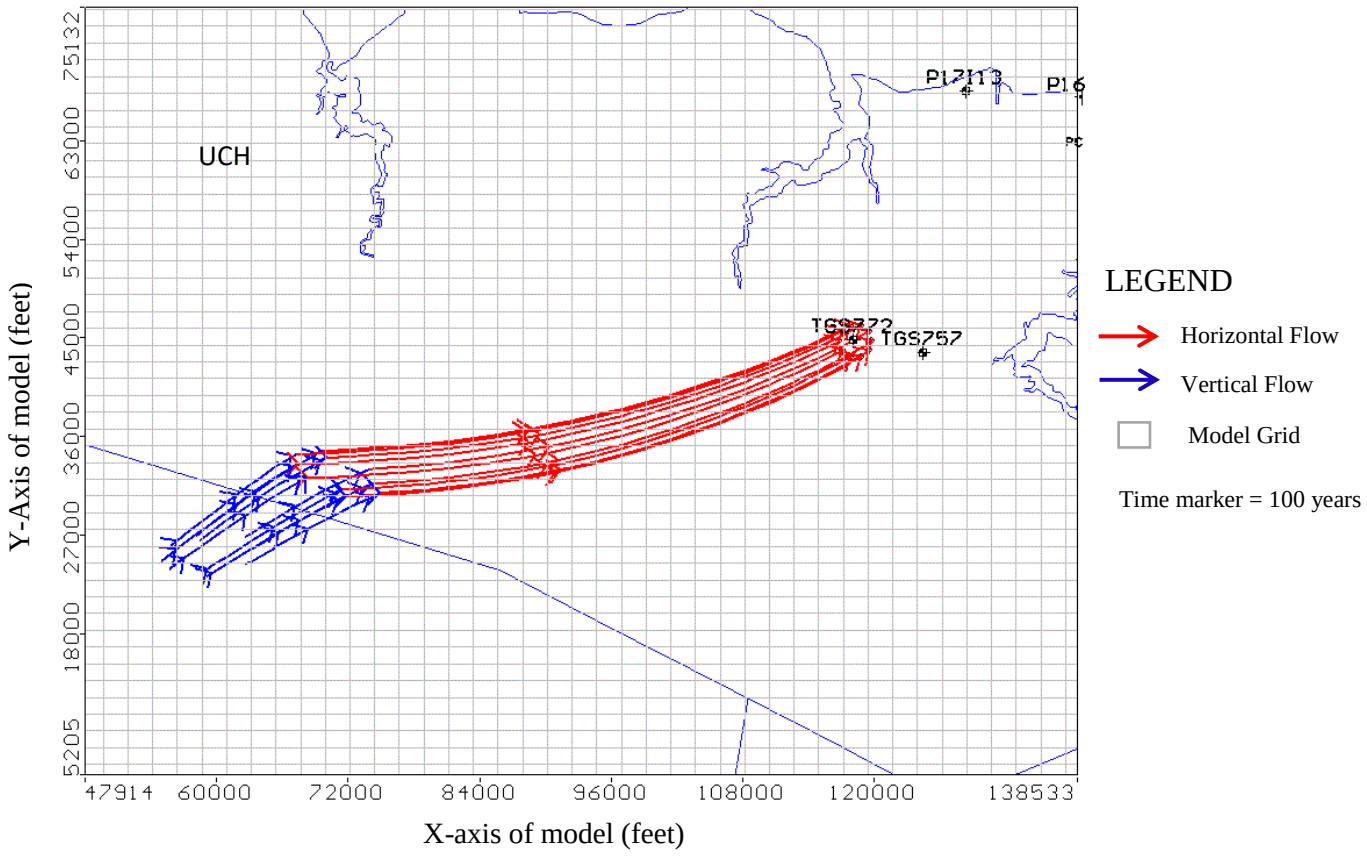

Sample TGS772 particle tracking. Travel time marker = 100 years.

MODPATH results indicate that the source of these groundwater particles comes from recharge infiltration. Under the current influence of groundwater pumping, it would take a minimum total travel time of 576 years for groundwater particles to travel from their source to the sample location. The minimum time required for particles to travel vertically through the units overlying the UCH is 376 years. Horizontal flow through the UCH (10 miles) requires approximately 200 years. Horizontal flow through the UCH occurs at an average rate of 0.05 miles/year.